REVIEWS OF MODERN PHYSICS, VOLUME 78, OCTOBER–DECEMBER 2006

The physics of hadronic tau decays

Michel Davier,* Andreas Höcker,† and Zhiqing Zhang‡

Laboratoire de l'Accélérateur Linéaire, IN2P3/CNRS and Université de Paris-Sud 11, BP34, F-91898 Orsay, France

(Published 4 October 2006)

Hadronic τ decays provide a clean laboratory for the precise study of quantum chromodynamics (QCD). Observables based on the spectral functions of hadronic τ decays can be related to QCD quark-level calculations to determine fundamental quantities like the strong-coupling constant, parameters of the chiral Lagrangian $|V_{us}|$, the mass of the strange quark, and to simultaneously test the concept of quark-hadron duality. Using the best available measurements and a revisited analysis of the theoretical framework, the value $\alpha_s(m_\tau^2)=0.345\pm0.004_{\rm exp}\pm0.009_{\rm th}$ is obtained. Taken together with the determination of $\alpha_s(M_Z^2)$ from the global electroweak fit, this result leads to the most accurate test of asymptotic freedom: the value of the logarithmic slope of $\alpha_s^{-1}(s)$ is found to agree with QCD at a precision of 4%. The τ spectral functions can also be used to determine hadronic quantities that, due to the nonperturbative nature of long-distance QCD, cannot be computed from first principles. An example for this is the contribution from hadronic vacuum polarization to loop-dominated processes like the anomalous magnetic moment of the muon. This article reviews the measurements of nonstrange and strange τ spectral functions and their phenomenological applications.

DOI: 10.1103/RevModPhys.78.1043 PACS number(s): 12.38.Bx, 12.38.Qk, 13.35.Dx, 13.40.Em

CONTENTS

*Electronic address: davier@lal.in2p3.fr
†Present address: CERN, PH Division, CH-1211 Geneva 23, Switzerland. Electronic address: hoecker@lal.in2p3.fr
‡Electronic address: zhangzq@lal.in2p3.fr

I. INTRODUCTION

Because of its relatively large mass and the simplicity of its decay mechanism, the τ lepton offers many interesting, and sometimes unique, possibilities for testing and improving the Standard Model (SM). These studies involve the leptonic and hadronic sectors and encompass a large range of topics, from the measurement of the leptonic couplings in the weak charged current and the search for lepton flavor violation, providing precise lepton universality tests, to a complete investigation of hadronic production from the quantum chromodynamics (QCD) vacuum. For the latter case, the τ decay results have proven to be complementary to those from e^+e^- data, allowing us to perform detailed studies at the fundamental level through the determination of the *spectral functions*, which embody both the rich hadronic structure seen at low energy and the quark behavior relevant in the higher-energy regime. The spectral functions play an important role in the understanding of hadronic dynamics in the intermediate-energy range. They represent the basic input for QCD studies and for evaluating low-energy contributions from hadronic vacuum polarization. This is required for the calculation of the muon anomalous magnetic moment and the running of the electromagnetic coupling constant. The topics of interest also include the following: studying isospin violation between the weak charged and electromagnetic hadronic currents, evaluation of chiral sum rules making use of the separate determination of vector and axial-vector components, and a global QCD analysis including perturbative and nonperturbative contributions, offering the possibility for a precise extraction of the strong coupling at a relatively low-energy scale, and hence providing a sensitive test of the running when compared to the value obtained at the M_Z scale. The spectral functions into strange ($|\Delta S|=1$) final states, though Cabibbo suppressed, can be used to determine the s-quark mass and the Cabibbo-Kobayashi-Maskawa (CKM) element $|V_{us}|$. In addition, the study of $\tau^+\tau^-$ pair production at the CERN LEP has proven to be an invaluable tool for investigating the neutral current sector of the electroweak theory, particularly through measurement of the τ polarization.

This article reviews measurements of nonstrange and strange τ spectral functions and their phenomenological applications. It is organized as follows. We begin in Sec. II with an overview on the experimental conditions leading to the measurement of the τ branching fractions (Sec. III) and hadronic spectral functions (Sec. IV) by the ALEPH and OPAL experiments at LEP as well as CLEO at CESR. Using isospin symmetry, the τ vector spectral functions are compared to the corresponding e^+e^- annihilation data in Sec. V. We discuss in this context isospin-breaking and radiative corrections. The use of spectral functions in dispersion relations to compute hadronic vacuum polarization is reviewed in Sec. VI. A comprehensive review of hadronic τ decays within QCD is presented in Secs. VII and VIII. The main topics here are determinations of the strong-coupling constant and mass of the strange quark at the scale of the τ mass together with $|V_{us}|$. We discuss nonperturbative contributions to the τ hadronic width and present results from chiral QCD sum rules.

For all topics we critically examine experimental and theoretical limitations, and provide detailed comparisons between experiments as well as perspectives for the future.

II. EXPERIMENTAL STAGE

A. Different experimental conditions

Tau physics in the nineties has been dominated by two rather different and in many views complementary experimental facilities: on one hand, the LEP experiments ALEPH, DELPHI, L3, and OPAL, operating at the Z resonance at center-of-mass (CM) energies of 91.2 GeV, and, on the other hand, CLEO at CESR running at the $\Upsilon(4S)$ resonance (10.6 GeV). The τ pair production and decay characteristics at LEP were

- a mean τ flight length of 2.2 mm;
- a strong boost of produced τ's leading to a collimated back-to-back event topology; hence tracks and photon clusters overlap in the detector, requiring excellent double hit resolution in the tracking system and a highly granular electromagnetic calorimeter;
- a large track reconstruction efficiency and low nuclear interactions and multiple scattering due to the high energetic particles in the final state;
- since hadronic background from Z decays occurs with significantly larger particle multiplicity, the selection of τ pairs is almost background free ($<1–2$ %), and the efficiency is large (up to 96% at ALEPH, depending on the final state);

- limited statistics of up to 1.6×10^5 τ pairs have been recorded by each of the LEP experiments between 1990 and 1995.

For CLEO, one has

- a mean τ flight length of 0.25 mm;
- well-separated τ decay products in the detector;
- significant hadronic background from $e^+e^-\to q\bar{q}$ continuum events due to the relatively low average multiplicity in the final state of these events. This requires τ tagging, i.e., one τ is reconstructed ("tagged") in a leptonic decay, or a hadronic mode with less than three hadrons in the final state. The recoil side of the tagged event is then used as an unbiased sample for physics studies;
- large statistics, for example, the $\tau^-\to\pi^-\pi^0\nu_\tau$ spectral function analysis (Anderson *et al.*, 2000) uses a data sample that contains 3.2×10^6 produced τ pairs.

Due to its superior statistics, CLEO discovered a number of rare modes and performed studies of their hadronic substructures. Examples for these are $\tau^-\to\eta K^-\nu_\tau$ (Bartelt *et al.*, 1996) and $\tau^-\to\eta\pi^-\pi^0\nu_\tau$ (Artuso *et al.*, 1992), the latter one proceeding through a vector current that is due to the Wess-Zumino chiral anomaly (Pich, 1987; Decker and Mirkes, 1993). The anomaly violates the rule that the weak vector and axial-vector currents produce an even and odd number of pseudoscalars, respectively. The $\tau^-\to\eta\pi^-\nu_\tau$ mode is a G-parity suppressed *second-class current*, which has not been observed yet.

For the τ decays with a branching fraction greater than 0.1%, the cleaner LEP events provided more precise branching fraction measurements, many of them with a subpercent relative accuracy, which are a crucial ingredient to the QCD study of hadronic τ decays. The Cabibbo-suppressed τ decays with $|\Delta S|=1$ have been studied by all experiments, albeit with limited success due to the restricted particle identification capabilities (except for DELPHI and CLEO III). Much progress is expected in this area from the B-Factory experiments *BABAR* and Belle, which have dedicated Cherenkov particle-identification devices.

B. Investigating the resonance structure in τ decays

Most of this review will be concerned with the interplay between measurements involving hadronic (or, more precisely, semileptonic) τ decays and QCD. This may appear a bit paradoxical in view of the relatively low-energy scale of τ physics. Indeed, τ decays to hadrons $(+\nu_\tau)$ reveal a rich structure of resonances, the study of which opens an interesting field of research on meson dynamics. The leptonic environment provides a significant advantage for isolating clean hadronic systems and measuring their parameters. Many τ decay modes have been investigated for their resonance structure. The phenomenologically important $\pi^-\pi^0$ vector state is analyzed in detail in Sec. V.

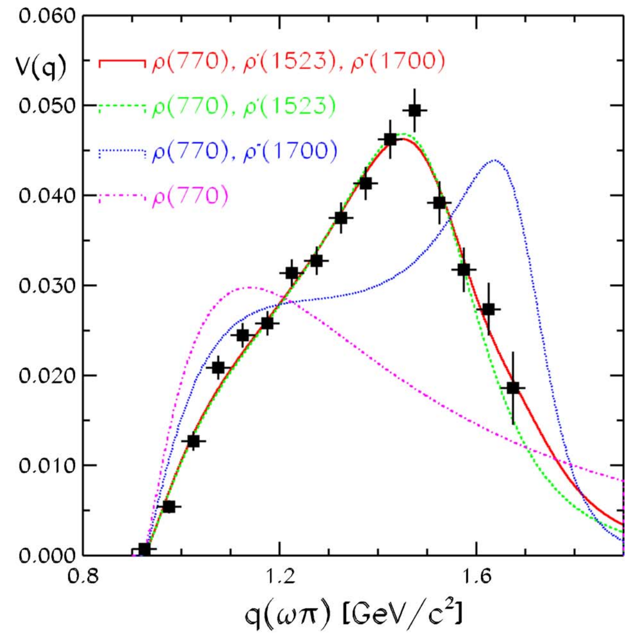

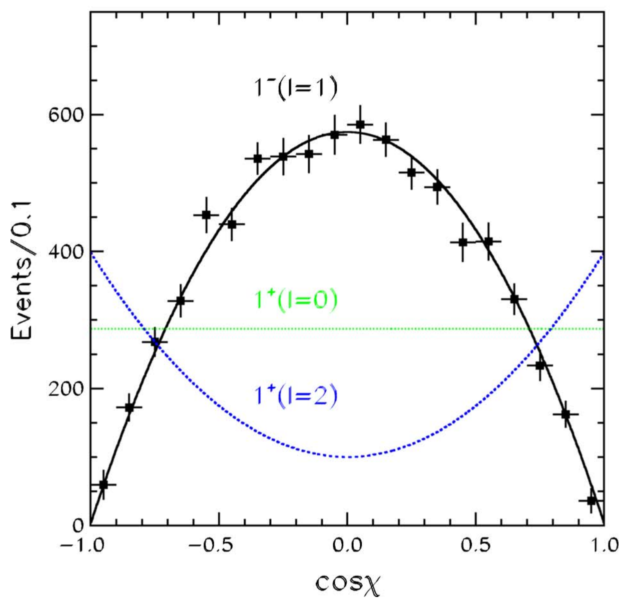

FIG. 1. (Color online) Upper: The spectral function (see Sec. IV for the definition) for the decay $\tau^-\to\omega\pi^-\nu_\tau$ vs the hadronic mass from the CLEO analysis (Edwards *et al.*, 2000). The curves are results of fits to various combinations of ρ, $\rho(1450)$, and $\rho(1700)$ resonance contributions. Lower: The angular distribution in the $\omega\pi$ center-of-mass frame compared to predictions for different (l) partial waves. Second-class currents would reveal themselves as $l=0,2$ waves.

Taking advantage of its large statistics sample, the CLEO Collaboration was able to perform partial-wave analyses of multihadron final states. In particular, the $(3\pi)^-\pi^0$ mode is expected to proceed through the vector current dominated by ρ, $\rho(1450)$, and $\rho(1700)$ isovector mesons. Resonances are also produced in two-body decays, such as $\omega\pi$, $\eta\pi$, and $a_1\pi$. CLEO measured (Edwards *et al.*, 2000) the $\omega\pi$ contribution, which they successfully modeled by interfering ρ, $\rho(1450)$, and $\rho(1700)$ resonances as shown in Fig. 1. At least the first two contributions are needed to reproduce the experimental mass spectrum. The helicity angle distribution in the $\omega\pi^-$ center of mass is found to be consistent with the expected $l=1$ wave (Fig. 1), whereas a wrong G-parity contribution arising from a weak second-class current, such as $\tau\to b_1^-\nu_\tau$ and $b_1^-\to\omega\pi^-$, would lead to an even l value. Such a contribution has been found to be less than 5.4% of the $\omega\pi^-$ rate. Besides $\omega\pi^-$, the total $(3\pi)^-\pi^0$ mode is shown to be dominated by $\rho\pi\pi$, consistent with originating from $a_1\pi$, $a_1\to\rho\pi$.

The decay $\tau\to\nu_\tau(3\pi)^-$ is the cleanest mode to study axial-vector resonance structure. The spectrum is dominated by the $J^P=1^+a_1$ state, known to decay essentially through $\rho\pi$. The hadronic structure of this decay has been studied in a model-independent analysis by the OPAL collaboration, where no evidence for vector or scalar currents has been found (Akers *et al.*, 1995, 1997). A comprehensive analysis of the $\pi^-2\pi^0$ channel has been presented by CLEO. First, a model-independent determination of the hadronic structure functions gave no evidence for non-axial-vector contributions [<17% at 90% (confidence limit) C.L.] (Browder *et al.*, 2000). Second, a partial-wave amplitude analysis was performed (Asner *et al.*, 2000): While the dominant $\rho\pi$ mode has been confirmed, it came as a surprise that an important contribution (~20%) from scalars [σ, $f_0(1470)$, and $f_2(1270)$] was found in the 2π subsystem. The precisely determined $a_1^-\to\pi^-2\pi^0$ line shape shows the opening of the K^*K decay channel. Some interference with a higher mass state (a_1') was advocated in Abreu *et al.* (1998). However, no conclusive evidence was found in the CLEO analysis, with a sensitivity about tenfold higher.

Evidence for the decay $\tau\to f_1(1285)\pi^-\nu_\tau$ has been obtained, with f_1 decay into $\eta\pi^+\pi^-$ and $\eta\pi^0\pi^0$ (Bergfeld *et al.*, 1997), and recently into $2\pi^+2\pi^-$ (by Aubert *et al.*, 2005b) the latter decay mode being consistent with $\rho^0\pi^+\pi^-$. Thus many spectroscopy issues can be tackled with τ leptons in a clean environment for single resonance studies.

III. TAU BRANCHING FRACTIONS

Tau hadronic spectral functions (Sec. IV) are obtained from the measured vector and axial-vector invariant mass spectra, normalized to the corresponding inclusive branching fractions. These are derived from the sum of exclusive branching fractions. Before discussing the spectral functions, we briefly review measurement of the τ branching fractions.

A. Measurement of branching fractions

In principle, measurement of branching fractions of exclusive τ decays relies on the identification of the corresponding final state and the knowledge of the produced τ leptons in the sample under study. The latter number can be derived from the production cross section, known to high precision in e^+e^- annihilation, and the measured luminosity. The measurement of the final state, however, requires excellence in many aspects of detector technology and analysis techniques: charged particle tracking and identification for $e/\mu/\pi/K$ separation, photon detection, and π^0 (η) reconstruction.

Since very clean and high-efficiency $\tau^+\tau^-$ samples have been produced at LEP, another approach can be considered where all decay channels are simultaneously measured. This global method was pioneered by the CELLO Collaboration at PETRA (Behrend *et al.*, 1990) with smaller statistics and less favorable conditions than those encountered at LEP. The detector performance achieved by ALEPH, in particular the granularity of its electromagnetic calorimeter, made it possible to implement this method and take full advantage of the LEP conditions on the Z peak (Decamp *et al.*, 1992; Buskulic *et al.*, 1996a, 1996b; Schael *et al.*, 2005).

The ALEPH global analysis of τ branching fractions proceeds from the selection of the $\tau^+\tau^-$ sample, based on the rejection of non-τ backgrounds: Z decays into e^+e^-, $\mu^+\mu^-$, and $q\bar{q}$ pairs, $\gamma\gamma$-induced processes $e^+e^-\to e^+e^-X$ (where X can be any fermion-antifermion pair), and cosmic-ray events. The kinematic properties of these backgrounds and their characteristic detector response permit us to achieve a high $\tau^+\tau^-$ selection efficiency of 78.9% (91.7% when the $\tau^+\tau^-$ direction points into the active area of the detector) and a low background fraction of 1.2%. Each τ decay is classified on the basis of charged particle and photon/π^0 multiplicities and the nature of the charged particles. Charged particle identification is achieved through the response of electromagnetic and hadronic calorimeters and the ionization loss measurement. Photons need to be identified among the neutral electromagnetic clusters, some of which are induced by charged hadron interactions or by spatial fluctuations of nearby showers (fake photons). Fourteen classes have been defined by Schael *et al.* (2005) for reconstructed decays, where the last one collects the fraction (3.6%) of rejected candidates corresponding to cases where particle identification is not reliable. The first 13 classes correspond to the following final states produced with ν_τ: $e^-\bar{\nu}_e$, $\mu^-\bar{\nu}_\mu$, h^-, $h^-\pi^0$, $h^-2\pi^0$, $h^-3\pi^0$, $h^-4\pi^0$, $2h^-h^+$, $2h^-h^+\pi^0$, $2h^-h^+2\pi^0$, $2h^-h^+3\pi^0$, $3h^-2h^+$, $3h^-2h^+\pi^0$, where h stands for a pion or kaon.

The branching fractions are determined using

$$n_i^{\mathrm{obs}} - n_i^{\mathrm{bkg}} = \sum_j \varepsilon_{ji} N_j^{\mathrm{prod}}, \qquad (1)$$

$$\mathcal{B}_j = \frac{N_j^{\mathrm{prod}}}{\sum_j N_j^{\mathrm{prod}}}, \qquad (2)$$

where n_i^{obs} (n_i^{bkg}) is the number of observed τ candidates (the non-τ background events) that are reconstructed in class i, ε_{ji} is the cross-talk efficiency of events that are produced in class j and reconstructed in class i, and N_j^{prod}

is the number of produced events in class j. The efficiency matrix ε_{ji} is determined from Monte Carlo simulation, based on the event generator KORALZ07 (Jadach *et al.*, 1994) and including the full detector response. The simulation has been calibrated using data for a large number of observables. Among these are particle-identification efficiencies, $\tau^+\tau^-$ selection efficiency, and the number of fake photon candidates. The selection efficiency remains constant within $\pm\sim 5\%$ for all 13 topologies considered. The linear system of equations (1) is solved for the N_j^{prod} unknown, hence the branching fractions $\mathcal{B}_j$.

Extensive systematic studies have been performed to assess possible biases in the decay assignment. These studies have been conducted on data samples in order not to rely on the detector simulation, however detailed it can be. They include event selection, non-τ background, particle identification, photon detection efficiency, converted photons, photon identification, fake photons, π^0 reconstruction, bremsstrahlung and radiative photons, π^0 Dalitz decays, secondary nuclear interactions, tracking of charged particles, and dynamics in the Monte Carlo generator. The dominant systematic uncertainties for hadronic modes stem from the photon/π^0 treatment and secondary interactions.

While measurements of branching fractions larger than 0.1% are more precise at LEP because of its small systematic uncertainties, the larger statistics accumulated by CLEO makes it more competitive for smaller branching fractions. The different experimental conditions also provide complementary information and valuable cross checks.

The ALEPH global analysis assumes a standard τ decay description. However, unknown decay modes not included in the simulation may exist. Since large detection efficiencies are achieved in the $\tau^-\tau^+$ selection, which is therefore robust, these decays would be difficult to pass unnoticed. An independent measurement of the branching fraction for undetected decay modes, i.e., modes not passing the selection cuts, using a direct search with a one-sided τ tag, was done by ALEPH (Snow, 1993), limiting this branching fraction to less than 0.11% at 95% C.L. This result justifies the assumption that the sum of the branching fractions for visible τ decays is equal to 1. The consistency between the results and τ decay description in the simulation can be investigated further by verifying that the "branching fraction" for a 14th class in the decay classification, which collects rejected events, turns out to be zero within the measurement errors. The result $\mathcal{B}_{14}=(0.066\pm 0.042)\%$ provides a nontrivial test of the overall procedure at the 0.1% level for branching fractions.

The global method at LEP reaches its limit for decay modes with small branching fractions, which compete with leading channels with fractions that could be more than two orders of magnitude larger. This limit is also determined by the overall τ statistics. It turns out that the two factors contribute at about the same level. Thus final states with more than five hadrons are poorly determined at LEP, whereas CLEO can use its larger statistics to apply stricter cuts for these higher-multiplicity decays with low branching ratios.

A final check of the global analysis can be performed by comparing the sums of the relevant exclusive decay fractions to the topological branching fractions $\mathcal{B}_i$, where i is the charged particle multiplicity in the decay. Even though the latter branching fractions have only limited direct physics implications, their determination represents a valuable cross check as the measurement does not depend on photon reconstruction in a calorimeter. Assuming a negligible contribution from charged-particle multiplicities larger than 5, in agreement with the 90% C.L. achieved by CLEO [$\mathcal{B}_7 < 2.4\times 10^{-6}$ (Edwards *et al.*, 1997)], ALEPH finds

$$\mathcal{B}_3 = (14.652 \pm 0.067 \pm 0.086)\,\%\,, \tag{3}$$

$$\mathcal{B}_5 = (0.093 \pm 0.009 \pm 0.012)\,\%\,, \tag{4}$$

in agreement with the values from a dedicated topological analysis performed by DELPHI (Abreu *et al.*, 2001),

$$\mathcal{B}_3^{\text{top}} = (14.569 \pm 0.093 \pm 0.048)\ \%\ , \tag{5}$$

$$\mathcal{B}_5^{\text{top}} = (0.115 \pm 0.013 \pm 0.006)\ \%\ . \tag{6}$$

B. Leptonic branching fractions

The measurement of two leptonic decay modes of τ is of great importance in our context, since they are complementary to the hadronic modes, the fraction of which can be determined by a simple difference. The leptonic branching ratios also turn out to be the most precisely determined τ decay fractions, not affected by systematic uncertainties that are specific to the presence of hadrons in the detector.

Before examining the experimental situation, we recall the theoretical expectations within the standard V-A theory with leptonic coupling g_ℓ at the $W\ell\bar{\nu}_l$ vertex. The $L=\mu,\tau$ leptonic ($\ell=e,\mu$) partial widths can be computed, including radiative corrections (Marciano and Sirlin, 1988) and safely neglecting neutrino masses:

$$\Gamma(L \to \nu_L \ell \bar{\nu}_\ell(\gamma)) = \frac{G_L G_\ell m_L^5}{192\pi^3} f\left(\frac{m_\ell^2}{m_L^2}\right) \delta_W^L \delta_\gamma^L, \tag{7}$$

where

$$G_\ell = \frac{g_\ell^2}{4\sqrt{2} M_W^2},$$

$$\delta_W^L = 1 + \frac{3}{5}\frac{m_L^2}{M_W^2},$$

$$\delta_\gamma^L = 1 + \frac{\alpha(m_L)}{2\pi}\left(\frac{25}{4} - \pi^2\right),$$

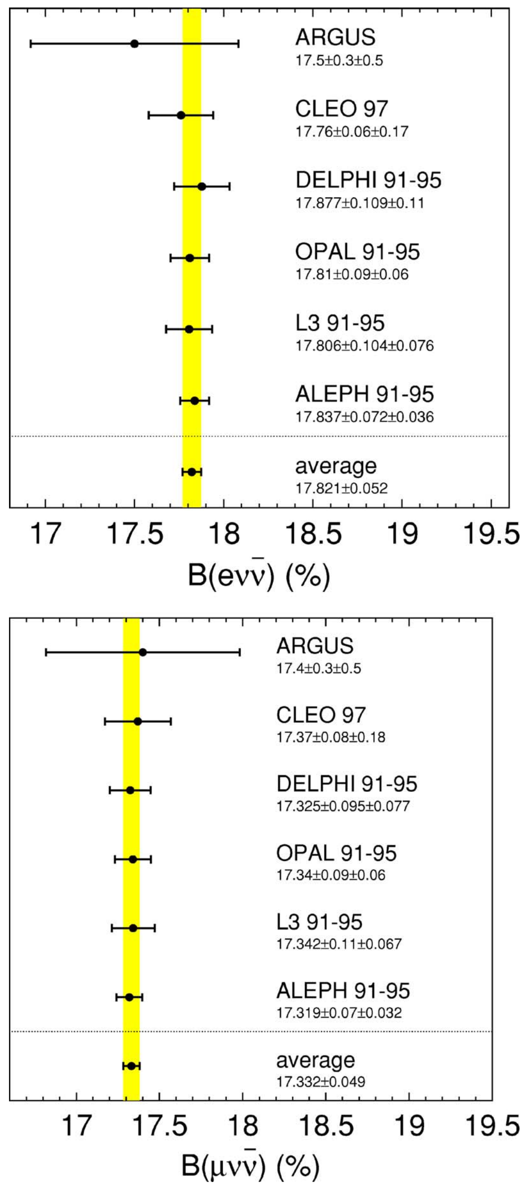

FIG. 2. (Color online) Measurements of the branching fraction for $\tau^- \to e^- \bar{\nu}_e \nu_\tau$ (upper) and $\tau^- \to \mu^- \bar{\nu}_\mu \nu_\tau$ (lower). References for experiments are Schael *et al.*, 2005; Albrecht *et al.*, 1993; Anastassov *et al.*, 1997; Abreu *et al.*, 1999; Acciarri *et al.*, 2001; Abbiendi *et al.*, 1999, 2003. The world averages are indicated by the shaded vertical bands.

$$f(x) = 1 - 8x + 8x^3 - x^4 - 12x^2 \ln x . \tag{8}$$

Numerically, the radiative and W propagator corrections are small: $\delta_W^\tau = 1 + 2.9 \times 10^{-4}$, $\delta_\gamma^\tau = 1 - 43.2 \times 10^{-4}$, $\delta_W^\mu = 1 + 1.0 \times 10^{-6}$, and $\delta_\gamma^\mu = 1 - 42.4 \times 10^{-4}$.

The experimental situation on the electronic and muonic branching fractions $\mathcal{B}_e$ and $\mathcal{B}_\mu$ is given in Fig. 2. The results for their average are

$$\mathcal{B}_e = (17.821 \pm 0.052)\,\% , \tag{9}$$

$$\mathcal{B}_\mu = (17.332 \pm 0.049)\,\% , \tag{10}$$

with a relative precision of 0.3%. The values for $\mathcal{B}_e$ and $\mathcal{B}_\mu$ agree with the universality assumption of equal leptonic couplings $g_e = g_\mu = g_\tau$. Their ratio

$$\frac{\mathcal{B}_\mu}{\mathcal{B}_e} = 0.9726 \pm 0.0041 \tag{11}$$

is consistent with the predicted value equal to $f(m_\mu^2/m_\tau^2)/f(m_e^2/m_\tau^2) = 0.972\,565 \pm 0.000\,009$, using lepton masses from the Particle Data Group (Eidelman *et al.*, 2004). The uncertainty arises essentially from the τ mass determination $m_\tau = (1777.03^{+0.30}_{-0.26})$ MeV dominated by the result of Bai *et al.* (2002).

The result for $\mathcal{B}_e$ can also be compared with the value obtained from the τ and μ masses and lifetimes $\tau_{\tau,\mu}$, under the assumption of $\tau - \mu$ universality, according to

$$\mathcal{B}_e = \frac{\tau_\tau}{\tau_\mu} \left(\frac{m_\tau}{m_\mu} \right)^5 \frac{f(m_e^2/m_\tau^2)}{f(m_e^2/m_\mu^2)} \frac{\delta_W^\tau \delta_\gamma^\tau}{\delta_W^\mu \delta_\gamma^\mu} = \frac{\tau_\tau}{(1\,631.9 \pm 1.4)\ \text{fs}} . \tag{12}$$

Using the τ lifetime (Eidelman *et al.*, 2004), $\tau_\tau = (290.6 \pm 1.1)$ fs, as well as the μ lifetime, one obtains $\mathcal{B}_e = (17.807 \pm 0.067)\,\%$, in excellent agreement with direct measurements.

The direct value for $\mathcal{B}_e$ and the two derived values from $\mathcal{B}_\mu$ and τ_τ are in good agreement with each other, providing a consistent and precise combined result for the electronic branching fraction,

$$\mathcal{B}_e^{\text{uni}} = (17.818 \pm 0.032)\,\% . \tag{13}$$

Hence we find for the branching fraction of $\mathcal{B}_{\text{had}}$, $\tau \to \nu_\tau$ hadrons assuming lepton universality and unitarity

$$\mathcal{B}_{\text{had}} = 1 - \mathcal{B}_e - \mathcal{B}_\mu = 1 - 1.972\,57 \mathcal{B}_e^{\text{uni}} = (64.853 \pm 0.063)\,\% . \tag{14}$$

C. Decay modes with kaons

Measurements of τ decay modes with kaons in the final state are important on at least two counts: (i) to determine the Cabibbo-suppressed component of the hadronic decay width, leading to interesting physics applications (see Sec. VIII), and (ii) to perform the necessary corrections to the measured topological branching fractions, based on charged particles and π^0 multiplicities. This latter step is made necessary by the difficulty separating charged pions and kaons and identifying K_L^0's at the level of an event. The subtraction of strange final states is then performed on a statistical basis.

The most complete measurements of τ branching fractions involving kaons are from ALEPH (Barate *et al.*, 1997a, 1998a, 1998b, 1999a, 1999b). From these results a comprehensive study of the strange sector has been performed, as well as some aspects of the dynamics in the final states with a $K\bar{K}$ pair. The experimental difficulty resides in the fact that both charged and neutral kaons have to be identified into multiparticle final states. The analyses involve the detection of charged kaons through the measurement of specific ionization losses and neutral kaons through either their decay into $\pi^+\pi^-$ (K_S^0) or their interactions in a calorimeter (K_L^0). Assuming *CP*

TABLE I. World average branching fractions (10^{-3}) for τ decays into strange final states and ν_τ from Barate *et al.* (1999b); Briere *et al.* (2003); Abbiendi *et al.* (2004); Eidelman *et al.* (2004); and Arms *et al.* (2005). The value for the $(\bar{K}3\pi)^-$ branching fraction takes into account measurements from ALEPH and CLEO, as well as estimates for unseen final states using isospin relations. The estimate for the very small $(\bar{K}4\pi)^-$ fraction, in addition to the measured $K^{*-}\eta$ rate (Bishai *et al.*, 1999), is obtained from an empirical observation of pionic modes and Cabibbo suppression.

Mode	$\mathcal{B}(10^{-3})$
K^-	6.81 ± 0.23
$K^-\pi^0$	4.54 ± 0.30
$\bar{K}^0\pi^-$	8.78 ± 0.38
$K^-\pi^0\pi^0$	0.58 ± 0.24
$\bar{K}^0\pi^-\pi^0$	3.60 ± 0.40
$K^-\pi^+\pi^-$	3.30 ± 0.28
$K^-\eta$	0.27 ± 0.06
$(\bar{K}3\pi)^-$ (estimated)	0.74 ± 0.30
$K_1(1270)^-\to K^-\omega$	0.67 ± 0.21
$(\bar{K}4\pi)^-$ (estimated) and $K^{*-}\eta$	0.40 ± 0.12
Sum	29.69 ± 0.86

invariance the K_S^0 and K_L^0 branching fractions can be averaged. The higher efficiency achieved for K_L^0 detection leads to smaller statistical uncertainties. Although the strange final states are Cabibbo suppressed, the precision achieved in these measurements is sufficient for various significant tests, ranging from τ-μ lepton universality to hadron dynamics, resonance production, QCD analyses, and the measurement of the Cabibbo angle. In addition, the consistency of the results is checked through the verification of isospin relations between rates observed for different charge configurations of the same final states.

New experimental results have been released by CLEO (Bishai *et al.*, 1999; Richichi *et al.*, 1999; Briere *et al.*, 2003; Arms *et al.*, 2005) and OPAL (Abbiendi *et al.*, 2004) achieving significant progress in the $\bar{K}\pi\pi$ modes. The new measurements tend to favor larger branching fractions. In particular, the branching fraction for the $K^-\pi^+\pi^-$ mode, $(2.14\pm0.47)\times10^{-3}$ for ALEPH, becomes in the world average $(3.30\pm0.28)\times10^{-3}$ with a χ^2 of 9.6 for 2 degrees of freedom (about 1% probability). Also, the branching fraction for $\bar{K}^0\pi^-\pi^0$, $(3.27\pm0.51)\times10^{-3}$ for ALEPH, becomes $(3.60\pm0.40)\times10^{-3}$ in the world average. A compilation of the world average $S=1$ branching fractions is given in Table I.

The branching fraction $\mathcal{B}_K$, for the decay $\tau^-\to K^-\nu$,

$$\mathcal{B}_K = (0.681 \pm 0.023)\,\%, \tag{15}$$

can be compared to the theoretical prediction assuming τ-μ universality in the charged weak current $\mathcal{B}_K^{\text{uni}}$ using the values (Eidelman *et al.*, 2004) for the τ and K lifetimes and masses, the $K^-\to\mu^-\bar{\nu}_\mu$ branching fraction, and a small radiative correction (Decker and Finkemeier, 1993) $\delta_{\tau/K}=1.0090\pm0.0022$,

$$\mathcal{B}_K^{\text{uni}} = \frac{\tau_\tau \mathcal{B}_{K\to\mu\nu}}{\tau_K}\frac{m_\tau^3}{2m_K m_\mu^2}\left(\frac{1-m_K^2/m_\tau^2}{1-m_\mu^2/m_K^2}\right)^2\delta_{\tau/K}$$
$$= \frac{\tau_\tau}{(40\,636\pm162)\ \text{fs}} = (0.715\pm0.003)\,\%. \tag{16}$$

D. Nonstrange hadronic branching fractions

Nonstrange hadronic branching fractions represent the largest part of τ decays and the physics goals require the achievement of small systematic uncertainties. The main experimental difficulty for this task is the photon/π^0 reconstruction. The high collimation of τ decays at LEP energies makes this task quite often difficult, since these photons are close to one another or close to showers generated by charged hadrons. Of particular relevance is the rejection of fake photons, which are due to hadronic interactions, fluctuations of electromagnetic showers, or an overlap of several showers. These problems reach a tolerable level in ALEPH due to the fine granularity of its electromagnetic calorimeter, comprising about 70 000 cells covering the detector angular acceptance, each cell being segmented threefold along the photon direction in order to discriminate between hadronic and electromagnetic showers. Even then, proper and reliable reconstruction methods had to be developed to correctly identify photon candidates. In the ALEPH analysis, a likelihood method is used for discriminating between genuine and fake photons, taking advantage of the detailed calorimeter information for each detected cluster of energy not associated to a charged track. Photons converted in the detector material are also included. Then π^0's are reconstructed: resolved π^0's from two-photon pairing, unresolved high-energy π^0's from merged clusters, and residual π^0's from the remaining single photons after removing radiative, bremsstrahlung, and fake photons with a likelihood method.

The 13 τ decay classes defined in Sec. III.A are not fully exclusive as they contain contributions from final states involving kaons. They come from charged kaons included in the class definition using hadrons (h) and from neutral kaons not taken into account in the classification. These contributions are subtracted on a statistical basis using the branching fractions measured separately (Sec. III.C).

The τ decays involving η or ω mesons also require special attention because of their electromagnetic decay modes. Indeed the final-state classification relies in part on the π^0 multiplicity, thereby assuming that all photons—except those specifically identified as bremsstrahlung or radiative—originate from π^0 decays. Therefore the non-π^0 photons from η and ω decays are treated as π^0 candidates in the ALEPH analysis and the systematic bias introduced by this effect must be evalu-

TABLE II. Results (Schael *et al.*, 2005) on exclusive hadronic branching fractions for modes without kaons. Contributions from channels with η and ω are given separately, the latter one only for electromagnetic ω decays. The measured branching ratio for $2\pi^-\pi^+3\pi^0$ is consistent with zero and the value listed has been estimated with the CLEO results (Bortoletto *et al.*, 1993b).

Mode	$\mathcal{B}\pm\sigma_{\rm stat}\pm\sigma_{\rm syst}$ (%)	
π^-	$10.828\pm0.070\pm0.078$	
$\pi^-\pi^0$	$25.471\pm0.097\pm0.085$	
$\pi^-2\pi^0$	$9.239\pm0.086\pm0.090$	
$\pi^-3\pi^0$	$0.977\pm0.069\pm0.058$	
$\pi^-4\pi^0$	$0.112\pm0.037\pm0.035$	
$\pi^-\pi^-\pi^+$	$9.041\pm0.060\pm0.076$	
$\pi^-\pi^-\pi^+\pi^0$	$4.590\pm0.057\pm0.064$	
$2\pi^-\pi^+2\pi^0$	$0.392\pm0.030\pm0.035$	
$2\pi^-\pi^+3\pi^0$	$0.013\pm0.000\pm0.010$	Estimate
$3\pi^-2\pi^+$	$0.072\pm0.009\pm0.012$	
$3\pi^-2\pi^+\pi^0$	$0.014\pm0.007\pm0.006$	
$\pi^-\pi^0\eta$	$0.180\pm0.040\pm0.020$	Barate *et al.*, 1997a
$\pi^-2\pi^0\eta$	$0.015\pm0.004\pm0.003$	Bergfeld *et al.*, 1997; Weinstein, 2001
$\pi^-\pi^-\pi^+\eta$	$0.024\pm0.003\pm0.004$	Bergfeld *et al.*, 1997; Weinstein, 2001
$a_1^-(\to\pi^-\gamma)$	$0.040\pm0.000\pm0.020$	Estimate
$\pi^-\omega(\to\pi^0\gamma,\pi^+\pi^-)$	$0.253\pm0.005\pm0.017$	Barate *et al.*, 1997a
$\pi^-\pi^0\omega(\to\pi^0\gamma,\pi^+\pi^-)$	$0.048\pm0.006\pm0.007$	Barate *et al.*, 1997a; Bortoletto *et al.*, 1993a
$\pi^-2\pi^0\omega(\to\pi^0\gamma,\pi^+\pi^-)$	$0.002\pm0.001\pm0.001$	Bergfeld *et al.*, 1997; Weinstein, 2001
$\pi^-\pi^-\pi^+\omega(\to\pi^0\gamma,\pi^+\pi^-)$	$0.001\pm0.001\pm0.001$	Bergfeld *et al.*, 1997; Weinstein, 2001

ated. The corrections are based on specific measurements by ALEPH of τ decay modes containing those mesons (Barate *et al.*, 1997a). Hence the final results correspond to exclusive branching fractions obtained from the values measured in the topological classification, corrected by contributions from K, η, and ω modes measured separately, taken into account through the simulation their specific selection and reconstruction efficiencies. This delicate bookkeeping takes into account all the major decay modes of the considered mesons (Eidelman *et al.*, 2004), including the isospin-violating $\omega\to\pi^+\pi^-$ decay mode. The main decay modes considered are $\pi^-\omega$, $\pi^-\pi^0\omega$, and $\pi^-\pi^0\eta$ with branching fractions of $(2.26\pm0.18)\times10^{-2}$, $(4.3\pm0.5)\times10^{-3}$, and $(1.80\pm0.45)\times10^{-3}$ (Barate *et al.*, 1997a), respectively. The first two values are derived from the branching fractions for the $2\pi^-\pi^+\pi^0$ and $2\pi^-\pi^+2\pi^0$ modes obtained in the global analysis and the measured ω fractions of 0.431 ± 0.033 from Barate *et al.* (1997a) and the average value, 0.78 ± 0.06, from Barate *et al.* (1997a) and Bortoletto *et al.* (1993a), respectively.

Small contributions from η and ω have been identified and measured by Bergefeld *et al.* (1997) and Weinstein (2001) with the decay modes $\tau^-\to\nu_\tau\eta\pi^-\pi^+\pi^-$ (2.4 ± 0.5), $\tau^-\to\nu_\tau\eta\pi^-2\pi^0$ (1.5 ± 0.5), $\tau^-\to\nu_\tau\omega\pi^-\pi^+\pi^-$ (1.2 ± 0.2), and $\tau^-\to\nu_\tau\omega\pi^-2\pi^0$ (1.5 ± 0.5), where the branching fractions are given in units of 10^{-4}. For the sake of completeness these modes have been included. Another small correction has been applied to take into account the a_1 radiative decay into $\pi\gamma$ with a branching fraction of $(2.1\pm0.8)\times10^{-3}$ (Zielinski, 1984).

The final ALEPH results on the hadronic branching fractions for τ decay modes not including kaons are given in Table II. The branching fractions obtained for the different channels are correlated with each other. On one hand, statistical fluctuations in the data and Monte Carlo samples are driven by the multinomial distribution of the corresponding events, producing well-understood correlations. On the other hand, systematic effects also induce significant correlations between the different channels. All systematic studies were done keeping track of the correlated variations in the final branching fraction results, thus allowing a proper propagation of errors. The full covariance matrices from statistical and systematic origins have been given by Schael *et al.* (2005).

The branching fraction $\mathcal{B}_\pi$ for the $\pi^-\nu$ decay mode,

$$\mathcal{B}_\pi=(10.83\pm0.11)\,\%\,, \tag{17}$$

agrees well with theoretical prediction depending only on the assumption of τ-μ universality $\mathcal{B}_\pi^{\rm uni}$ using the values (Eidelman *et al.*, 2004) for the τ and π lifetimes and masses, the $\pi^-\to\mu^-\bar{\nu}_\mu$ branching fraction, and a small radiative correction (Decker and Finkemeier, 1993) $\delta_{\tau/\pi}=1.0016\pm0.0014$,

$$\mathcal{B}_\pi^{\rm uni}=\frac{\tau_\tau\mathcal{B}_{\pi\to\mu\nu}}{\tau_\pi}\frac{m_\tau^3}{2m_\pi m_\mu^2}\left(\frac{1-m_\pi^2/m_\tau^2}{1-m_\mu^2/m_\pi^2}\right)^2\delta_{\tau/\pi}$$

$$=\frac{\tau_\tau}{2663.7\pm4.0\ \text{fs}}=(10.910\pm0.044)\,\%\,, \tag{18}$$

where the error in the denominator of the prediction is dominated by the uncertainty on the structure-dependent radiative correction.

Concerning the $(3\pi)^-\nu$ decay mode, which is dominated by the a_1 resonance, it is interesting to compare the rates in the $2\pi^-\pi^+$ and $\pi^-2\pi^0$ channels. Dominance of the $\rho\pi$ intermediate state in the a_1 decay predicts equal rates, but (small) isospin-breaking effects are expected from different charged and neutral π (and possibly ρ) masses, slightly favoring the $\pi^-2\pi^0$ channel. However, a partial-wave analysis of the $\pi^-2\pi^0$ final state performed by CLEO (Asner *et al.*, 2000) revealed that this decay is in fact rather complicated involving many intermediate states, in particular isoscalars, which amount to about 20% of the total rate and produce strong interference effects. A good description of the a_1 decays was achieved in this study, which can be applied to the $(3\pi)^-$ final state. Including known isospin-breaking effects from the pion masses, it predicts a ratio of the $2\pi^-\pi^+$ to the $\pi^-2\pi^0$ rate of 0.985. This value is in agreement with the ALEPH measurement (Schael *et al.*, 2005)

$$\frac{\mathcal{B}_{2\pi^-\pi^+}}{\mathcal{B}_{\pi^-2\pi^0}} = 0.979 \pm 0.018, \qquad (19)$$

supporting the expected trend.

A comparison of recent measurements of the dominant hadronic branching fractions is provided in Fig. 3. To compare with other experiments, results are given without charged hadron identification, i.e., the branching fractions correspond to the sum of all branching fractions with the same charged particle topology, whether pions or kaons.

E. Separation of vector and axial-vector contributions

From the complete analysis of the τ branching fractions presented by Schael *et al.* (2005) it is possible to determine the nonstrange vector (V) and axial-vector (A) contributions to the total τ hadronic width. It is conveniently expressed in terms of their ratios to the leptonic width, denoted $R_{\tau,V}$ and $R_{\tau,A}$, respectively, while the inclusive strange counterpart is denoted $R_{\tau,S}$. Only limited attempts to separate vector and axial-vector $|\Delta S|=1$ currents have been performed by experiments so far (Barate *et al.*, 1999b).

The ratio R_τ for the total hadronic width is calculated from the leptonic branching fractions alone, and eventually from the (massless) electronic branching fraction only,[1]

$$R_\tau = \frac{\Gamma(\tau^- \to \nu_\tau \,\mathrm{hadrons}^-)}{\Gamma(\tau^- \to \nu_\tau e^- \bar{\nu}_e)} = \frac{1-\mathcal{B}_e-\mathcal{B}_\mu}{\mathcal{B}_e} = \frac{1}{\mathcal{B}_e^{\mathrm{uni}}} - 1.9726 = 3.642 \pm 0.012, \qquad (20)$$

for ALEPH, assuming universality in the leptonic weak current. All R values given below are rescaled so that the sum of the hadronic and leptonic branching fractions, the latter one computed using the “universal” value $\mathcal{B}_e^{\mathrm{uni}}$(ALEPH), add up to 1. Deviations introduced in this way are small, less than 10% of the experimental error, but this procedure guarantees the consistency of all values. Using the ALEPH measurement of the strange branching fractions (Barate *et al.*, 1999b), supplemented by a (small) contribution from the $K^{*-}\eta$ channel measured by CLEO (Barate *et al.*, 1999a), one finds (see footnote 1)

$$\mathcal{B}_S = (2.85 \pm 0.11)\,\%,$$

$$R_{\tau,S} = 0.1603 \pm 0.0064, \qquad (21)$$

and consequently

$$\mathcal{B}_{V+A} = (62.01 \pm 0.14)\,\%,$$

$$R_{\tau,V+A} = 3.482 \pm 0.014, \qquad (22)$$

for the nonstrange component.

Separation of V and A components in hadronic final states with only pions is straightforward. An even number of pions has $G=1$ corresponding to vector states, while an odd number of pions has $G=-1$, which tags axial-vector states. This property places a requirement on knowledge of the π^0 reconstruction efficiency in the detector.

Modes with a $K\bar{K}$ pair are not in general eigenstates of G parity and contribute to both V and A channels. While the decay to K^-K^0 is pure vector, the situation is *a priori* not clear in the $K\bar{K}\pi$ channel observed in three charged modes: $K^-K^+\pi^-$, $K^-K^0\pi^0$, and $K^0\bar{K}^0\pi^-$. Three sources of information exist on the possible V/A content in these decays:

(1) In the ALEPH analysis of τ decay modes with kaons (Barate *et al.*, 1999b), an estimate of the vector contribution was obtained using available e^+e^- annihilation data in the $K\bar{K}\pi$ channel, extracted in the $I=1$ state. This contribution was found to be small, yielding the branching fraction $\mathcal{B}_{\mathrm{CVC}}(\tau^- \to \nu_\tau (K\bar{K}\pi)^-_V) = (0.26\pm0.39)\times10^{-3}$, which corresponds to an axial fraction of $f_{A,\mathrm{CVC}}=0.94^{+0.06}_{-0.08}$.

(2) The CVC result is corroborated by a partial-wave and line-shape analysis of the a_1 resonance from τ decays in the $\nu_\tau\pi^-2\pi^0$ mode by Asner *et al.* (2000). The observation through unitarity of the K^*K decay

[1] The branching ratios $\mathcal{B}_e^{\mathrm{uni}}(\mathrm{ALEPH})=(17.810\pm0.039)\%$ and $\mathcal{B}_S(\mathrm{ALEPH})=(2.85\pm0.11)\%$ used are from the ALEPH analysis only (Schael *et al.*, 2005) and differ slightly from the world average values given in Secs. III.B and III.C.

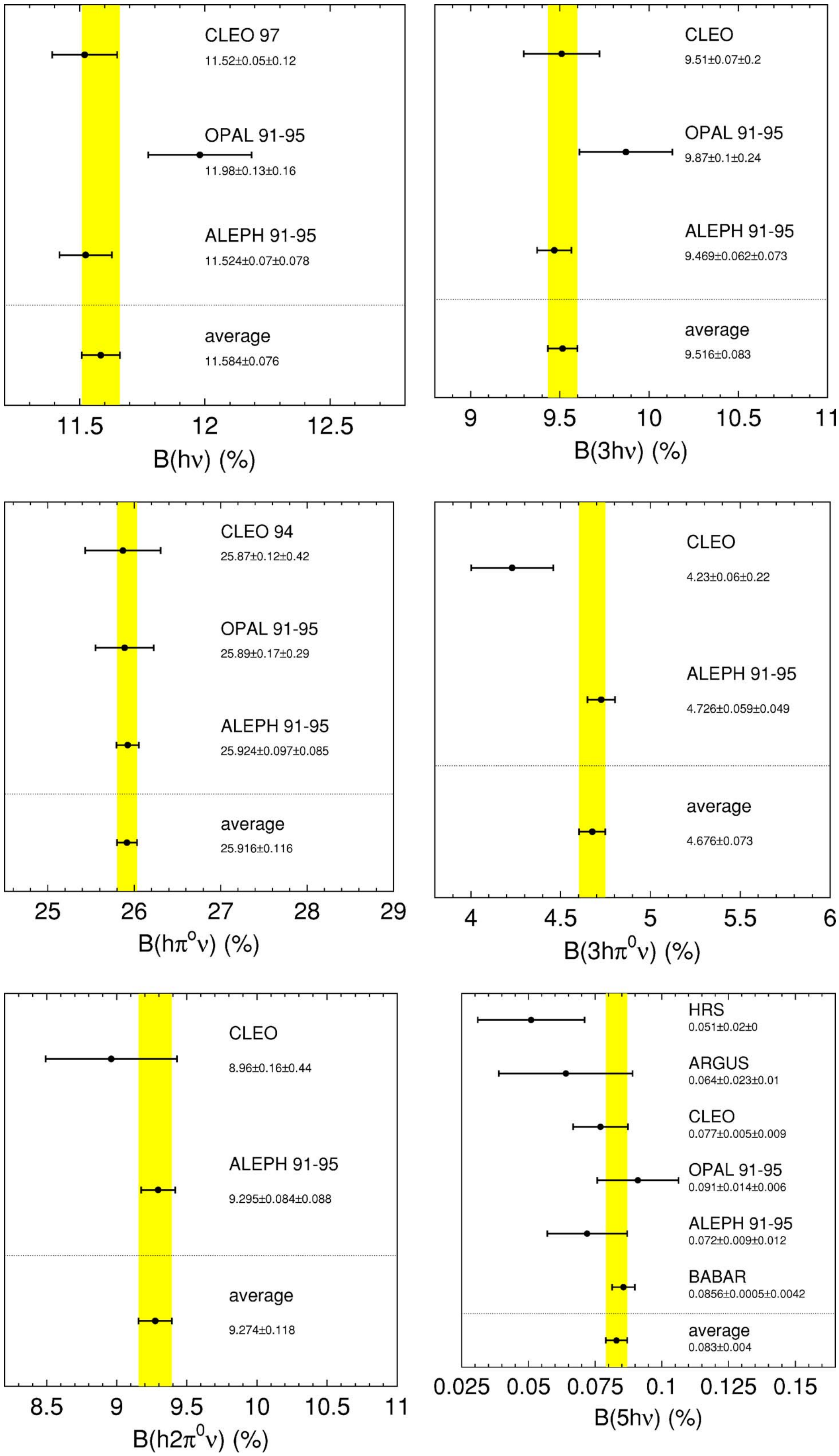

FIG. 3. (Color online) Comparison of results on the main branching fractions for τ hadronic modes (Bylsma *et al.*, 1987; Albrecht *et al.*, 1988; Procario *et al.*, 1993; Artuso *et al.*, 1994; Gibaut *et al.*, 1994; Balest *et al.*, 1995; Anastassov *et al.*, 1997; Ackerstaff *et al.*, 1998, 1999b; Aubert *et al.*. 2005b; Schael *et al.*, 2005). World averages are indicated by the shaded vertical bands.

mode opening with a_1 is postulated and the branching fraction $\mathcal{B}(a_1 \to K^* K) = (3.3 \pm 0.5)\%$ is derived. With the known decay rate of $\tau^- \to \nu_\tau a_1^-$, it is easy to see that such a result saturates, and even exceeds, the total rate for the $K\bar{K}\pi$ channel. The corresponding axial fraction is $f_{A,3\pi} = 1.30 \pm 0.24$.

(3) A new piece of information, also contributed by CLEO, but conflicting with the two previous results, was recently published (Coan *et al.*, 2004). It is based on a partial-wave analysis in the $K^-K^+\pi^-$ channel using two-body resonance production and including many possibly contributing channels. A much

smaller axial contribution is found here: $f_{A,K\bar{K}\pi} = 0.56 \pm 0.10$.

Since the three determinations are inconsistent, a conservative value of $f_A = 0.75 \pm 0.25$ is assumed. It encompasses the range allowed by previous results and still represents some progress over earlier analyses (Barate *et al.*, 1997b, 1998c), where a value of 0.5 ± 0.5 was used. For decays into $K\bar{K}\pi\pi$ no information is available in this respect, and a fraction of 0.5 ± 0.5 is used.

The total nonstrange vector and axial-vector contributions obtained by (Schael *et al.*, 2005) are

$$\mathcal{B}_V = (31.82 \pm 0.18 \pm 0.12)\,\%, \tag{23}$$

$$R_{\tau,V} = 1.787 \pm 0.011 \pm 0.007, \tag{24}$$

$$\mathcal{B}_A = (30.19 \pm 0.18 \pm 0.12)\,\%, \tag{25}$$

$$R_{\tau,A} = 1.695 \pm 0.011 \pm 0.007, \tag{26}$$

where the second errors reflect the uncertainties in the V/A separation in the channels with $K\bar{K}$ pairs. Taking care of (anti)correlations between the respective uncertainties, one obtains the difference between the vector and axial-vector components, which is physically related to the amount of nonperturbative contributions in the nonstrange hadronic τ decay width (see Sec. VII)

$$\mathcal{B}_{V-A} = (1.63 \pm 0.34 \pm 0.24)\,\%, \tag{27}$$

$$R_{\tau,V-A} = 0.092 \pm 0.018 \pm 0.014, \tag{28}$$

where the second error has the same meaning as in Eqs. (23) and (25). The ratio

$$\frac{R_{\tau,V-A}}{R_{\tau,V+A}} = 0.026 \pm 0.007 \tag{29}$$

is a measure of the relative importance of nonperturbative contributions. Its smallness, in spite of our subtraction of observables with very different spectral contributions from hadronic resonances, represents a proof of the remarkable property that is referred to as *quark-hadron duality*[2] (Shifman *et al.*, 1979a, 1979b, 1979c). It is the basis of the QCD analyses of hadronic τ decays presented in this review.

The inclusive vector and axial-vector branching fractions provide normalization of the corresponding spectral functions, which will be discussed below and which are the ingredients for the vacuum-polarization calculations and QCD analysis of hadronic τ decays.

[2] Blok *et al.* (1998) give the following definition of quark-hadron duality. "In a nutshell, a *truncated* OPE is analytically continued, term by term, from the Euclidean to the Minkowski domain. A smooth quark curve obtained in this way is supposed to coincide at high energies (energy releases) with the actual hadronic cross section."

IV. TAU HADRONIC SPECTRAL FUNCTIONS

The τ is the only lepton of the three-generation SM that is heavy enough to decay into hadrons. It is therefore an ideal laboratory for studying charged weak hadronic currents and QCD. In analogy to purely leptonic τ decays, the invariant amplitude for hadronic decays can be written in the form of a factorized current-current interaction,

$$\mathcal{M}(\tau^- \to \text{hadrons}^- \nu_\tau) = \frac{G_F}{\sqrt{2}} |V_{\rm CKM}| \ell_\mu h^\mu, \tag{30}$$

with the corresponding nonstrange or strange CKM matrix element $|V_{\rm CKM}|$, and where ℓ_μ describes the leptonic V-A current

$$\ell_\mu = \bar{\nu}_\tau \gamma_\mu (1 - \gamma_5) \tau \tag{31}$$

of the weak interaction. The hadronic transition current h_μ is the piece of interest here. It probes the matrix element of the left-handed charged current between the vacuum and hadronic final state. Restricting to a V-A structure, one can write

$$h_\mu = \langle \text{hadrons} | V_\mu(0) - A_\mu(0) | 0 \rangle. \tag{32}$$

The differential τ hadronic width can be expressed as follows:

$$d\Gamma(\tau^- \to \text{hadrons}^- \nu_\tau) = \frac{G_F^2}{4M_\tau} |V_{\rm CKM}|^2 L_{\mu\nu} H^{\mu\nu} d\text{PS}, \tag{33}$$

with the leptonic (hadronic) tensor $L_{\mu\nu}$ ($H_{\mu\nu}$) and the Lorentz invariant phase-space element dPS. The hadronic tensor obeys a Lorentz-invariant decomposition, the dynamical structure being embedded in so-called structure functions (Kühn and Mirkes, 1992).

For the simplest hadronic decay modes $\tau^- \to h^- \nu_\tau$ ($h = \pi, K$), the structure functions reduce to δ distributions, whereas resonances appear in τ decays into multiple hadrons. The hadronic structure is described by spectral functions. The quantum number corresponding to the (conserved) vector and axial-vector currents is the isotopic G parity. It is a generalized multiplicative symmetry of multipion systems under successive operations C and R, where C conjugates the charge and R rotates the system around the second axis in the $I=1$ isospace. The measurement of the τ vector and axial-vector current spectral functions requires selection and identification of τ decay modes with a defined G parity $G=+1$ and $G=-1$, and hence hadronic channels with an even and odd number of neutral *or* charged pions, respectively. Since hadronic final states of different G parity differ also in their J^P quantum numbers, there is no interference between these two states. Hence the total hadronic width separates into $\Gamma_{\rm tot} = \Gamma_V + \Gamma_A$.

A. Definitions

The spectral function v_1 (a_1, a_0), where the subscript refers to the spin J of the hadronic system, is defined for a nonstrange ($|\Delta S|=0$) or strange ($|\Delta S|=1$) vector (axial-vector) hadronic τ decay channel $V^-\nu_\tau$ ($A^-\nu_\tau$). The spectral function is obtained by dividing the normalized invariant mass-squared distribution $(1/N_{V/A})(dN_{V/A}/ds)$ for a given hadronic mass $\sqrt{s}$ by the appropriate kinematic factor

$$v_1(s)/a_1(s) = \frac{m_\tau^2}{6|V_{\rm CKM}|^2 S_{\rm EW}} \frac{\mathcal{B}(\tau^- \to V^-/A^-\nu_\tau)}{\mathcal{B}(\tau^- \to e^-\bar{\nu}_e\nu_\tau)} \times \frac{dN_{V/A}}{N_{V/A}ds}\left[\left(1-\frac{s}{m_\tau^2}\right)^2\left(1+\frac{2s}{m_\tau^2}\right)\right]^{-1}, \quad (34)$$

$$a_0(s) = \frac{m_\tau^2}{6|V_{\rm CKM}|^2 S_{\rm EW}} \frac{\mathcal{B}(\tau^- \to \pi^-(K^-)\nu_\tau)}{\mathcal{B}(\tau^- \to e^-\bar{\nu}_e\nu_\tau)} \times \frac{dN_A}{N_A ds}\left(1-\frac{s}{m_\tau^2}\right)^{-2}, \quad (35)$$

where $S_{\rm EW}$ accounts for electroweak radiative corrections (Marciano and Sirlin, 1988) (see Sec. V.A for the relevant values of $S_{\rm EW}$). Since CVC is a very good approximation for the nonstrange sector, the $J=0$ contribution to the nonstrange vector spectral function is put to zero, while the main contributions to a_0 are from the pion or kaon poles, with $dN_A/N_A ds = \delta(s-m_{\pi,K}^2)$. They are connected through partial conservation of the axial-vector current (PCAC) to the corresponding decay constants $f_{\pi,K}$. The spectral functions are normalized by the ratio of the vector/axial-vector branching fraction $\mathcal{B}(\tau^- \to V^-/A^-\nu_\tau)$ to the branching fraction of the massless leptonic, i.e., electron, channel (discussed in Sec. III.B).

Values for the CKM matrix elements V_{ud} and V_{us} have been recently much debated, because determinations from nuclear β decays and semileptonic kaon decays did not satisfy the unitarity relation in the first row of the CKM matrix, that is, $|V_{ud}|^2+|V_{us}|^2+|V_{ub}|^2=1$ (for this comparison, the V_{ub} element has a negligible contribution). The situation has improved with the availability of new results from $K_{\ell 3}$ and $K_{\mu 2}$ decays with revisited corrections from chiral perturbation theory, on one hand, and more precise radiative corrections for the nuclear β decays (Marciano, 2005), on the other hand. The current results (Isidori, 2005), which are still preliminary,[3]

$$|V_{ud}| = 0.9739 \pm 0.0003, \quad \text{nuclear } \beta \text{ decays}, \quad (36)$$

$$|V_{us}| = 0.2248 \pm 0.0016, \quad K_{\ell 3} + K_{\mu 2}, \quad (37)$$

are consistent with CKM unitarity and provide a new level of precision in this sector. The $|V_{ud}|$ value gives $|V_{us}|=0.2269\pm0.0013$ if CKM unitarity is used.

Using unitarity and analyticity, the spectral functions are connected to the imaginary part of the two-point correlation (or hadronic vacuum-polarization) functions

$$\Pi_{ij,U}^{\mu\nu}(q) \equiv i \int d^4x e^{iqx}\langle 0|T[U_{ij}^\mu(x)U_{ij}^\nu(0)^\dagger]|0\rangle = (-g^{\mu\nu}q^2 + q^\mu q^\nu)\Pi_{ij,U}^{(1)}(q^2) + q^\mu q^\nu \Pi_{ij,U}^{(0)}(q^2) \quad (38)$$

of vector ($U_{ij}^\mu = V_{ij}^\mu = \bar{q}_j\gamma^\mu q_i$) or axial-vector ($U_{ij}^\mu = A_{ij}^\mu = \bar{q}_j\gamma^\mu\gamma_5 q_i$) color-singlet quark currents, and for timelike momenta squared $q^2>0$. Lorentz decomposition is used to separate the correlation function into its $J=1$ and $J=0$ parts. The polarization functions $\Pi_{ij,U}^{\mu\nu}(s)$ have a branch cut along the real axis in the complex $s=q^2$ plane. Their imaginary parts give the spectral functions defined in Eq. (34), for nonstrange (strange) quark currents

$$\text{Im}\,\Pi_{\bar{u}d(s),V/A}^{(1)}(s) = \frac{1}{2\pi}v_1/a_1(s),$$

$$\text{Im}\,\Pi_{\bar{u}d(s),A}^{(0)}(s) = \frac{1}{2\pi}a_0(s), \quad (39)$$

which provide the basis for comparing short-distance theory with hadronic data.

The analytic vacuum-polarization function $\Pi_{ij,U}^{(J)}(q^2)$ obeys the dispersion relation

$$\Pi_{ij,U}^{(J)}(q^2) = \frac{1}{\pi}\int_0^\infty ds \frac{\text{Im}\,\Pi_{ij,U}^{(J)}(s)}{s-q^2-i\varepsilon} + \text{subtractions}, \quad (40)$$

where the unknown but in general irrelevant subtraction constants can be removed by taking the derivative of $\Pi_{ij,U}(q^2)$. The dispersion relation allows one to connect the experimentally accessible spectral functions to the correlation functions $\Pi_{ij,U}^{(J)}(q^2)$, which can be derived from theory (QCD).

B. Physical mass spectra and their unfolding

Measurement of the τ spectral functions defined in Eq. (34) requires determination of the invariant mass-squared distributions, obtained from experimental distributions after unfolding from the effects of measurement distortion. The unfolding procedure used by the ALEPH Collaboration (Barate *et al.*, 1997b, 1998c) follows a method based on the regularized inversion of the simulated detector response matrix using the singular value decomposition technique (Höcker and Kartvelishvili, 1996). The regularization function

[3]We thank V. Cirigliano and G. Isidori for their advice on the current best values for $|V_{ud}|$ and $|V_{us}|$.

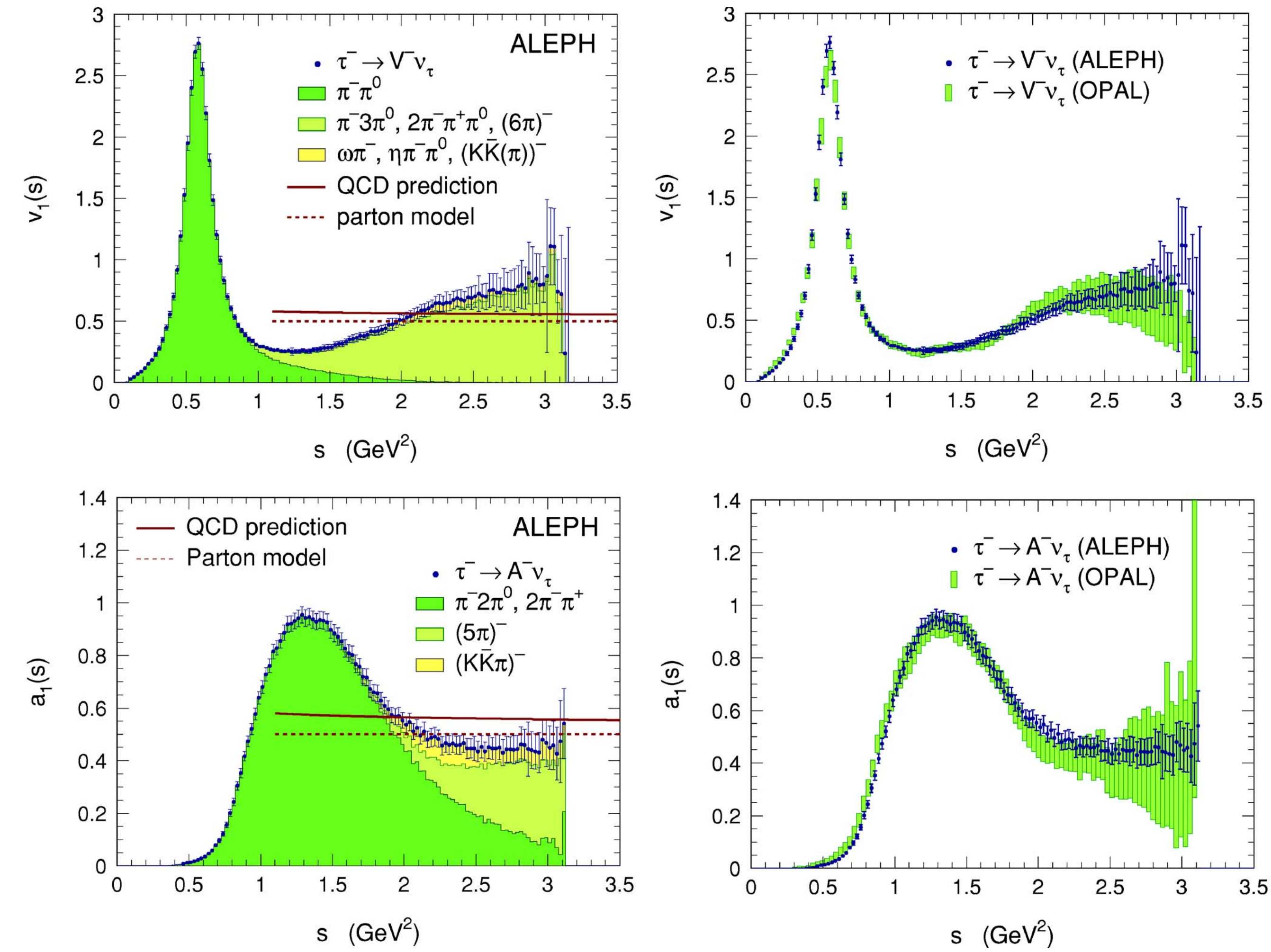

FIG. 4. (Color online) Left-hand plots: The inclusive vector (upper) and axial-vector (lower) spectral functions as measured by Schael *et al.* (2005). Shaded areas indicate the contributing exclusive τ decay channels. Curves show predictions from the parton model (dotted) and from massless perturbative QCD using $\alpha_s(M_Z^2)=0.120$ (solid). Right-hand-plots: Comparison of the inclusive vector (upper) and axial-vector (lower) spectral functions obtained by ALEPH and OPAL (Ackerstaff *et al.*, 1999a).

applied[4] minimizes the average curvature of the distribution. The optimal choice of the regularization strength is found by means of the Monte Carlo simulation where the true distribution is known and chosen to be close to the expected physical distribution. The OPAL Collaboration (Ackerstaff *et al.*, 1999a) employed a similar regularized unfolding technique (Blobel, 1984), which is, however, based on cubic splines instead of the binned histograms used by ALEPH. Due to the superior mass resolution, the CLEO collaboration considers it to be sufficient to only apply a bin-to-bin migration correction (Anderson *et al.*, 2000).

To measure exclusive spectral functions, individual unfolding procedures with specific detector response matrices and regularization parameters are applied for each τ decay channel considered. An iterative procedure is followed to correct the Monte Carlo spectral functions used to subtract the cross-feed among the modes.

Before unfolding the mass distributions, the τ and non-τ backgrounds are subtracted. In the case of τ feedthrough the Monte Carlo distributions normalized to the measured branching fractions are used. When the spectral functions are measured for nonstrange exclusive final states, contributions from strange modes classified in the same topology are subtracted using their Monte Carlo spectral functions normalized by measured branching fractions.

The systematic uncertainties affecting the decay classification of the exclusive modes are contained in the systematic errors on the branching fractions. Additional systematic uncertainties related to the shape of the unfolded mass-squared distributions, and not its normalization, are included. They are dominated by the photon and π^0 reconstruction.

[4]Regularization is necessary since in certain cases unfolding produces results with unphysical behavior: statistically insignificant components in the detector response matrix can lead to large oscillations in the unfolded distribution. The regularization is achieved by applying a smooth damping function to the unfolded distribution.

C. Inclusive nonstrange spectral functions

1. Vector and axial-vector spectral functions

The inclusive τ vector and axial-vector spectral functions are shown in the upper and lower plots of Fig. 4, respectively. The left-hand plots give the ALEPH result (Barate *et al.*, 1997b, 1998c; Schael *et al.*, 2005) together with its most important exclusive contributions, and the right-hand plots compare ALEPH with OPAL (Ackerstaff *et al.*, 1999a). The agreement between experiments is satisfying with the exception of the $\pi^-\pi^0$ (vector) mode, where some discrepancies occur. We note that the branching fraction used for this mode to obtain the inclusive spectral function is not the same in both experiments. The branching fraction used by ALEPH (Schael *et al.*, 2005) exceeds the one used by OPAL (Ackerstaff *et al.*, 1999a) by 0.9% (relative).

The curves in the left-hand plots of Fig. 4 represent the parton model (leading-order QCD) prediction (dotted) and improved (massless) perturbative QCD prediction (solid), assuming the relevant physics to be governed by short distances (Sec. VII). The difference between the two curves is due to higher-order terms in the strong coupling $[\alpha_s(s)/\pi]^n$ with $n=1,2,3$. At high energies the spectral functions are assumed to be dominated by continuum production, which locally agrees with perturbative QCD. This asymptotic region is not yet reached at $s=m_\tau^2$ for the vector and axial-vector spectral functions.

To build the vector spectral function ALEPH has measured the two- and four-pion final states exclusively, while only parts of the six-pion state. The total six-pion branching fraction has been determined using isospin symmetry (Barate *et al.*, 1997b). However, one has to account for the fact that the six-pion channel is contaminated by isospin-violating $\tau^-\to\eta(3\pi)^-\nu_\tau$ decays, as reported by CLEO (Bergfeld *et al.*, 1997; Weinstein, 2001). A small fraction of the $\omega\pi^-\nu_\tau$ decay channel that is not reconstructed in the four-pion final state is added using the simulation. Similarly, one corrects for the $\eta\pi^-\pi^0\nu_\tau$ decay mode where the η decays into pions. For the $\eta\to2\gamma$ mode, the τ decay is classified in the $h^-3\pi^0\nu_\tau$ final state, since the two-photon mass is inconsistent with the π^0 mass and consequently each photon is reconstructed as a π^0. The $K^-K^0\nu_\tau$ mass distribution is taken entirely from the simulation (recall that this mode is pure vector). The spectral functions for the final states $K\bar{K}\pi$ and $K\bar{K}\pi\pi$ (see Sec. III.E for discussion on the G parity of these modes) are obtained from the Monte Carlo simulation, where large systematic errors are applied to cover this approximation (Barate *et al.*, 1997b).

In analogy to the vector spectral function, the inclusive axial-vector spectral function is obtained by summing exclusive axial-vector spectral functions with the addition of small unmeasured modes taken from the Monte Carlo simulation. The small fraction of the $\omega\pi^-\pi^0\nu_\tau$ decay channel that is not accounted for in the $2\pi^-\pi^+2\pi^0\nu_\tau$ final state is added from the simulation. Also considered are the axial-vector $\eta(3\pi)^-\nu_\tau$ final states (Bergfeld *et al.*, 1997; Weinstein, 2001). CLEO observed that the dominant part of this mode issues from the $\tau^-\to f_1(1285)\pi^-\nu_\tau$ intermediate state, with $\mathcal{B}(\tau^-\to f_1\pi^-\nu_\tau)=(0.068\pm0.030)\%$, measured in the $f_1\to\eta\pi^+\pi^-$ and $f_1\to\eta2\pi^0$ decay modes (Bergfeld *et al.*, 1997; Weinstein, 2001). Since the f_1 meson is isoscalar, the branching fractions relate as $\mathcal{B}(\tau^-\to\eta\pi^-\pi^+\pi^-\nu_\tau)=2\mathcal{B}(\tau^-\to\eta\pi^-2\pi^0\nu_\tau)$. The distributions are taken from the ordinary six-pion phase-space simulation accompanied by large systematic errors. The $K\bar{K}\pi$ final states contribute mostly to the inclusive axial-vector spectral function, with errors that are fully anticorrelated with the inclusive vector spectral function. The invariant mass distributions for these channels are taken from the simulation.

2. Inclusive $V\pm A$ spectral functions

For the total v_1+a_1 hadronic spectral function it is not necessary to distinguish in experiment whether a given event belongs to one or the other current. The one-, two-, and three-pion final states dominate and their exclusive measurements are added with proper accounting for (anti)correlations. The remaining contributing topologies are treated inclusively, i.e., without separation of the vector and axial-vector decay modes. This reduces the statistical uncertainty. The effect of the feed-through between τ final states on the invariant mass spectrum is described by the Monte Carlo simulation and resolution effects are corrected by the data unfolding. In this procedure simulated mass distributions are iteratively corrected using the exclusive vector/axial-vector unfolded mass spectra. Also, one does not have to separate the vector/axial-vector currents of the $K\bar{K}\pi$ and $K\bar{K}\pi\pi$ modes. The v_1+a_1 spectral functions for ALEPH and OPAL are plotted in the upper plot of Fig. 5. The improvement in precision when comparing to a sum of the two parts in Fig. 4 is significant at higher mass-squared values.

One nicely identifies the oscillating behavior of the spectral function and it is interesting to observe that, unlike the vector/axial-vector spectral functions, it does approximately reach the asymptotic limit predicted by perturbative QCD at $s\to m_\tau^2$. Also, the $V+A$ spectral function, including the pion pole, exhibits the features expected from global quark-hadron duality: Despite oscillations due to the prominent π, $\rho(770)$, a_1, and $\rho(1450)$ resonances, the spectral function qualitatively averages out to the quark contribution from perturbative QCD.

In the case of the v_1-a_1 spectral function, uncertainties on the V/A separation are reinforced due to their anticorrelation. In addition, anticorrelations in the branching fractions between τ final states with adjacent numbers of pions increase the errors. The v_1-a_1 spectral functions for ALEPH and OPAL are shown in the lower plot of Fig. 5. The oscillating behavior of the respective v_1 and a_1 spectral functions is emphasized and the asymptotic regime is not reached at $s=m_\tau^2$. However again, the strong oscillation generated by the hadron

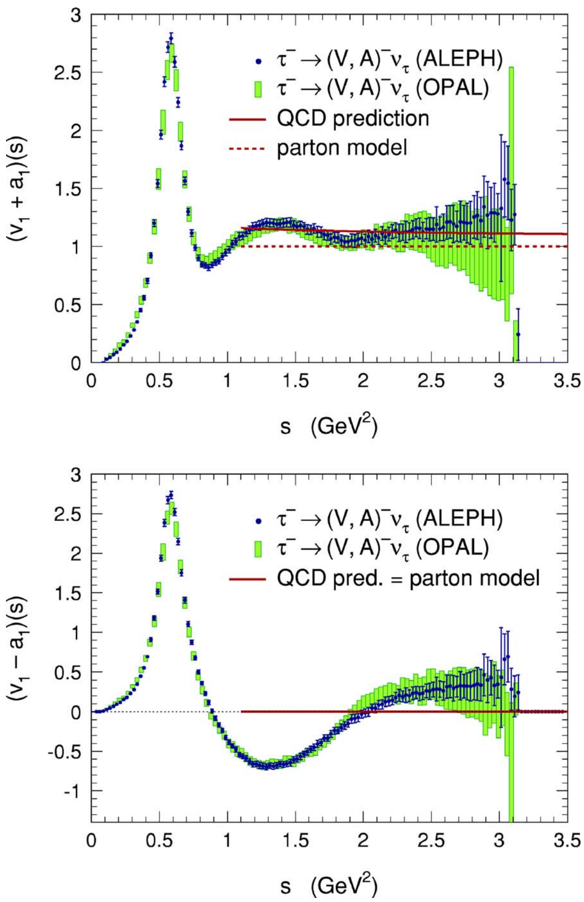

FIG. 5. (Color online) Inclusive vector plus axial-vector (upper) and vector minus axial-vector spectral function (lower) as measured by Schael *et al.* (2005) (dots with errors bars) and Ackerstaff *et al.* (1999a) (shaded 1 standard deviation errors). Lines show predictions from the parton model (dotted) and from massless perturbative QCD using $\alpha_s(M_Z^2)=0.120$ (solid). They cancel to all orders in the difference.

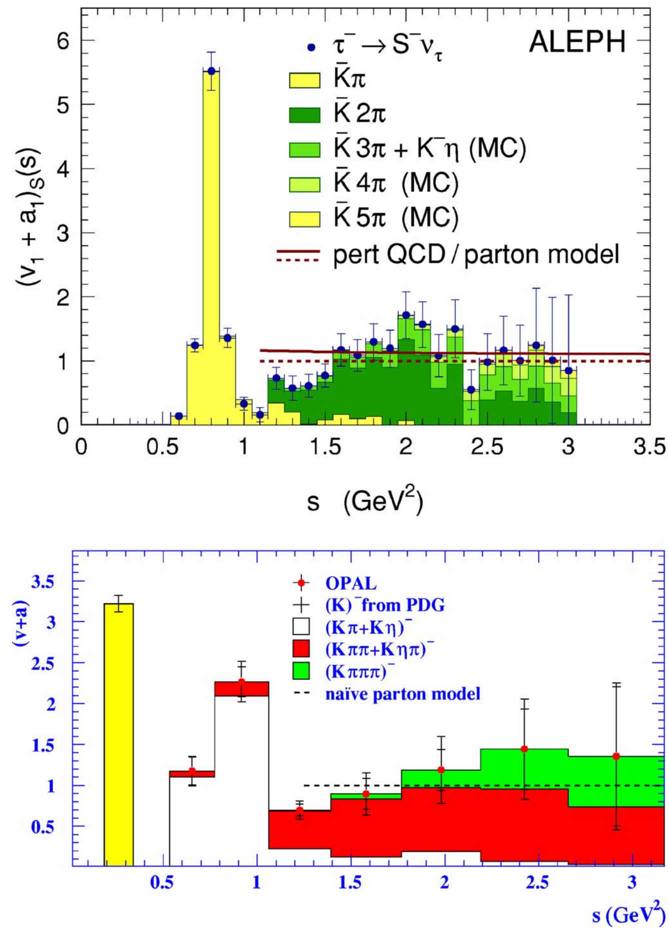

FIG. 6. (Color online) Inclusive hadronic vector plus axial-vector spectral function from τ decays into $S=\pm 1$ final states with its different contributions as indicated from Barate *et al.* (1999b) and Abbiendi *et al.* (2004). The kaon pole is not included in the ALEPH plot. The parton model prediction is given by the dashed line.

resonances mostly averages out to zero, as predicted by perturbative QCD.

D. Strange spectral functions

The total $|\Delta S|=1$ spectral functions from the ALEPH and OPAL analyses are shown in Fig. 6. For ALEPH, the spectra for the $\bar{K}\pi$ and $\bar{K}\pi\pi$ modes are obtained from the corrected mass spectra, taking into account acceptance and bin migration corrections. The spectrum for the $\bar{K}\pi$ mode is taken from the $K^-\pi^0$ and $K_S^0\pi^-$ final states because of their superior mass resolution as compared to the higher statistics $K_L^0\pi$ state where K_L^0 detection suffers from poor energy resolution. For the other modes a phase-space generator is used to simulate the mass distributions. The contributions from the respective channels are normalized to the corresponding branching fractions.

Since OPAL normalizes each channel using the corresponding world average branching fraction, which is dominated by the ALEPH measurement, the added information is on the shape, however limited by the relatively low statistics. As a consequence the OPAL and ALEPH spectral functions are correlated.

The $K^*(892)^-$ resonance stands out clearly on the low mass side, while within a large uncertainty [dominated by background subtraction in the $(\bar{K}\pi\pi)^-$ modes] the higher-energy part is consistent with the parton model (or perturbative QCD) expectation.

V. COMPARING TAU SPECTRAL FUNCTIONS WITH ELECTRON-POSITRON ANNIHILATION DATA VIA THE CONSERVED VECTOR CURRENT

The vacuum-polarization functions (38) for various types of quark currents ij carry dynamical information for the theoretical evaluation of total cross sections and decay widths. In the limit of isospin invariance the vector current is conserved (CVC) so that the spectral function of a vector τ decay mode $X^-\nu_\tau$ in a given isospin state for the hadronic system is related to the e^+e^- annihilation cross section of the corresponding isovector final state X^0,

$$\sigma^{I=1}_{e^+e^-\to X^0}(s) = \frac{4\pi\alpha^2}{s} v_{1,X^-}(s), \tag{41}$$

where α is the electromagnetic fine-structure constant.

A. Isospin breaking and radiative corrections

Since the breaking of isospin symmetry is expected at some level, in particular from electromagnetic effects, it is useful to carefully write down all factors involved in the comparison of τ and e^+e^- spectral functions in order to make explicit the possible sources causing the breakdown of CVC. For the dominant $\pi\pi$ spectral functions, we have on the e^+e^- side

$$\sigma(e^+e^- \to \pi^+\pi^-) = \frac{4\pi\alpha^2}{s} v_0(s), \tag{42}$$

where the spectral function $v_0(s)$ is related to the pion form factor $F^0_\pi(s)$ by

$$v_0(s) = \frac{\beta_0^3(s)}{12} |F^0_\pi(s)|^2, \tag{43}$$

and where $\beta_0^3(s)$ is the threshold kinematic factor. Similarly, on the τ side the relation between the spectral function (34) and the charged pion form factor reads

$$v_-(s) = \frac{\beta_-^3(s)}{12} |F^-_\pi(s)|^2. \tag{44}$$

Isospin symmetry implies $v_-(s) = v_0(s)$. The threshold functions $\beta_{0,-}$ are defined by

$$\beta_{0,-} = \beta(s, m_{\pi^-}, m_{\pi^{+,0}}), \tag{45}$$

where

$$\beta(s, m_1, m_2) = \left[\left(1 - \frac{(m_1+m_2)^2}{s}\right) \times \left(1 - \frac{(m_1-m_2)^2}{s}\right)\right]^{1/2}. \tag{46}$$

Experiments measure τ decays inclusively with respect to radiative photons, i.e., for $\tau^- \to \nu_\tau \pi^-\pi^0(\gamma)$. The measured spectral function is hence $v_-^*(s) = v_-(s)G(s)$, where $G(s)$ is a radiative correction.

Several levels of SU(2) breaking can be identified:

- *Electroweak radiative corrections to τ decays* are contained in the $S_{\rm EW}$ factor (Marciano and Sirlin, 1988; Braaten and Li, 1990), which is dominated by short-distance effects. It is expected to be weakly dependent on the specific hadronic final state, as verified for the $\tau^- \to (\pi^-, K^-)\nu_\tau$ decays (Decker and Finkemeier, 1993). Detailed calculations have been performed for the $\pi^-\pi^0$ channel (Cirigliano *et al.*, 2001, 2002), which also confirm the relative smallness of long-distance contributions. The total correction is $S_{\rm EW} = S^{\rm had}_{\rm EW} S^{\rm had}_{\rm EM} / S^{\rm lep}_{\rm EM}$, where $S^{\rm had}_{\rm EW}$ is the leading-log short-distance electroweak factor (which vanishes for leptons) and $S^{\rm had,lep}_{\rm EM}$ are nonleading electromagnetic corrections. The latter corrections have been calculated at the quark level (Braaten and Li, 1990), at the hadron level for the $\pi^-\pi^0$ decay mode (Cirigliano *et al.*, 2001), and for leptons (Marciano and Sirlin, 1988; Braaten and Li, 1990). The total correction amounts to (Davier *et al.*, 2003a) $S^{\rm incl}_{\rm EW} = 1.0198 \pm 0.0006$ for the inclusive hadron decay rate and $S^{\pi\pi^0}_{\rm EW} = (1.0232 \pm 0.0006) \times G^{\pi\pi^0}_{\rm EM}(s)$ for the $\pi\pi^0$ decay mode, where $G^{\pi\pi^0}_{\rm EM}(s)$ is an s-dependent long-distance radiative correction (Cirigliano *et al.*, 2001).
- *The pion mass splitting* breaks isospin symmetry in the spectral functions (Alemany *et al.*, 1998; Czyż and Kühn, 2001) since $\beta_-(s) \neq \beta_0(s)$.
- Isospin symmetry is also broken in *the pion form factor* due to the π mass splitting (Alemany *et al.*, 1998; Cirigliano *et al.*, 2001).
- A similar effect is expected from ρ *mass splitting*. The theoretical expectation (Bijnens and Gosdzin-

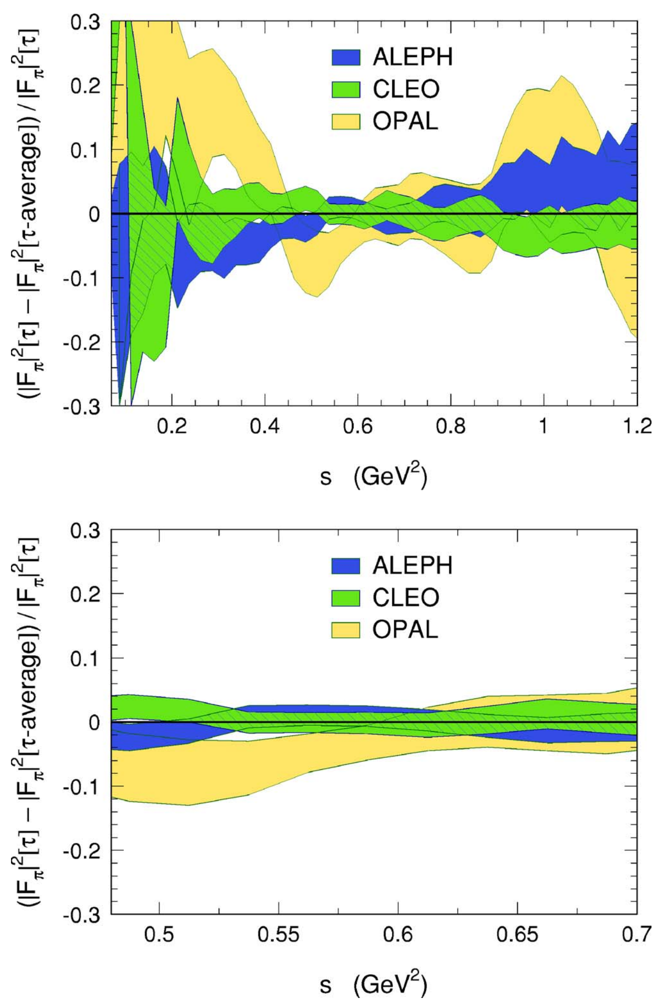

FIG. 7. (Color online) Upper: Relative comparison of the $\pi^+\pi^-$ spectral functions extracted from τ data for the different experiments, expressed as a ratio to the average τ spectral function. Lower: The ρ region. For CLEO only statistical errors are shown.

sky, 1996) gives a limit <0.7 MeV, but this is only a rough estimate. Hence the question must be investigated experimentally, the best approach being the explicit comparison of τ and e^+e^- 2π spectral functions after correction for other isospin-breaking effects. No correction for ρ mass splitting is applied initially.

- Explicit *electromagnetic decays* such as $\pi\gamma$, $\eta\gamma$, $\ell^+\ell^-$, and $\pi\pi\gamma$ introduce small differences between the widths of the charged and neutral ρ's.
- Isospin violation in the strong amplitude through the *mass difference between u and d quarks* is expected to be negligible.
- When comparing τ with e^+e^- data, an obvious and locally large correction must be applied to the τ spectral function to introduce the effect of ρ-ω *mixing*, only present in the neutral channel. This correction is computed using the parameters determined from e^+e^- experiments in their form factor fits to the $\pi^+\pi^-$ line-shape modeling ρ-ω interference (Akhmetshin *et al.*, 2004).

B. Tau spectral functions and e^+e^- data

Data from τ decays into two- and four-pion final states $\tau^-\to\nu_\tau\pi^-\pi^0$, $\tau^-\to\nu_\tau\pi^-3\pi^0$, and $\tau^-\to\nu_\tau 2\pi^-\pi^+\pi^0$ are available from ALEPH (Schael *et al.*, 2005), CLEO (Anderson *et al.*, 2000; Edwards *et al.*, 2000), and OPAL (Ackerstaff *et al.*, 1999a). For the two-pion final states, they are compared in Fig. 7 in the region around the ρ resonance. For this comparison, each data set is normalized to the world average branching fraction and plotted with respect to their weighted average. The two most precise results from ALEPH and CLEO are in agreement. The statistics are comparable in the two cases, however, due to a flat acceptance in ALEPH and a strongly increasing one (with the mass squared) in CLEO, the ALEPH data are more precise below the ρ peak while CLEO has the better precision above. In the following we will use the $\tau^-\to\pi^-\pi^0\nu_\tau$ spectral function averaged over the three experiments.

Exclusive low-energy e^+e^- cross sections have been mainly measured by experiments running at e^+e^- colliders in Novosibirsk and Orsay. The most precise $e^+e^-\to\pi^+\pi^-$ measurements come from CMD-2, which are now available in their final form (Akhmetshin *et al.*, 2004), after a significant revision where problems related to radiative corrections have been removed. The overall systematic error of the final data is quoted to be 0.6% and is dominated by uncertainties in the radiative corrections (0.4%).

Recently, new data on the $\pi^+\pi^-$ spectral function in the mass region between 0.60 and 0.97 GeV were presented by the KLOE Collaboration (Aloisio *et al.*, 2005), using—for the purpose of precision measurements—the innovative technique of the radiative return (Binner *et*

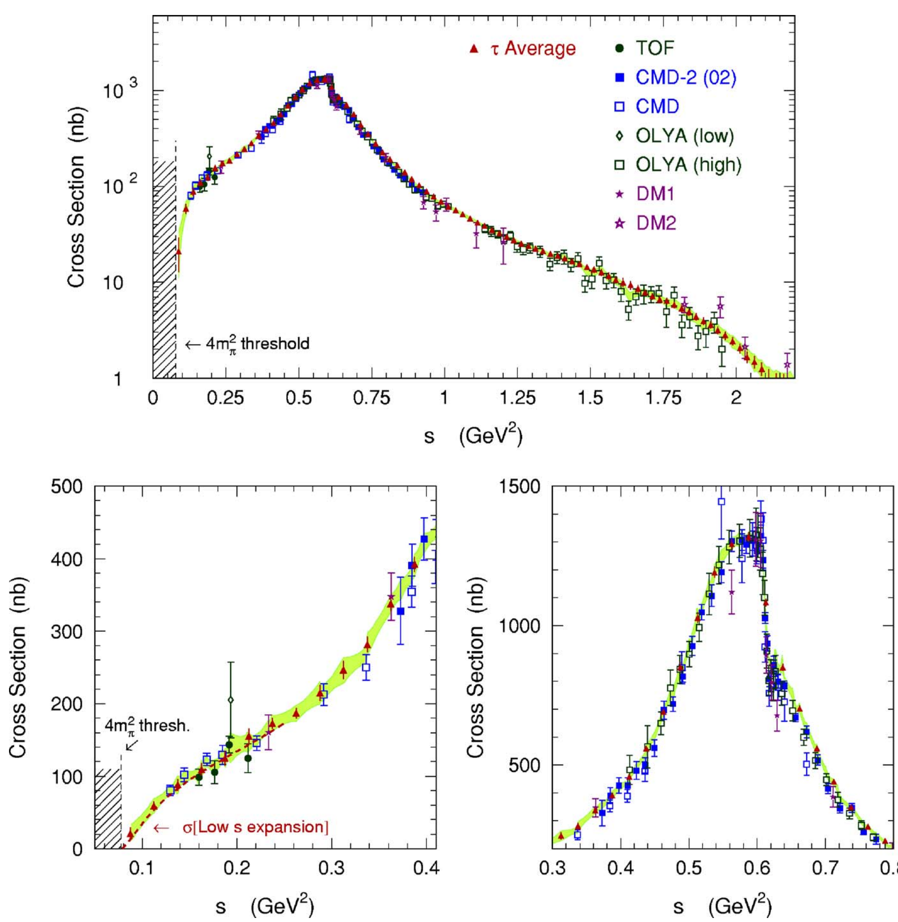

FIG. 8. (Color online) Comparison of $\pi^+\pi^-$ spectral functions from isospin-breaking corrected τ data (world average) expressed as e^+e^- cross sections and e^+e^- annihilation. The band indicates the combined τ and e^+e^- result within 1σ errors. It is given for illustration purpose only. A compendium of references for the e^+e^- data has been given by Davier *et al.* (2003a, 2003b).

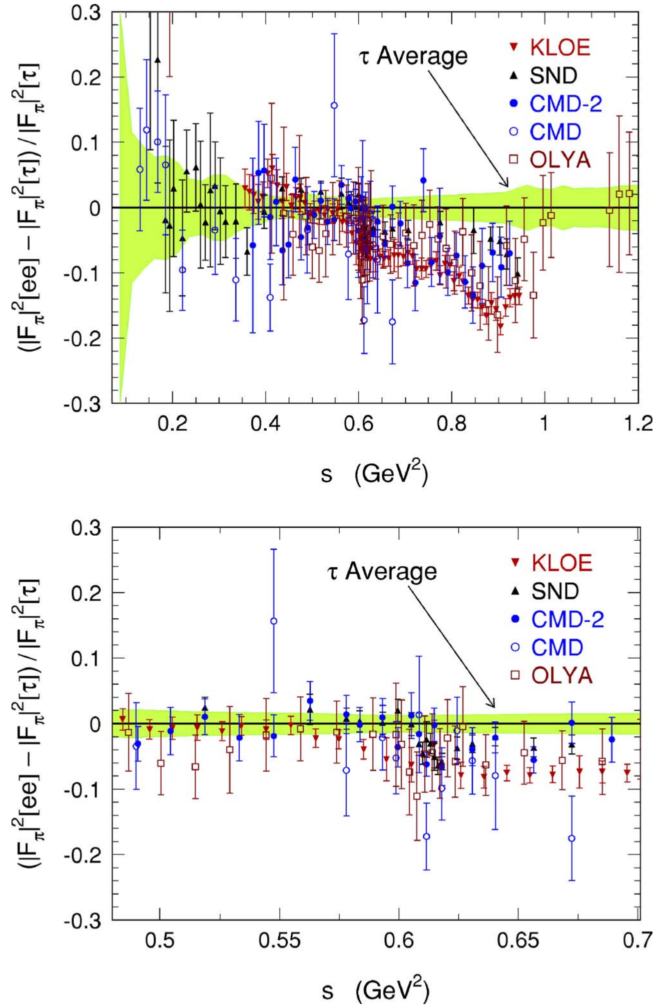

FIG. 9. (Color online) Relative comparison of the isospin-breaking corrected τ data (world average) and $\pi^+\pi^-$ spectral functions from e^+e^- annihilation, expressed as a ratio to the τ spectral function. The shaded band gives the uncertainty on the τ spectral function. The lower plot zooms into the $\rho(770)$ peak region where the data density is high. The ρ-ω mixing has been phenomenologically corrected using a fit to the CMD-2 data. The larger mixing observed in the SND data, expressed as a 40% increase in the value for the $\omega \to \pi^+\pi^-$ branching fraction (Achasov *et al.*, 2005), is responsible for the residual effect after correction seen in the lower plot.

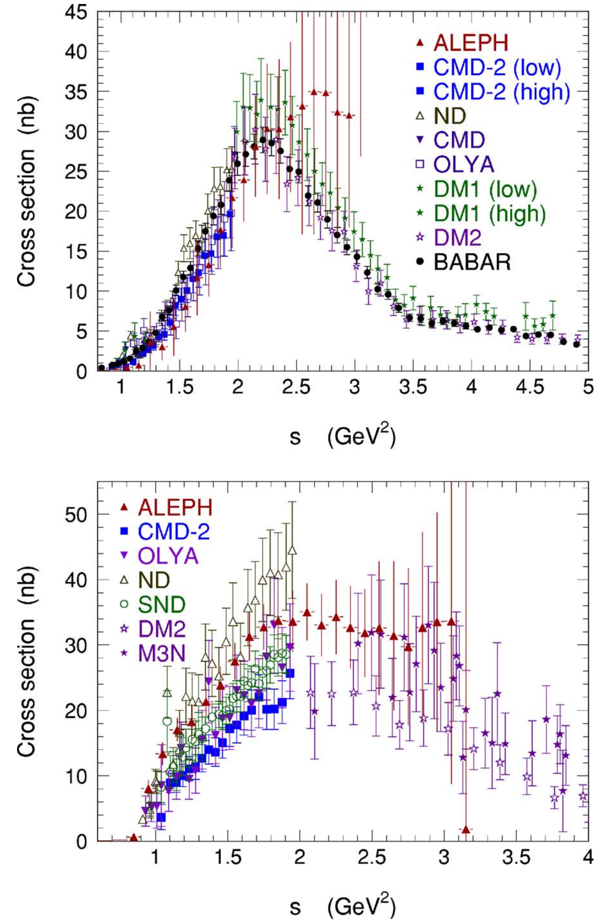

FIG. 10. (Color online) Comparison of the $2\pi^+2\pi^-$ (upper) and $\pi^+\pi^-2\pi^0$ (lower) spectral functions from e^+e^- and isospin-breaking corrected τ data (ALEPH), expressed as e^+e^- cross sections. References for the e^+e^- data have been given by Davier *et al.* (2003a, 2003b). The *BABAR* results are taken from Aubert *et al.* (2005a).

al., 1999; Czyż *et al.*, 2002). The statistical precision of these data by far outperforms the Novosibirsk sample, but systematic errors are about twice as large as those assigned by CMD-2.

C. Comparing τ with e^+e^- data

1. 2π spectral function

2π spectral functions extracted from τ decays and e^+e^- annihilation data are compared in Fig. 8. The e^+e^- data are taken from Quenzer *et al.* (1978); Vasserman *et al.* (1979, 1981); Barkov *et al.* (1985); Bisello *et al.* (1989); Akhmetshin *et al.* (2004). All error bars shown contain statistical and systematic errors. Visually, the agreement appears to be satisfactory, however, the large dynamical range involved does not permit an accurate test. To do so, the e^+e^- data are plotted as a point-by-point ratio to the τ spectral function in Fig. 9. In these latter plots we also show more recent e^+e^--annihilation results from the SND Collaboration (Achasov *et al.*, 2005)[5] and from the radiative return analysis performed by the KLOE Collaboration (Aloisio, 2005). Several observations can be made.

- A significant discrepancy mainly above the ρ peak is found between τ and the e^+e^- data from CMD-2 as well as older data from OLYA.
- Overall, the KLOE data seem to confirm the trend exhibited by the other (older) e^+e^- data.
- Some disagreement between KLOE and CMD-2 oc-

[5]The SND results have just been updated by correcting mistakes in the treatment of radiative corrections (Achasov *et al.*, 2006). After correction they are in better agreement with CMD-2.

TABLE III. Branching fractions of τ vector decays into two and four pions in the final state (Schael *et al.*, 2005). Second column: τ decay measurements. Third column: Results inferred from e^+e^- spectral functions using the isospin relations (41), (44), and (47) and correcting for isospin breaking (Davier *et al.*, 2003a, 2003b). The two-pion prediction does not include recent KLOE and SND data. Experimental errors, including uncertainties on the integration procedure, and theoretical errors (missing radiative corrections for e^+e^-, and isospin-breaking corrections and $|V_{ud}|$ for τ) are shown separately. Last column: Differences between direct measurements in τ decays and CVC evaluations, where various errors have been added in quadrature.

Mode	Branching fractions (%)		
	τ	e^+e^- via CVC	$\Delta(\tau - e^+e^-)$
$\tau^- \to \nu_\tau \pi^- \pi^0$	25.47 ± 0.13	$24.52 \pm \underbrace{0.26_{\rm exp} \pm 0.11_{\rm rad} \pm 0.12_{\rm SU(2)}}_{0.31}$	$+0.95 \pm 0.33$
$\tau^- \to \nu_\tau \pi^- 3\pi^0$	0.98 ± 0.09	$1.09 \pm \underbrace{0.06_{\rm exp} \pm 0.02_{\rm rad} \pm 0.05_{\rm SU(2)}}_{0.08}$	-0.11 ± 0.12
$\tau^- \to \nu_\tau 2\pi^- \pi^+ \pi^0$	4.59 ± 0.09	$3.63 \pm \underbrace{0.19_{\rm exp} \pm 0.04_{\rm rad} \pm 0.09_{\rm SU(2)}}_{0.21}$	$+0.96 \pm 0.23$

curs on the low mass side (KLOE data are large), on the ρ peak (KLOE below CMD-2), as well as on the high mass side (KLOE data are low).

- A significant discrepancy between the (most recent) SND data and KLOE is observed in the energy domain above the $\rho(770)$ peak. The SND data largely dissolve the discrepancy observed with the τ data.

At this stage, the τ spectral function has not been corrected for a possible $\rho^- - \rho^0$ mass and width splitting (Davier, 2003; Ghozzi and Jegerlehner, 2004; Schael *et al.*, 2005). In contrast to earlier experimental (Barate *et al.*, 1997b) and theoretical results (Bijnens and Gosdzinsky, 1996), a combined pion form factor fit to the new precise data on τ spectral functions and e^+e^- leads to $m_{\rho^-} - m_{\rho^0} = 2.4 \pm 0.8$ MeV (Sec. V.D.2), while no significant width splitting is observed within the fit error of 1.0 MeV.

Considering the mass splitting in the isospin-breaking correction of the τ spectral function tends to locally improve though not restore the agreement between τ and CMD-2 data, leaving an overall normalization discrepancy. Increasing the $\Gamma_{\rho^-} - \Gamma_{\rho^0}$ width splitting by +3 MeV improves the agreement between τ and KLOE data in the peak region, while it cannot correct the discrepancies in the tails. Note that a correction of the mass splitting alone would *increase* the discrepancy between the τ- and e^+e^--based results for $a_\mu^{\rm had,LO}$ (Sec. VI.F).

In light of the new SND data (Achasov *et al.*, 2005), it seems appropriate to consider the possibility of a bias in the KLOE results, and one may also question the small systematic uncertainties claimed by CMD-2. We also point out that application of the τ long-distance correction $G_{\rm EM}^{\pi\pi^0}(s)$ (Cirigliano *et al.*, 2001) worsens the agreement with the SND data in the energy domain above the $\rho(770)$ peak.

2. 4π spectral functions

The spectral function measurements of the τ vector-current final states $\pi^- 3\pi^0$ and $\pi^-\pi^-\pi^+\pi^0$ are compared to the cross sections of the corresponding e^+e^- annihilation into the isovector states $2\pi^- 2\pi^+$ and $\pi^-\pi^+ 2\pi^0$. Using Eq. (35) and isospin invariance, the following relations hold:

$$\sigma^{I=1}_{e^+e^- \to \pi^+\pi^-\pi^+\pi^-} = 2\frac{4\pi\alpha^2}{s} v_{1,\pi^- 3\pi^0 \nu_\tau}, \qquad (47)$$

$$\sigma^{I=1}_{e^+e^- \to \pi^+\pi^-\pi^0\pi^0} = \frac{4\pi\alpha^2}{s}[v_{1,2\pi^-\pi^+\pi^0\nu_\tau} - v_{1,\pi^- 3\pi^0\nu_\tau}]. \qquad (48)$$

The comparison of these cross sections is given in Fig. 10 for $2\pi^+ 2\pi^-$ (upper plot) and $\pi^+\pi^- 2\pi^0$ (lower plot). The latter mode suffers from discrepancies between results from various e^+e^- experiments. The τ data, combining two measured spectral functions according to Eq. (48), and (coarsely) corrected for isospin breaking originating from the pion mass splitting (Czyż and Kühn, 2001), lie somewhat in between, with large uncertainties above 1.4 GeV because of the lack of statistics and a large feed-through background in the mode with three neutral pions. In spite of these difficulties the $\pi^- 3\pi^0$ spectral function is in agreement with e^+e^- data as can be seen in Fig. 10. Due to inconsistencies among e^+e^- experiments a quantitative test of CVC in the $\pi^+\pi^- 2\pi^0$ channel is premature.

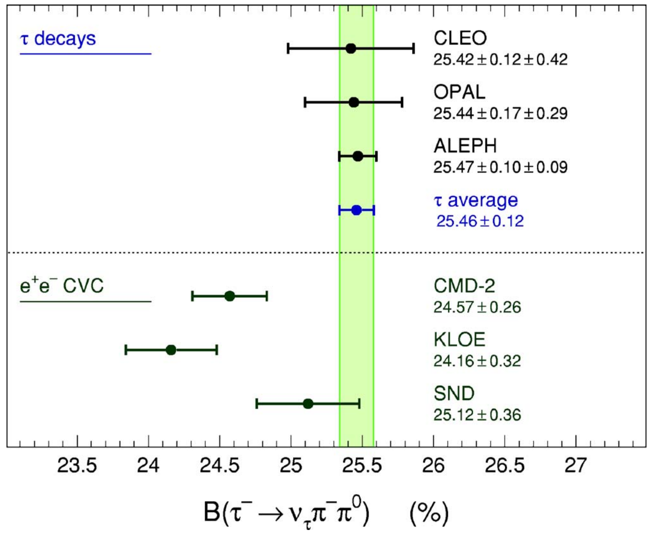

FIG. 11. (Color online) Measured branching fractions for $\tau^- \to \pi^-\pi^0\nu_\tau$ (Artuso *et al.*, 1994; Ackerstaff *et al.*, 1998; Schael *et al.*, 2005) compared to the predictions from $e^+e^- \to \pi^+\pi^-$ spectral functions, applying the isospin-breaking correction factors discussed in Sec. V.A. For e^+e^- results we have used only data from indicated experiments where they are available (0.61–0.96 GeV for CMD-2, 0.60–0.97 GeV for KLOE, and 0.39–0.97 GeV for SND), and all data combined in the remaining energy domains below m_τ. Since the compatibility between e^+e^- data is marginal (cf. Fig. 9), we have refrained from taking their average.

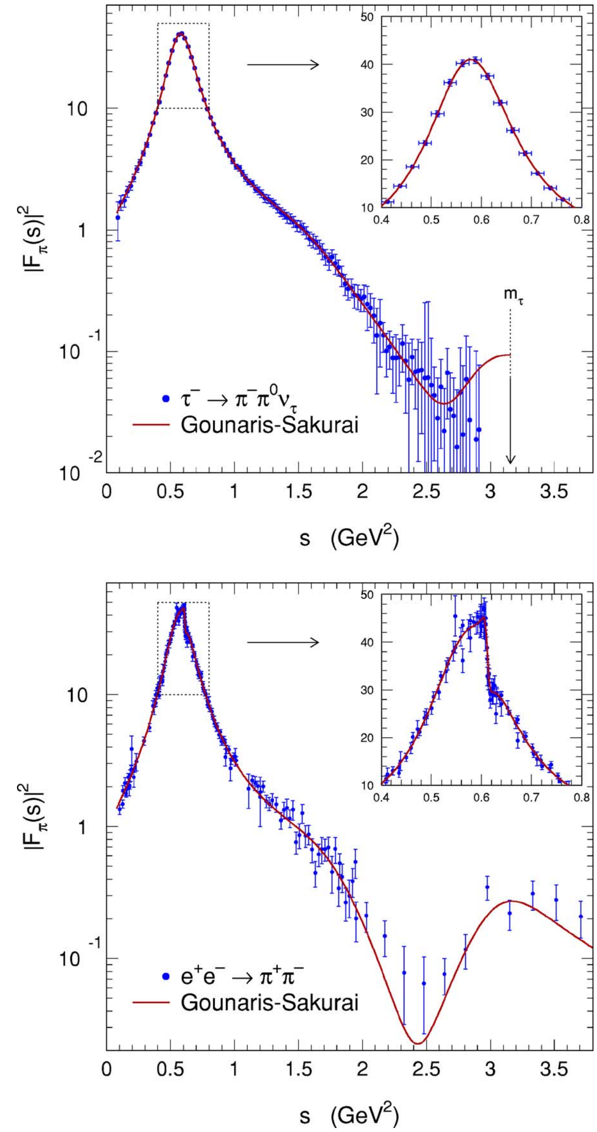

FIG. 12. (Color online) Phenomenological fit to the ALEPH $\pi^+\pi^0$ spectral function (upper) and to e^+e^- annihilation data (lower) using the Gounaris-Sakurai parametrization. From Schael *et al.*, 2005.

3. Branching fractions in τ decays and CVC

It is instructive to compare the τ and e^+e^- spectral functions in a more quantitative way by calculating weighted integrals over the mass range of interest up to the τ mass. One convenient choice is provided by τ branching fractions, which for the spin-1 part involve as a weight the kinematic factor $(1-s/m_\tau^2)^2(1+2s/m_\tau^2)$ coming from the $V-A$ charged current in τ decay. It is then possible to directly compare measured τ branching fractions to their prediction through isospin invariance (CVC), with the e^+e^- isovector spectral functions as input.

Using the universality-improved branching fraction (13), one finds the results given for the dominant channels in Table III. The errors quoted for the CVC values are split into uncertainties from (i) the experimental input (the e^+e^- annihilation cross sections) and the numerical integration procedure, (ii) additional radiative corrections applied to some of the e^+e^- data (Davier *et al.*, 2003a), and (iii) the isospin-breaking corrections when relating τ and e^+e^- spectral functions.

As expected from the preceding discussion, a discrepancy is observed for the $\tau^- \to \pi^-\pi^0\nu_\tau$ branching fraction, with a difference of $(0.95 \pm 0.13_\tau \pm 0.26_{\mathrm{ee}} \pm 0.11_{\mathrm{rad}} \pm 0.12_{\mathrm{SU(2)}})\%$, where uncertainties are from the τ branching fraction, e^+e^- cross section e^+e^- missing radiative corrections, and isospin-breaking corrections (also including the uncertainty on $|V_{ud}|$), respectively. Adding all errors in quadrature gives a 2.9σ effect. Including new SND measurements (Achasov *et al.*, 2005) into the $\pi^+\pi^-$ data sample would decrease this discrepancy to approximately 2.5σ. The improvement would have been stronger if we had discarded older data sets. In effect, using only SND data in the region where these are available (0.39–0.97 GeV), and all other data elsewhere, one finds for the predicted branching fraction: $\mathcal{B}_{\mathrm{CVC}}(\tau^- \to \nu_\tau\pi^-\pi^0) = (25.12 \pm 0.36)\%$, which is in agreement with the τ result.[6] More informa-tion on this comparison is displayed in Fig. 11, where we also give results for using only CMD-2 and only KLOE data, respectively, in the available energy regions (and the aver-

[6]However, we point out that the scarce SND data points in the tails of the $\rho(770)$ resonance, where the line shape is concave, may lead to an overestimate of the integral computed by the trapezoidal rule as done here.

age of all other data elsewhere). The discrepancy between the e^+e^--based prediction using the KLOE data and the τ result is at the 3.8σ level.

The situation in 4π channels is different. While there is agreement for the $\pi^- 3\pi^0$ mode within a relative accuracy of 12%, comparison is not satisfactory for $2\pi^-\pi^+\pi^0$. In the latter case, the relative difference is very large, $(23\pm6)\%$, compared to a reasonable level of isospin symmetry breaking. As such, these discrepancies point to experimental problems that require further investigation. These are emphasized by the scatter observed among the different e^+e^- results.

D. Fits to the $\pi\pi$ spectral function

Phenomenological fits to the pion form factor have been performed by the ALEPH and CLEO Collaborations (Barate *et al.*, 1997b; Anderson *et al.*, 2000; Schael *et al.*, 2005) (see Fig. 12). Appropriate parametrizations, e.g., the one proposed by Kühn and Santamaria (1990), employ relativistic P-wave Breit-Wigner propagators, and coherent summation of resonance amplitudes using the isobar model. The $\pi\pi$ spectral function is dominated by the broad ρ resonance, parametrized by both collaborations following Gounaris and Sakurai (1968). The Gounaris-Sakurai parametrization takes into account analyticity and unitarity properties. We will in the following discuss the fits performed by Schael *et al.* (2005).

Assuming vector dominance, the pion form factor is given by interfering amplitudes from the known isovector meson resonances $\rho(770)$, $\rho(1450)$, and $\rho(1700)$ with relative strengths 1, β, and γ. Although one could expect from the quark model that β and γ are real and, respectively, negative and positive, the phase ϕ_β of β is left free in the fits, and only the much smaller γ is assumed to be real for lack of precise experimental information at large masses. Taking into account ρ-ω mixing, one writes for the $\pi^+\pi^-$ form factor in e^+e^- annihilation

$$F_\pi^{I=1,0}(s) = \frac{\mathrm{BW}_{\rho(770)}(s)[1+\delta \mathrm{BW}_{\omega(783)}(s)]/(1+\delta) + \beta \mathrm{BW}_{\rho(1450)}(s) + \gamma \mathrm{BW}_{\rho(1700)}(s)}{1+\beta+\gamma}, \tag{49}$$

with the Breit-Wigner propagators

$$\mathrm{BW}^{\mathrm{GS}}_{\rho(m_\rho)}(s) = \frac{m_\rho^2(1+d\Gamma_\rho/m_\rho)}{m_\rho^2 - s + f(s) - i\sqrt{s}\Gamma_\rho(s)}, \tag{50}$$

where

$$f(s) = \Gamma_\rho \frac{m_\rho^2}{k^3(m_\rho^2)}\Bigg[k^2(s)[h(s)-h(m_\rho^2)] + (m_\rho^2 - s)k^2(m_\rho^2)\left.\frac{dh}{ds}\right|_{s=m_\rho^2}\Bigg] \tag{51}$$

and $\Gamma_\rho = \Gamma_\rho(m_\rho^2)$. The P-wave energy-dependent width is given by

$$\Gamma_\rho(s) = \Gamma_\rho \frac{m_\rho}{\sqrt{s}}\left(\frac{k(s)}{k(m_\rho^2)}\right)^3, \tag{52}$$

where $k(s) = \frac{1}{2}\sqrt{s}\beta_\pi^-(s)$ and $k(m_\rho^2)$ are pion momenta in the ρ rest frame. The function $h(s)$ is defined as

$$h(s) = \frac{2}{\pi}\frac{k(s)}{\sqrt{s}} \ln \frac{\sqrt{s}+2k(s)}{2m_\pi}, \tag{53}$$

with $dh/ds|_{m_\rho^2} = h(m_\rho^2)\{[8k^2(m_\rho^2)]^{-1} - (2m_\rho^2)^{-1}\} + (2\pi m_\rho^2)^{-1}$. Since interference with the isospin-violating electromagnetic $\omega \to \pi^+\pi^-$ decay occurs only in e^+e^- annihilation, δ is fixed to zero when fitting τ data. The normalization $\mathrm{BW}^{\mathrm{GS}}_{\rho(m_\rho)}(0)=1$ fixes the parameter $d = f(0)/\Gamma_\rho m_\rho$, which is found to be (Gounaris and Sakurai, 1968)

$$d = \frac{3}{\pi}\frac{m_\pi^2}{k^2(m_\rho^2)} \ln\left(\frac{m_\rho + 2k(m_\rho^2)}{2m_\pi}\right) + \frac{m_\rho}{2\pi k(m_\rho^2)} - \frac{m_\pi^2 m_\rho}{\pi k^3(m_\rho^2)}. \tag{54}$$

1. Fit to τ data

The fit of the Gounaris-Sakurai model to the isovector τ data establishes the need for the $\rho(1450)$ contribution to the weak pion form factor (Barate *et al.*, 1997b; Schael *et al.*, 2005). Only weak evidence is found for a $\rho(1700)$ contribution lying close to the τ end point. Most of the fit parameters exhibit large correlations, which have to be taken into account when interpreting the results. The ρ mass uncertainty is found to be dominated by systematic effects, the largest being knowledge of the π^0 energy scale (calibration).

2. Combined fit to τ and e^+e^- data

The ALEPH Collaboration has performed a combined fit using τ (ALEPH and CLEO) and e^+e^- data (not yet including KLOE and SND) in order to better constrain the lesser known parameters in the phenomenological form factor (Barate *et al.*, 1997b; Schael *et al.*, 2005). For this study, the τ spectral function is duly corrected for the isospin-breaking effects identified in Sec. V.A. Also photon vacuum-polarization contributions are removed in the e^+e^- spectral function since they are absent in the τ data. In this way, the mass and width of the dominant $\rho(770)$ resonance in the two isospin states can be determined. For the subleading amplitudes from higher vector mesons, isospin symmetry is assumed so that common masses and widths can be used in the fit.

The result of the combined fit is given in Table IV. The differences between the masses and widths of the charged and neutral $\rho(770)$'s are found to be (Schael *et al.*, 2005)

$$m_{\rho^-} - m_{\rho^0} = 2.4 \pm 0.8 \text{ MeV}, \tag{55}$$

$$\Gamma_{\rho^-} - \Gamma_{\rho^0} = 0.2 \pm 1.0 \text{ MeV}. \tag{56}$$

The mass splitting is somewhat larger than the theoretical prediction (<0.7 MeV) (Bijnens and Gosdzinsky, 1996), but only at the 2σ level. The expected width splitting, known from isospin breaking, but not taking into account any ρ mass splitting, is 0.7 ± 0.3 MeV (Cirigliano *et al.*, 2001; Davier *et al.*, 2003a). However, if the mass difference is taken as an experimental fact, a larger width difference would be expected. From the chiral model of the ρ resonance (Guerrero and Pich, 1997; Gómez Dumm *et al.*, 2000; Cirigliano *et al.*, 2001), one expects a total width difference of 2.1 ± 0.5 MeV, which is only marginally consistent with the observed value.

As seen in previous applications, the situation should improve with the inclusion of the new SND data (Achasov *et al.*, 2005). Also the observed ρ mass difference (55) is expected to decrease in this case.

VI. TAU DECAYS AND HADRONIC VACUUM POLARIZATION

Hadronic vacuum polarization in the photon propagator plays an important role in precision tests of the SM. This is the case for the evaluation of the electromagnetic coupling at the Z mass scale, $\alpha(M_Z^2)$, which receives a contribution $\Delta\alpha_{\rm had}(M_Z^2)$ of the order of 2.8×10^{-2}. This correction must be known to a relative accuracy of better than 1% so that it does not limit the accuracy on the indirect determination of the Higgs-boson mass from measurement of $\sin^2\theta_W$. Another example is provided by the anomalous magnetic moment $a_\mu = (g_\mu - 2)/2$ of the muon, where the lowest-order hadronic vacuum-polarization component $a_\mu^{\rm had,LO}$ is the leading contributor to the uncertainty of the theoretical prediction.

Starting with the results of Cabibbo and Gatto (1960, 1961) and Bouchiat and Michel (1961) there is a long history of calculating contributions from hadronic vacuum polarization in these processes. As they cannot be obtained from first principles because of the low-energy scale involved, the computation relies on analyticity and unitarity so that the relevant integrals can be expressed in terms of an experimentally determined spectral function, which is proportional to the cross section for e^+e^- annihilation into hadrons. The accuracy of the calculations has therefore followed the progress in the quality of the corresponding data (Eidelman and Jegerlehner, 1995). Because the data were not always suitable, it was deemed necessary to resort to other sources of information. One such possibility was the use of vector spectral functions derived from the study of hadronic τ decays for an energy range less than m_τ (Alemany *et al.*, 1998). Also, it was demonstrated that essentially perturbative QCD could be applied to energy scales as low as 1–2 GeV (Barate *et al.*, 1998c; Ackerstaff *et al.*, 1999a), thus offering a way to replace poor e^+e^- data in some energy regions by a reliable and precise theoretical prescription (Martin and Zeppenfeld, 1995; Davier and Höcker, 1998a, 1998b; Groote *et al.*, 1998; Kühn and Steinhauser, 1998; Erler, 1999). Finally, without any further theoretical assumption, it was proposed to use QCD sum rules (Davier and Höcker, 1998b; Groote *et al.*, 1998) in order to improve the evaluation in energy regions dominated by resonances where one has to rely only on experimental data. The complete theoretical prediction includes in addition quantum electrodynamics (QED), weak and higher-order hadronic contributions.

Since in this review of hadronic τ decays we are mostly dealing with the low-energy region,[7] common to both τ and e^+e^- data, and because of the current interest in the muon magnetic moment prompted by recent experimental results (see below), the emphasis will be on $a_\mu^{\rm had,LO}$ rather than $\Delta\alpha_{\rm had}(M_Z^2)$. We note that the presently achieved accuracy on $\Delta\alpha_{\rm had}(M_Z^2)$ is meeting the goals for the LEP/SLC/FNAL global electroweak fit. However, the situation will change in the long run when precise determinations of $\sin^2\theta_W$, as could be available from the beam polarization asymmetry at the International Linear Collider, require a significant increase in the accuracy of $\Delta\alpha_{\rm had}(M_Z^2)$ (Abe *et al.*, 2001).

A. Muon magnetic anomaly

One of the great successes of the Dirac (1928) equation was its prediction that the magnetic dipole moment $\vec{\mu}$ of a spin $|\vec{s}| = 1/2$ particle such as the electron (or muon) is given by

$$\vec{\mu}_\ell = g_\ell \frac{e}{2m_\ell}\vec{s}, \quad \ell = e, \mu, \ldots \tag{57}$$

with gyromagnetic ratio $g_\ell = 2$, a value already implied by early atomic spectroscopy. Later it was realized that a relativistic quantum field theory such as QED can give rise via quantum fluctuations to a shift in g_ℓ,

$$a_\ell \equiv \frac{g_\ell - 2}{2}, \tag{58}$$

called the magnetic anomaly. In a now classic QED calculation, Schwinger (1948) found the leading (one-loop)

[7] It is the property of the dispersion relation describing the hadronic contribution to $(g-2)_\mu$ that the $\pi\pi$ spectral function provides the major part of the total hadronic vacuum-polarization contribution. Hence the experimental effort focuses on this channel.

TABLE IV. Combined fit to the pion form factor squared from ALEPH, CLEO, τ, and all e^+e^- data, where vacuum polarization and known sources of isospin violation have been excluded from the latter data. Parametrization of the $\rho(770)$, $\rho(1450)$, and $\rho(1700)$ line shapes follows the Gounaris-Sakurai formula. Separate masses and widths are fit for the $\rho(770)$, while common values are kept for higher vector mesons. All mass and width values are in units of MeV and phases are in degrees. The value of the χ^2 estimator per degree of freedom (DF) is also quoted.

Simultaneous fit to τ and e^+e^- spectral functions (χ^2/DF=383/326)					
$m_{\rho^-(770)}$	775.5 ± 0.6	$\Gamma_{\rho^-(770)}$	148.2 ± 0.8	δ	$(2.03\pm0.10)\times10^{-3}$
$m_{\rho^0(770)}$	773.1 ± 0.5	$\Gamma_{\rho^0(770)}$	148.0 ± 0.9	ϕ_δ	13.0 ± 2.3
$m_{\rho(1450)}$	1409 ± 12	$\Gamma_{\rho(1450)}$	501 ± 37	β	0.166 ± 0.005
$m_{\rho(1700)}$	1740 ± 20	$\Gamma_{\rho(1700)}$	$\equiv235$	ϕ_β	177.8 ± 5.2
				γ	0.071 ± 0.006
				ϕ_γ	$\equiv0$

effect [Fig. 13(b)] $a_\ell=\alpha/2\pi\simeq0.001\,16$, with $\alpha\equiv e^2/4\pi \simeq 1/137.036$, which agreed beautifully with experiment (Nagle, Julian, and Zacharias, 1947; Nagle, Nelson, and Rabi, 1947), thereby providing confidence in the validity of perturbative QED. Today, the tradition of testing QED and its $SU(3)_C\times SU(2)_L\times U(1)_Y$ SM extension is continued (which includes strong and electroweak interactions) by measuring $a_\ell^{\rm exp}$ for the electron and muon more precisely and comparing with $a_\ell^{\rm SM}$ expectations, calculated to higher order in perturbation theory. Such comparisons test the validity of the SM and probe for new physics effects, which if present in quantum loop fluctuations should cause disagreement at some level. An experiment underway at Harvard (Gabrielse and Tan, 1994) aims to improve the present measurement (Van Dyck *et al.*, 1987) of a_e by about a factor of 15. Combined with an improved independent determination of α, it would significantly test the validity of perturbative QED. It should be noted, however, that a_e is in general not very sensitive to new physics at a high mass scale Λ because its effect on a_e is expected to be quadratic in $1/\Lambda$ (Czarnecki and Marciano, 2001),

$$\Delta a_e(\Lambda) \sim \mathcal{O}\left(\frac{m_e^2}{\Lambda^2}\right) \tag{59}$$

and hence highly suppressed by the smallness of the electron mass. It would be much more sensitive if Δa_e were linear in $1/\Lambda$; but that is unlikely if chiral symmetry is present in the $m_e\to0$ limit.

The muon magnetic anomaly has recently been measured for positive and negative muons with a relative precision of 5×10^{-7} by the E821 Collaboration at Brookhaven National Laboratory (Bennett *et al.*, 2004). Combined with the older, less precise results from CERN (Bailey *et al.*, 1977), and averaging over charges, gives

$$a_\mu^{\rm exp} = (11\,659\,208.0 \pm 5.8) \times 10^{-10}. \tag{60}$$

Although the accuracy is 200 times worse than $a_e^{\rm exp}$, a_μ is about $m_\mu^2/m_e^2\simeq40\,000$ times more sensitive to new physics and hence a better place (by about a factor of 200) to search for a deviation from the SM expectation. Of course, strong and electroweak contributions to a_μ are also enhanced by m_μ^2/m_e^2 relative to a_e; so, they must be evaluated much more precisely in any meaningful comparison of $a_\mu^{\rm SM}$ with Eq. (60). Fortunately, the recent experimental progress in $a_\mu^{\rm exp}$ has stimulated much theoretical improvement of $a_\mu^{\rm SM}$, uncovering errors and inspiring new computational approaches along the way, among these the use of hadronic τ decays.

It is convenient to separate the SM prediction for the anomalous magnetic moment of the muon into its different contributions,

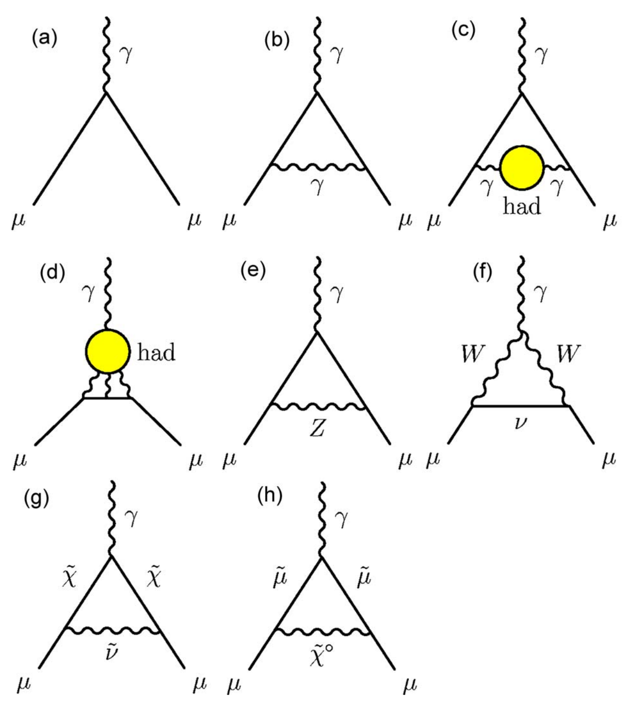

FIG. 13. (Color online) Representative diagrams contributing to a_μ. Lowest-order diagram (a) and first-order QED correction (b); lowest-order hadronic contribution (c) and hadronic light-by-light scattering (d); weak interaction diagrams (e), (f); possible contributions from lowest-order supersymmetry (g), (h).

$$a_\mu^{\rm SM} = a_\mu^{\rm QED} + a_\mu^{\rm weak} + a_\mu^{\rm had}, \tag{61}$$

where $a_\mu^{\rm QED} = (11\,658\,472.0 \pm 0.2) \times 10^{-10}$ is the pure electromagnetic contribution [see Czarnecki and Marciano (1999) and Hughes and Kinoshita (1999), and references therein],[8] $a_\mu^{\rm weak} = (15.4 \pm 0.1 \pm 0.2) \times 10^{-10}$, with the first error being the hadronic uncertainty and the second due to the Higgs-mass range accounts for corrections due to exchange of weakly interacting bosons up to two loops [Czarnecki *et al.*, 2003] [see Figs. 13(e) and 13(f)]. The term $a_\mu^{\rm had}$ can be further decomposed into

$$a_\mu^{\rm had} = a_\mu^{\rm had,LO} + a_\mu^{\rm had,HO} + a_\mu^{\rm had,LBL}, \tag{62}$$

where $a_\mu^{\rm had,LO}$ is the lowest-order contribution from hadronic vacuum polarization and $a_\mu^{\rm had,HO}$ the corresponding higher-order part (Sec. VI.E). At the three-loop level in α, the so-called hadronic light-by-light (LBL) scattering contributions $a_\mu^{\rm had,LBL}$ must be estimated in a model-dependent approach. Those estimates have been plagued by errors, which now seem to be sorted out (Sec. VI.E). Nevertheless, the remaining overall uncertainties from hadronic vacuum polarization and LBL scattering in $a_\mu^{\rm had}$ represent the main theoretical error in $a_\mu^{\rm SM}$.

Owing to unitarity and to the analyticity of the vacuum-polarization function,[9] the lowest-order hadronic vacuum-polarization contribution to a_μ can be computed via the dispersion integral (Gourdin and de Rafael, 1969)

$$a_\mu^{\rm had,LO} = \frac{1}{3}\left(\frac{\alpha}{\pi}\right)^2 \int_{m_\pi^2}^{\infty} ds \frac{K(s)}{s} R^{(0)}(s), \tag{63}$$

where $K(s)$ is the QED kernel (Brodsky and de Rafael, 1968),

$$K(s) = x^2\left(1 - \frac{x^2}{2}\right) + (1+x)^2\left(1 + \frac{1}{x^2}\right) \times \left[\ln(1+x) - x + \frac{x^2}{2}\right] + x^2 \ln x \frac{1+x}{1-x}, \tag{64}$$

with $x = (1-\beta_\mu)/(1+\beta_\mu)$ and $\beta_\mu = (1-4m_\mu^2/s)^{1/2}$. In Eq. (63), $R^{(0)}(s)$ denotes the ratio of the "bare" cross section for e^+e^- annihilation into hadrons to the pointlike muon-pair cross section at center-of-mass energy $\sqrt{s}$. The bare cross section is defined as the measured cross section corrected for initial-state radiation, electron-vertex loop contributions, and vacuum-polarization effects in the photon propagator. As the only QED effect, photon radiation in the final state is to be included. The reason for using the bare (i.e., lowest-order) cross section is that a full treatment of higher orders is anyhow needed at the level of a_μ, so that the use of the "dressed" cross section would entail the risk of double counting some higher-order contributions.

The function $K(s) \sim 1/s$ in Eq. (63) gives weight to the low-energy part of the integral. About 91% of the total contribution to $a_\mu^{\rm had,LO}$ is accumulated at center-of-mass energies $\sqrt{s}$ below 1.8 GeV and 73% of $a_\mu^{\rm had,LO}$ is covered by the $\pi\pi$ final state, which is dominated by the $\rho(770)$ resonance.

B. Input data and their treatment

Information used for evaluation of the integral (63) comes mainly from direct measurements of the cross sections in e^+e^- annihilation and via CVC from τ spectral functions. In addition to data with two- and four-pion final states shown in Sec. V.B, other final states and at different energies are also used [references for experimental data can be found in the work of Davier *et al.* (2003a)]. However, due to the higher hadron multiplicity at energies above ~2.5 GeV, exclusive measurement of many hadronic final states is not practicable. Consequently, experiments at high-energy colliders ADONE, SPEAR, DORIS, PETRA, PEP, VEPP-4, CESR, and BEPC have measured the total inclusive cross-section ratio R. In some cases measurements are incomplete, as, for example, $e^+e^- \to K\bar{K}\pi\pi$ or $e^+e^- \to 6\pi$, and one has to rely on isospin symmetry to estimate or bound the unmeasured cross sections (Davier *et al.*, 2003a). To obtain the corresponding e^+e^- annihilation cross sections using τ data, the isospin rotations (41) and (47) are applied, and all identified sources of isospin breaking are corrected.

---

[8] An improved calculation including all mass-dependent α^4 QED contributions has been published with a slightly different result (Kinoshita and Nio, 2004): $a_\mu^{\rm QED} = 116\,584\,719.58(0.02)(1.15)(0.85) \times 10^{-11}$. Here, 0.02 and 1.15 are uncertainties in the α^4 and α^5 terms, and 0.85 is from the uncertainty in α measured by atom interferometry.

[9] The photon vacuum-polarization function is a spin-1 component of the time-ordered product of two electromagnetic currents $\Pi_\gamma(q^2)$ [cf. Eq. (38)]. Due to Ward identities, contributions from self-energy and vertex correction graphs to $\Pi_\gamma(q^2)$ cancel, and only vacuum polarization modifies the charge of an elementary particle. One can therefore write for the running electron charge (charge screening) at energy scale s, $\alpha(s) = \alpha(0)/[1-\Delta\alpha(s)]$, where $\alpha(0)$ is the fine-structure constant in the long-wavelength Thomson limit and $\Delta\alpha(s) = \Delta\alpha_{\rm lep}(s) + \Delta\alpha_{\rm had}(s) = -4\pi\alpha\,{\rm Re}[\Pi_\gamma(s) - \Pi_\gamma(0)]$. The leptonic part $\Delta\alpha_{\rm lep}(s)$ is calculable within QED and known up to three loops (Steinhauser, 1998). However, quark loops are modified by long-distance hadronic physics that cannot be calculated within QCD. Instead, the optical theorem

$$12\pi\,{\rm Im}\,\Pi_\gamma(s) = \sigma(e^+e^- \to {\rm hadrons})/\sigma(e^+e^- \to \mu^+\mu^-) \equiv R(s),$$

and, owing to the analyticity of Π_γ, the dispersion relation

$$\Pi_\gamma(s) - \Pi_\gamma(0) = \frac{s}{\pi}\int_0^\infty ds' \frac{{\rm Im}\,\Pi_\gamma(s')}{s'(s'-s) - i\varepsilon},$$

lead to

$$\Delta\alpha_{\rm had}(s) = -\frac{\alpha(0)s}{3\pi}\,{\rm Re}\int_0^\infty ds' \frac{R(s')}{s'(s'-s) - i\varepsilon}.$$

Its right-hand side can be obtained with the use of experimental data for $R(s)$. Similarly, one obtains Eq. (63) for the hadronic vacuum-polarization contribution to a_μ.

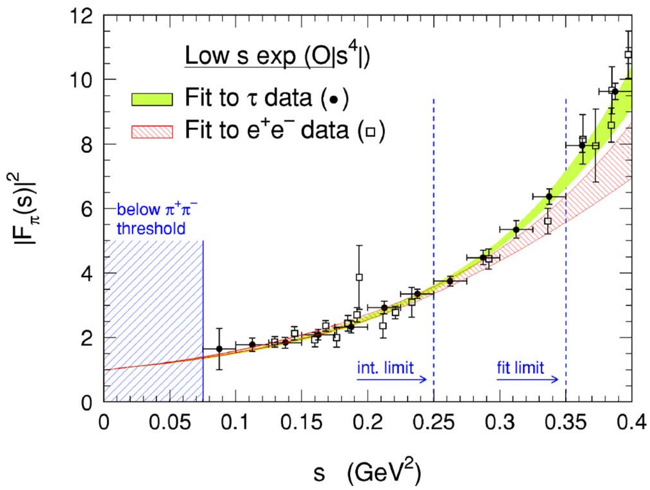

FIG. 14. (Color online) Fit of the pion form factor from $4m_\pi^2$ to 0.35 GeV^2 using a third-order expansion with constraints at $s=0$ and measured pion rms charge radius from spacelike data (Amendolia *et al.*, 1986). The result of the fit is integrated only up to 0.25 GeV^2. The e^+e^- data do not yet include the recent SND measurement (Achasov *et al.*, 2005).

To exploit the maximum information from available data, weighted measurements of different experiments at a given energy should be combined instead of calculating integrals for every experiment and finally averaging them. Different averaging methods are used in the literature varying from classical χ^2 minimization methods (Alemany *et al.*, 1998; Menke, 2001; Davier *et al.*, 2003a) to the so-called clustering method (Hagiwara *et al.*, 2004) in which a cluster of arbitrary size is predefined and precise data are used to rescale imprecise measurements within (correlated) systematic errors of the imprecise data set.

To overcome the lack of precise data at threshold energies, a phenomenological expansion in powers of s is used:

$$|F_\pi^0| = 1 + \tfrac{1}{6}\langle r_\pi^2\rangle s + c_1 s^2 + c_2 s^3. \qquad (65)$$

This interpolating function satisfies the known form-factor constraints at $s=0$. Above the 2π threshold, where a branch cut develops in the form factor, such parametrization has been derived within the framework of chiral perturbation theory (Colangelo *et al.*, 1996). Exploiting precise results from spacelike data (Amendolia *et al.*, 1986), the pion charge radius squared is constrained to

$$\langle r_\pi^2\rangle = 0.439 \pm 0.008\ \mathrm{fm}^2, \qquad (66)$$

and the two parameters $c_{1,2}$ are fit to the data in the range $[2m_\pi, 0.6\ \mathrm{GeV}]$. Good agreement is observed in the low-energy region and this parametrization is used for evaluating integrals up to 0.5 GeV (Davier *et al.*, 2003a) (see Fig. 14).

C. QCD for high-energy contributions

Since problems still remain regarding the spectral functions from low-energy data, the prediction from essentially perturbative QCD is used above an energy of 1.8 and 5 GeV, respectively. Details of the calculation are given by Davier and Höcker (1998a, 1998b), and references therein.

The perturbative QCD prediction uses a next-to—next-to—leading-order $O(\alpha_s^3)$ expansion of the Adler D function (Gorishnii *et al.*, 1991; Surguladze and Samuel, 1991), with second-order quark mass corrections included (Chetyrkin *et al.*, 1996). $R(s)$ is obtained by evaluating numerically a contour integral in the complex s plane (cf. the detailed discussion of this technique in Sec. VII). Nonperturbative effects are considered through the operator product expansion, giving small power corrections controlled by gluon and quark condensates. The value $\alpha_s(M_Z^2)=0.1193\pm0.0026$, used for the evaluation of the perturbative part, is taken as the average of the results from the analyses of τ decays (Barate *et al.*, 1998c) (see Sec. VII) and of the Z width in the global electroweak fit (Abbaneo *et al.*, 2002). Uncertainties on the QCD prediction are taken to be equal to the common error on $\alpha_s(M_Z^2)$, to half of the quark mass corrections and to full nonperturbative contributions. A local test of the QCD prediction can be performed in the energy range between 1.8 and 3.7 GeV. The contribution to $a_\mu^{\mathrm{had,LO}}$ in this region is computed to be $(33.87\pm0.46)\times10^{-10}$ using QCD, to be compared with the result $(34.9\pm1.8)\times10^{-10}$ from data. The two values agree within the 5% accuracy of the measurements.

The evaluation of $a_\mu^{\mathrm{had,LO}}$ was shown to be improved by applying QCD sum rules (Davier and Höcker, 1998b; Groote *et al.*, 1998). The latest full reanalyses (Davier *et al.*, 2003a, 2003b), however, did not consider this possibility since the main problem at energies below 2 GeV was the inconsistency between the e^+e^- and τ input data, which had to be resolved with priority. Also the improvement provided by the use of QCD sum rules results from a balance between the experimental accuracy of the data and theoretical uncertainties. With an increase in the experimental precision, the gain from the theoretical constraint would be smaller than before.

D. Results for the lowest-order hadronic vacuum polarization

Many calculations of the hadronic vacuum-polarization contribution have been carried out in the past, taking advantage of the e^+e^- data available at that time and benefiting from a more complete treatment of isospin-breaking corrections (Cirigliano *et al.*, 2001, 2002). In this review, we will follow the latest published analysis by Davier *et al.* (2003b) [and the update (Höcker, 2004) including data from KLOE; see also the result in de Troconiz and Yndurain (2005)], which considers input from both τ and e^+e^- data.

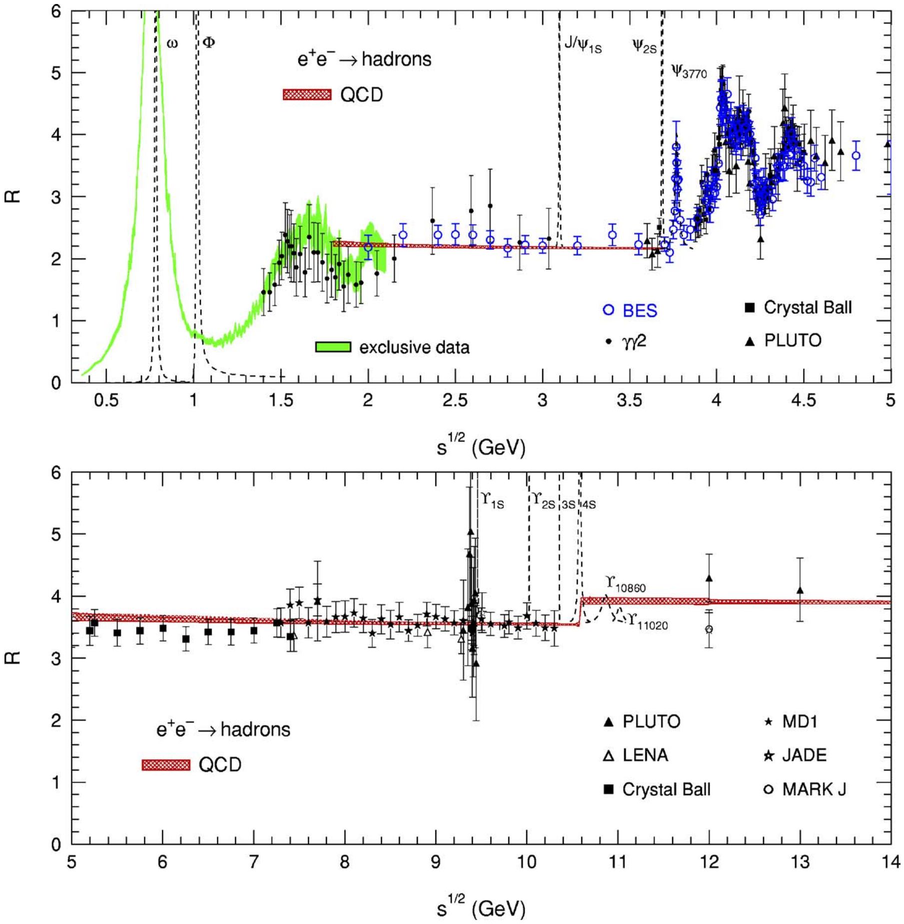

FIG. 15. (Color online) Compilation of data contributing to $a_\mu^{\rm had,LO}$. Shown is the total hadronic over muonic cross-section ratio R. The shaded band below 2 GeV represents the sum of exclusively measured channels, with the exception of contributions from narrow resonances that are given as dashed lines. All data points shown correspond to inclusive measurements. The cross-hatched band gives the prediction from (essentially) perturbative QCD (see text).

Figure 15 gives a panoramic view of the e^+e^- data in the relevant energy range. The shaded band below 2 GeV represents the sum of exclusive channels. The QCD prediction is indicated by the cross-hatched band. Note that the QCD band is plotted taking into account thresholds for open flavor B states, in order to facilitate comparison with data in the continuum. However, for evaluating the integral, the $b\bar{b}$ threshold is taken at twice the pole mass of the b quark, so that the contribution includes the narrow Υ resonances according to global quark-hadron duality.

Compiling all contributions, the e^+e^--based result (including the KLOE data, but not yet SND) for the lowest-order hadronic contribution is (Höcker, 2004)

$$a_\mu^{\rm had,LO} = (693.4 \pm 5.3 \pm 3.5_{\rm rad}) \times 10^{-10}, \quad (67)$$

where the second error is due to the treatment of (potentially) missing radiative corrections in the older data (Davier *et al.*, 2003a). The new KLOE data decreased the contribution by about 3×10^{-10}. For a comparison we also give results without KLOE for the e^+e^-- and τ-based analyses (Davier *et al.*, 2003b): $a_\mu^{\rm had,LO}[e^+e^-\text{-based}]=(696.3\pm6.2_{\rm exp}\pm3.6_{\rm rad})\times10^{-10}$ and $a_\mu^{\rm had,LO}[\tau\text{-based}]=(711.0\pm5.0_{\rm exp}\pm0.8_{\rm rad}\pm2.8_{\rm SU(2)})\times10^{-10}$.

E. Hadronic three-loop effects

The three-loop hadronic contributions to $a_\mu^{\rm SM}$ involve one hadronic vacuum-polarization insertion with an additional loop (either photonic or another leptonic or hadronic vacuum polarization). They can be evaluated (Krause, 1997) with the same $e^+e^-\to$hadrons data sets used for $a_\mu^{\rm had,LO}$. Denoting that subset of $\mathcal{O}(\alpha/\pi)^3$ hadronic contributions $a_\mu^{\rm had,NLO}$, we quote the result of a recent analysis (Hagiwara *et al.*, 2004),

$$a_\mu^{\rm had,NLO} = (-9.8 \pm 0.1) \times 10^{-10}, \quad (68)$$

which is consistent with earlier studies (Krause, 1997; Alemany *et al.*, 1998). It would change by about -0.3×10^{-10} if the τ data were also used.

More controversial are the hadronic light-by-light scattering contributions illustrated in Fig.13(d). Since it invokes a four-point correlation function, a dispersion relation approach using data is not possible and a first-principles calculation [e.g., lattice gauge theory (Blum, 2003)] has so far not been carried out. Instead, calculations involving pole insertions, short-distance quark loops (Bijnens *et al.*, 1996; Hayakawa *et al.*, 1996), and charged-pion loops have been individually performed in a large N_C QCD approach. The pseudoscalar poles (π^0, η, and η') dominate such a calculation. Unfortunately, in early studies the sign of the contribution was incorrect. Its correction (Hayakawa and Kinoshita, 1998; Bijnens *et* al., 2002; Blokland et al., 2002; Knecht and Nyffeler, 2002; Knecht et al., 2002) led to a large shift in the $a_\mu^{\rm SM}$ prediction. A representative estimate (Davier et al., 2003a) of the LBL contribution, which includes π, η, and η' poles as well as other resonances, charged pion loops, and quark loops, currently gives $a_\mu^{\rm had,LBL} \simeq (8.6 \pm 3.5) \times 10^{-10}$ (representative).

A new analysis of LBL scattering (Melnikov and Vainshtein, 2004) takes into account the proper matching of the asymptotic short-distance behavior of pseudoscalar and axial-vector contributions with the free quark loop behavior. It yields the somewhat larger result $a_\mu^{\rm had,LBL} = (13.6 \pm 2.5) \times 10^{-10}$.

As pointed out by Davier and Marciano (2004), several small but (likely) negative contributions such as charged pion loops and scalar resonances were not included in the work of Melnikov and Vainshtein (2004) and could reduce somewhat the magnitude of the result. Melnikov and Vainshtein (2004) provided a consistency check on their result much in the spirit of the electroweak hadronic triangle diagram study (Czarnecki et al., 2003; Vainshtein, 2003) discussed by Davier and Marciano (2004). Using constituent quark masses in the LBL diagram combined with a pion pole contribution that properly accounts for the chiral properties of massless QCD and avoiding short-distance double counting, they find $a_\mu^{\rm had,LBL} \simeq 12.0 \times 10^{-10}$ with about half of the contribution coming from quark diagrams and the other half from the pion pole. Using that result along with an inflated error assigned so that the representative result and the one obtained by Melnikov and Vainshtein (2004) overlap within their errors (Davier and Marciano, 2004) suggest the value

$$a_\mu^{\rm had,LBL} \simeq (12.0 \pm 3.5) \times 10^{-10}. \tag{69}$$

Further resolution of the LBL scattering contribution is very important.

Combining Eqs. (68) and (69), one finds

$$a_\mu^{\rm had,3\text{-}loop} = (2.2 \pm 3.5) \times 10^{-10}, \tag{70}$$

which we identify with $a_\mu^{\rm had,HO}$ in Eq. (62).

F. Comparing a_μ between theory and experiment

Summing the results from the previous sections on $a_\mu^{\rm QED}$, $a_\mu^{\rm EW}$, $a_\mu^{\rm had,LO}$, $a_\mu^{\rm had,NLO}$, and $a_\mu^{\rm had,LBL}$, one obtains the SM prediction for a_μ. The newest e^+e^--based result reads (Höcker, 2004)

$$a_\mu^{\rm SM} = (11\,659\,182.8 \pm 6.3_{\rm had,LO+NLO} \pm 3.5_{\rm had,LBL} \pm 0.3_{\rm QED+EW}) \times 10^{-10}. \tag{71}$$

This value can be compared to the present measurement (60); adding all errors in quadrature, the difference between experiment and theory is

$$a_\mu^{\rm exp} - a_\mu^{\rm SM} = (25.2 \pm 9.2) \times 10^{-10}, \tag{72}$$

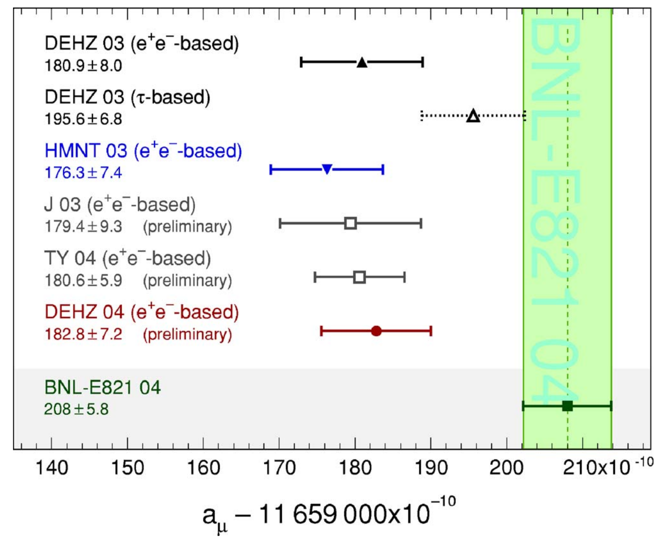

FIG. 16. (Color online) Comparison of the result (71) (Höcker, 2004) labeled DEHZ 04 with the BNL measurement (Bennett et al., 2004). Also given are the previous estimate (Davier et al., 2003b), where the triangle with the dotted error bar indicates the τ-based result, as well as estimates from Hagiwara et al. (2004); Jegerlehner (2004); de Troconiz and Yndurain (2005), not yet including the KLOE data.

which corresponds to 2.7 "standard deviations" (to be interpreted with care due to the dominance of experimental and theoretical systematic errors in the SM prediction). A graphical comparison of the result (71) with previous evaluations (also those containing τ data) and the experimental value is given in Fig. 16.

Whereas the evaluation based on the e^+e^- data only disagrees with measurement, evaluation including the tau data is consistent with it. The dominant contribution to the discrepancy between the two evaluations stems from the $\pi\pi$ channel with a difference of $[-11.9 \pm 6.4_{\rm exp} \pm 2.4_{\rm rad} \pm 2.6_{\rm SU(2)} (\pm 7.3_{\rm total})] \times 10^{-10}$, and a more significant energy-dependent deviation.[10] As a consequence, during the previous evaluations of $a_\mu^{\rm had,LO}$ the results using, respectively, the τ and e^+e^- data were quoted individually, but on the same footing since the e^+e^--based evaluation was dominated by the data from a single experiment (CMD-2).

The seeming confirmation of the e^+e^- data by KLOE could lead to the conclusion that the τ-based result be discredited for the use in the dispersion integral (Höcker, 2004). However, the newest SND data (Achasov et al., 2005) alter this picture in favor of the τ data, along with prompting doubts on the validity of the KLOE results (see discussion in Sec. V.C). Comparing

[10] The systematic problem between τ and e^+e^- data is more noticeable when comparing the $\tau^- \to \pi^-\pi^0\nu_\tau$ branching fraction with the prediction obtained from integrating the corresponding isospin-breaking-corrected e^+e^- spectral function (cf. Sec. V).

the SND and CMD-2 data in the overlapping energy region between 0.61 and 0.96 GeV, the SND-based evaluation of $a_\mu^{\rm had,NLO}$ is found to be larger by $(9.1\pm6.3)\times10^{-10}$. However, once these two experiments are averaged using the trapezoidal rule, the increase over the CMD-2 only evaluation is reduced to 2×10^{-10} due to the much smaller systematic errors and the higher density of the CMD-2 measurements.

The proper response to problems in the LO hadronic contribution is to further improve the experimental precision by a renewed experimental effort, and to continue to improve theory. In this respect, new $e^+e^-\to$hadrons data and further study of LBL scattering could potentially reduce the overall theoretical uncertainty. The excitement that was caused by the deviation (72) stems from the expectation that new physics could cause an effect of similar magnitude, some examples of which have been discussed by Marciano (1996) and Davier and Marciano (2004).

G. Conclusions and perspectives

After considerable effort, the experiment E821 at Brookhaven has improved the determination of a_μ by about a factor of 14 relative to the classic CERN results of the 1970s (Bailey *et al.*, 1977; Farley and Picasso, 1990). The result is still statistics limited and could be improved by another factor of 2 or so (to a precision of 3.0×10^{-10}) before systematic effects become a limitation. Pushing the experiment to that level seems to be an obvious goal for the near term. In the longer term, a new experiment with improved muon acceptance and magnetic fields could potentially reach 0.6×10^{-10} (Roberts, 1999; Hertzog, 2005).

In spite of the new and precise data on the two-pion spectral function from the KLOE and SND Collaborations, the lowest-order hadronic vacuum-polarization contribution remains the most critical component in the SM prediction of a_μ. The publication of the KLOE results led to an outward confirmation of the discrepancy between the τ data and e^+e^- annihilation observed in the $\pi^+\pi^-$ channel (Davier *et al.*, 2003b). Including the KLOE data in the hadronic evaluation, the e^+e^--based SM prediction of a_μ was found to differ from the experimental value by 2.7 standard deviations.

An opposite point view has been advocated by Maltman (2006). A QCD sum-rule analysis of low-energy e^+e^- data results in the value $\alpha_s(M_Z^2)=0.1150\pm0.0024$, which is somewhat lower than the world average (Eidelman *et al.*, 2004), 0.1187 ± 0.0020, and even less consistent with the average 0.1200 ± 0.0020, which excludes τ data, for the sake of comparison, and heavy quarkonium results [the accuracy of which has been questioned by Brambilla *et al.* (2004)]. The same analysis using the τ vector spectral function provides agreement, with a value of $\alpha_s(M_Z^2)=0.1201\pm0.0021$. Although the disagreement between the e^+e^- data and other measurements is not yet significant, the observed trend is worth more investigations. It is supported by the newest measurement from SND that tends to amend the compatibility with the τ data in the two-pion channel.

Further improvement of the e^+e^- data is the better route and one is looking forward to the forthcoming results on the low- and high-energy two-pion spectral function from the CMD-2 Collaboration. These data will help to significantly reduce the systematic uncertainty due to the corrective treatment of radiative effects, often omitted by part by the previous experiments. The initial-state-radiation program of the *BABAR* Collaboration has already proved its performance by publishing the spectral functions for $\pi^+\pi^-\pi^0$ (Aubert *et al.*, 2004) and $2\pi^+2\pi^-$ (Aubert *et al.*, 2005a), while results for the two-pion final state are expected. All sources considered, and assuming all discrepancies to be resolved, it appears, however, difficult to reach an uncertainty much better than 3×10^{-10} in this sector.[11]

The 30% uncertainty in the hadronic LBL contribution (3.5×10^{-10}) is largely model dependent. Here one could conceive that further work following the approach of Melnikov and Vainshtein (2004) or lattice calculations could help to reduce the error. Doing much better will be difficult, but an improvement in the precision by about a factor of 2 would well match short-term experimental capabilities.

If the above experimental and theoretical improvements do occur, they will lead to a total uncertainty in $\Delta a_\mu=a_\mu^{\rm exp}-a_\mu^{\rm SM}$ of about 5.0×10^{-10}, i.e., a factor of 2 reduction with respect to today. This would provide an important step towards a better test of the SM. The result could be used in conjunction with future collider discoveries to sort out the properties of new physics (e.g., the size of $\tan\beta$ in supersymmetry) or to further constrain possible extensions of the SM.

VII. HADRONIC TAU DECAYS AND QCD

Tests of quantum chromodynamics and the precise measurement of the strong-coupling constant α_s at the τ mass scale (Narison and Pich, 1988; Braaten, 1989; Braaten *et al.*, 1992; Le Diberder and Pich, 1992b) carried out for the first time by the ALEPH (Buskulic *et al.*, 1993) and CLEO (Coan *et al.*, 1995) Collaborations have triggered many theoretical developments. They concern primarily the perturbative expansion for which different optimized rules have been suggested. Among these are contour-improved (resummed) fixed-order perturbation theory (Pivovarov, 1991, 1992; Le Diberder and Pich, 1992a), effective charge and minimal sensitivity schemes (Grunberg, 1980, 1984; Stevenson, 1981; Dhar, 1983; Dhar and Gupta, 1983), the large-β_0 expansion (Altarelli *et al.*, 1995; Ball *et al.*, 1995; Neubert, 1996), as well as combinations of these approaches. They mainly distinguish themselves in how they deal with the fact that the perturbative series is truncated at an order where the

[11] We also point out that lattice gauge theories with dynamical fermions can in principle provide a determination of $a_\mu^{\rm had,LO}$ (Blum, 2003).

missing part is not expected to be small. Also, in the discussion of the so-called *contour improved* approach we point out the importance to fully retain the complete information from the renormalization group when computing integrals of perturbatively expanded quantities. With the publication of the full vector and axial-vector spectral functions by the ALEPH (Barate *et al.*, 1997b, 1998c) and OPAL (Ackerstaff *et al.*, 1999a) Collaborations it became possible to directly study the nonperturbative properties of QCD through vector minus axial-vector sum rules. These analyses are described in Sec. IX.

One could wonder how τ decays may at all allow us to learn something about perturbative QCD. The hadronic decay of the τ is dominated by resonant single-particle final states. The corresponding QCD interactions that bind the quarks and gluons into these hadrons necessarily involve small momentum transfers, which are outside the domain of perturbation theory. On the other hand, perturbative QCD describes interactions of quarks and gluons with large momentum transfer. Indeed, it is the inclusive character of the sum of all hadronic τ decays that allows us to probe fundamental short-distance physics. Inclusive observables like the total hadronic τ decay rate R_τ, Eq. (20), can be accurately predicted as function of $\alpha_s(m_\tau^2)$ using perturbative QCD, and including small nonperturbative contributions within the framework of the operator product expansion (OPE) (Shifman *et al.*, 1979a, 1979b, 1979c). In effect, R_τ is a doubly inclusive observable since it is the result of an integration over all hadronic final states at a given invariant mass and further over all masses between m_π and m_τ. Hadronic τ decays are more inclusive than e^+e^- annihilation data, since vector and axial-vector contributions are of approximately equal size, while the isospin-zero component in e^+e^- data is three times smaller than the isovector part, which is (about) equal to the vector contribution in τ decays. The scale m_τ lies in a compromise region where $\alpha_s(m_\tau^2)$ is large enough so that R_τ is sensitive to its value, yet still small enough so that the perturbative expansion converges safely and nonperturbative power terms are small.

If strong and electroweak radiative corrections are neglected, the theoretical parton level prediction for $SU_C(N_C)$, $N_C=3$, reads

$$R_\tau = N_C(|V_{ud}|^2 + |V_{us}|^2) = 3, \tag{73}$$

so that we can estimate a perturbative correction to this value of approximately 21% to obtain Eq. (20), assuming other sources to be small. One realizes the increase in sensitivity to α_s compared to the Z hadronic width, where due to the three times smaller $\alpha_s(M_Z^2)$ the perturbative QCD correction reaches only about 4%.

The nonstrange inclusive observable R_τ can be theoretically separated into contributions from specific quark currents, namely, vector (V) and axial-vector (A) $\bar{u}d$ and $\bar{u}s$ quark currents. It is therefore appropriate to decompose

$$R_\tau = R_{\tau,V} + R_{\tau,A} + R_{\tau,S}, \tag{74}$$

where for the strange hadronic width $R_{\tau,S}$ vector and axial-vector contributions are not separated so far due to the lack of the corresponding experimental information for the Cabibbo-suppressed modes. Parton-level and perturbative terms do not distinguish vector and axial-vector currents (for massless partons). Thus the corresponding predictions become $R_{\tau,V/A}=(N_C/2)|V_{ud}|^2$ and $R_{\tau,S}=N_C|V_{us}|^2$, which add up to Eq. (73).

A crucial issue of the QCD analysis at the τ mass scale concerns the reliability of the theoretical description, i.e., the use of the OPE to organize the perturbative and nonperturbative expansions, and the control of unknown higher-order terms in these series. A reasonable stability test is to continuously vary m_τ to lower values $\sqrt{s_0} \le m_\tau$ for both theoretical prediction and measurement, which is possible since the shape of the full τ spectral function is available. The kinematic factor that takes into account the τ phase-space suppression at masses near to m_τ is correspondingly modified so that $\sqrt{s_0}$ represents the new mass of the τ.

A. Renormalization-group equations

Like in QED, the subtraction of divergences in QCD is equivalent to the renormalization of the coupling ($\alpha_s \equiv g_s^2/4\pi$), the quark masses ($m_q$), etc, and fields in the bare (superscript B) Lagrangian such as $\alpha_s^B = s^\varepsilon Z_{\alpha_s}\alpha_s$, $m_q^B = s^\varepsilon Z_m m_q$, etc. Here s is the renormalization scale, ε the dimensional regularization parameter, and Z denotes a series of renormalization constants obtained from the generating functional of the bare Green's function. The renormalization procedure introduces an energy scale s, which represents the point at which the subtraction to remove the divergences is actually performed. This leads to the differential *renormalization-group equations* (RGEs),

$$\frac{da_s}{d\ln s} = \beta(a_s) = -a_s^2 \sum_n \beta_n a_s^n, \tag{75}$$

$$\frac{1}{m_q}\frac{dm_q}{d\ln s} = \gamma(a_s) = -a_s \sum_n \gamma_n a_s^n, \tag{76}$$

with $a_s = \alpha_s/\pi$. Expressed in the *modified minimal subtraction renormalization scheme* ($\overline{\rm MS}$) ('t Hooft and Veltman, 1972; Bardeen *et al.*, 1978) and for three active quark flavors at the τ mass scale, the perturbative coefficients known to four loops (van Ritbergen *et al.*, 1997a, 1997b) are[12]

$$\beta_0 = 2.25, \quad \beta_1 = 4, \quad \beta_2 \approx 10.059\,89,$$

$$\beta_3 \approx 47.228\,04, \tag{77}$$

$$\gamma_0 = 1, \quad \gamma_1 = 3.791\,66, \quad \gamma_2 \approx 12.420\,18, \tag{78}$$

$$\gamma_3 \approx 44.262\,78.$$

The solutions for the evolutions (75) and (76) are obtained from integration[13] (Stevenson, 1981; Chetyrkin, Kniehl, and Steinhauser, 1997)

$$\ln \frac{s}{\Lambda^2} = \int_0^{a_s(s)} da_s' \left(\frac{1}{\beta(a_s')} + \frac{1}{\beta_0 (a_s')^2 + \beta_1 (a_s')^3} \right) + \int_{a_s(s)}^{\infty} da_s' \frac{1}{\beta_0 (a_s')^2 + \beta_1 (a_s')^3}, \tag{79}$$

$$\ln \frac{m_q(s)}{m_q(s_0)} = \int_{a_s(s_0)}^{a_s(s)} da_s' \frac{\gamma(a_s')}{\beta(a_s')}, \tag{80}$$

where the $\overline{\mathrm{MS}}$ asymptotic scale parameter Λ and the RG-invariant quark mass $\hat{m}_q$ [which appears after evaluating the integral (80)] are fixed by referring to known values $a_s(s_0)$ and $m_q(s_0)$, respectively, at scale s_0.

For most practical purposes, it is, however, unnecessary to explicitly perform the integrations (79) and (80), since the evolution of the differential RGEs can be solved numerically by means of *single-step integration* using a modified Euler method. It consists of Taylor developing, say, Eq. (75) around the reference scale s_0 in powers of $\eta \equiv \ln(s/s_0)$, and reordering the perturbative series in powers of $a_s \equiv a_s(s_0)$,

$$\begin{aligned} a_s(s) = {} & a_s - \beta_0 \eta a_s^2 + (-\beta_1 \eta + \beta_0^2 \eta^2) a_s^3 + \Big(-\beta_2 \eta \\ & + \frac{5}{2} \beta_0 \beta_1 \eta^2 - \beta_0^3 \eta^3 \Big) a_s^4 + \Big(-\beta_3 \eta + \frac{3}{2} \beta_1^2 \eta^2 \\ & + 3 \beta_0 \beta_2 \eta^2 - \frac{13}{3} \beta_0^2 \beta_1 \eta^3 + \beta_0^4 \eta^4 \Big) a_s^5 + \Big(-\beta_4 \eta \\ & + \frac{7}{2} \beta_1 \beta_2 \eta^2 + \frac{7}{2} \beta_0 \beta_3 \eta^2 - \frac{35}{6} \beta_0 \beta_1^2 \eta^3 - 6 \beta_0^2 \beta_2 \eta^3 \\ & + \frac{77}{12} \beta_0^3 \beta_1 \eta^4 - \beta_0^5 \eta^5 \Big) a_s^6 + \mathcal{O}(a_s^7). \end{aligned} \tag{81}$$

For later use, we have expressed the expansion up to order a_s^6, which involves the unknown five-loop coefficient β_4. An efficient integration of the RGEs can also be obtained using the CERNLIB routine "RKSTP," which performs a fourth-order Runge-Kutta single step approximation with excellent accuracy.

B. Theoretical prediction of R_τ

According to Eq. (39) the absorptive parts of the vector and axial-vector two-point correlation functions $\Pi^{(J)}_{\bar{u}d,V/A}(s)$, with the spin J of the hadronic system, are proportional to the τ hadronic spectral functions with corresponding quantum numbers. The nonstrange ratio $R_{\tau,V+A}$ can be written as an integral of these spectral functions over the invariant mass squared s of final-state hadrons (Braaten *et al.*, 1992),

$$R_{\tau,V+A}(s_0) = 12\pi S_{\mathrm{EW}} \int_0^{s_0} \frac{ds}{s_0} \left(1 - \frac{s}{s_0}\right)^2 \left[\left(1 + 2\frac{s}{s_0}\right) \times \mathrm{Im}\,\Pi^{(1)}(s + i\epsilon) + \mathrm{Im}\,\Pi^{(0)}(s + i\epsilon) \right], \tag{82}$$

where $\Pi^{(J)}$ can be decomposed as $\Pi^{(J)} = |V_{ud}|^2 (\Pi^{(J)}_{ud,V} + \Pi^{(J)}_{ud,A})$. The lower integration limit is zero because the pion pole is at zero mass in the chiral limit.

The correlation function $\Pi^{(J)}$ is analytic in the complex s plane everywhere except on the positive real axis

---

[12] Full expressions for an arbitrary number of quark flavors (n_f) are (van Ritbergen *et al.*, 1997a, 1997b)

$$\beta_0 = \frac{1}{4}\left(11 - \frac{2}{3} n_f\right), \quad \beta_1 = \frac{1}{16}\left(102 - \frac{38}{3} n_f\right),$$

$$\beta_2 = \frac{1}{64}\left(\frac{2857}{2} - \frac{5033}{18} n_f + \frac{325}{54} n_f^2\right),$$

$$\beta_3 = \frac{1}{256}\left[\frac{149753}{6} + 3564\zeta_3 - \left(\frac{1078361}{162} + \frac{6508}{27}\zeta_3\right) n_f + \left(\frac{50065}{162} + \frac{6472}{81}\zeta_3\right) n_f^2 + \frac{1093}{729} n_f^3\right],$$

and

$$\gamma_0 = 1, \quad \gamma_1 = \frac{1}{16}\left(\frac{202}{3} - \frac{20}{9} n_f\right),$$

$$\gamma_2 = \frac{1}{64}\left[1249 - \left(\frac{2216}{27} + \frac{160}{3}\zeta_3\right) n_f - \frac{140}{81} n_f^2\right],$$

$$\begin{aligned} \gamma_3 = \frac{1}{256}\Big[& \frac{4603055}{162} + \frac{135680}{27}\zeta_3 - 8800\zeta_5 + \Big(-\frac{91723}{27} \\ & - \frac{34192}{9}\zeta_3 + 880\zeta_4 + \frac{18400}{9}\zeta_5 \Big) n_f + \Big(\frac{5242}{243} + \frac{800}{9}\zeta_3 \\ & - \frac{160}{3}\zeta_4 \Big) n_f^2 + \Big(-\frac{332}{243} + \frac{64}{27}\zeta_3 \Big) n_f^3 \Big], \end{aligned}$$

where the $\zeta_{i=\{3,4,5\}} = \{1.202\,056\,9, \pi^4/90, 1.036\,927\,8\}$ are the Riemann ζ functions.

[13] Note that the integration is only defined for a nonvanishing derivative $\beta(a_s) \neq 0$. Vanishing $\beta(a_s)$ may indeed occur, for example, in effective charge schemes with large K_4 or K_5 coefficients (see later in this section).

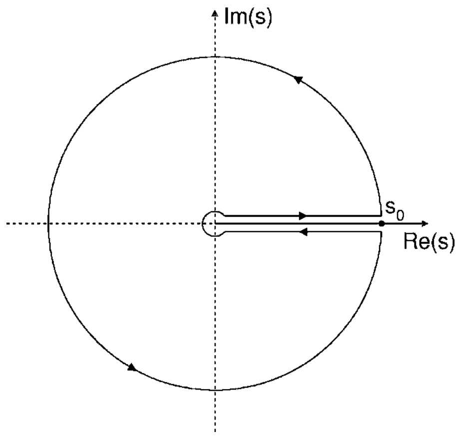

FIG. 17. Integration contour for the right-hand side of Eq. (83).

where singularities exist. Hence by Cauchy's theorem, the imaginary part of $\Pi^{(J)}$ is proportional to the discontinuity across the positive real axis,

$$\frac{1}{\pi}\int_0^{s_0} ds w(s) \mathrm{Im}\,\Pi(s) = -\frac{1}{2\pi i}\oint_{|s|=s_0} ds w(s)\Pi(s), \quad (83)$$

where $w(s)$ is an arbitrary analytic function and the contour integral runs counterclockwise around the circle from $s=s_0+i\epsilon$ to $s=s_0-i\epsilon$ as indicated in Fig. 17.

The energy scale $s_0=m_\tau^2$ is large enough that contributions from nonperturbative effects are expected to be subdominant and the use of the OPE is appropriate. The kinematic factor $(1-s/s_0)^2$ suppresses the contribution from the region near the positive real axis where $\Pi^{(J)}(s)$ has a branch cut and the OPE validity is restricted due to large possible quark-hadron duality violations (Poggio *et al.*, 1976; Braaten, 1988).

The theoretical prediction of the vector and axial-vector ratio $R_{\tau,V/A}$ can hence be written as

$$R_{\tau,V/A} = \tfrac{3}{2}|V_{ud}|^2 S_{\mathrm{EW}}\Big(1 + \delta^{(0)} + \delta'_{\mathrm{EW}} + \delta^{(2,m_q)}_{ud,V/A} + \sum_{D=4,6,\ldots} \delta^{(D)}_{ud,V/A}\Big), \quad (84)$$

with the massless perturbative contribution $\delta^{(0)}$, the residual nonlogarithmic electroweak correction $\delta'_{\mathrm{EW}}=0.0010$ (Braaten and Li, 1990) (cf. the discussion on radiative corrections in Sec. V.A), and the dimension $D=2$ *perturbative* contribution $\delta^{(2,m_q)}_{ud,V/A}$ from quark masses, which is lower than 0.1% for u,d quarks. The term $\delta^{(D)}$ denotes the OPE contributions of mass dimension D,

$$\delta^{(D)}_{ud,V/A} = \sum_{\dim\mathcal{O}=D} C_{ud,V/A}(s,\mu)\frac{\langle\mathcal{O}_{ud}(\mu)\rangle_{V/A}}{(-\sqrt{s_0})^D}, \quad (85)$$

where the scale parameter μ separates the long-distance nonperturbative effects, absorbed into the vacuum expectation elements $\langle\mathcal{O}_{ud}(\mu)\rangle$, from the short-distance effects that are included in the Wilson coefficients $C_{ud,V/A}(s,\mu)$ (Wilson, 1969). Note that $\delta^{(D)}_{ud,V+A}=(\delta^{(D)}_{ud,V}+\delta^{(D)}_{ud,A})/2$.

1. Perturbative prediction

The perturbative prediction used by experiments follows the work of Le Diberder and Pich (1992a). The perturbative contribution is given in the chiral limit. Effects from quark masses have been calculated by Chetyrkin and Kwiatkowski (1993) and are found to be well below 1% for the light quarks. As a consequence, contributions from vector and axial-vector currents coincide to any given order of perturbation theory and the results are flavor independent.

For evaluation of the perturbative series, it is convenient to introduce the analytic Adler (1974) function

$$D(s) \equiv -s\frac{d\Pi(s)}{ds} = \frac{s}{\pi}\int_0^\infty ds' \frac{\mathrm{Im}\,\Pi(s')}{(s'-s)^2}, \quad (86)$$

where the second identity is the dispersion relation (cf. Sec. VI.A). The derivative of the correlator avoids extra subtractions (renormalization) on the right-hand side of Eq. (86), which are unrelated to QCD dynamics. The function $D(s)$ calculated in perturbative QCD within the $\overline{\mathrm{MS}}$ renormalization scheme depends on a nonphysical parameter μ occurring as $\ln(\mu^2/s)$. Furthermore, it is a function of α_s. On the other hand, since $D(s)$ is connected to a physical quantity, the spectral function $\mathrm{Im}\,\Pi(s)$, it cannot depend on the subjective choice of μ. This can be achieved if α_s becomes a function of μ providing independence of $D(s)$ of the choice of μ. Nevertheless, in the realistic case of a truncated series, some μ dependence remains and represents an irreducible systematic uncertainty. $D(s)$ is then a function of μ^2/s, α_s and can be understood as an effective charge (see below) that obeys the RGE. Choosing $\mu^2=s$, the perturbative series reads

$$D[\alpha_s(s)] = \sum_{n=0}^{\infty} r_n a_s^n(s), \quad (87)$$

with renormalization scheme dependent coefficients r_n.

To introduce the Adler function in Eqs. (82) and (83) one uses partial integration

$$\oint_{|s|=s_0} dsg(s)\Pi(s) = -\oint_{|s|=s_0}\frac{ds}{s}[G(s)-G(s_0)]s\frac{d\Pi(s)}{ds}, \quad (88)$$

with the kernel $g(s)=(1-s/s_0)^2(1+2s/s_0)/s_0$ and $G(s)=\int_0^s ds' g(s')$. This gives (Le Diberder and Pich, 1992a)

$$1+\delta^{(0)} = -2\pi i\oint_{|s|=s_0}\frac{ds}{s}\left[1-2\frac{s}{s_0}+2\left(\frac{s}{s_0}\right)^3 - \left(\frac{s}{s_0}\right)^4\right]D(s). \quad (89)$$

The perturbative expansion of the Adler function can be inferred from the third-order calculation of the

e^+e^- inclusive cross-section ratio $R_{e^+e^-}(s)=\sigma(e^+e^- \to \mathrm{hadrons}(\gamma))/\sigma(e^+e^-\to\mu^+\mu^-(\gamma))$ (Chetyrkin *et al.*, 1979; Dine and Sapirstein, 1979; Celmaster and Gonsalves, 1980; Gorishnii *et al.*, 1991; Surguladze and Samuel, 1991; Le Diberder and Pich, 1992a)

$$D(s) = \frac{1}{4\pi^2}\sum_{n=0}^{\infty}\tilde{K}_n(\xi)a_s^n(-\xi s), \tag{90}$$

with the $\tilde{K}_n(\xi)$ functions up to order $n=5$ (Le Diberder and Pich, 1992a),

$$\tilde{K}_0(\xi)=K_0,\quad \tilde{K}_1(\xi)=K_1,\quad \tilde{K}_2(\xi)=K_2+L,$$

$$\tilde{K}_3(\xi)=K_3+(b_1+2K_2)L+L^2,$$

$$\tilde{K}_4(\xi)=K_4+(b_2+2b_1K_2+3K_3)L+(\tfrac{5}{2}b_1+3K_2)L^2 + L^3,$$

$$\tilde{K}_5(\xi)=K_5+(b_3+2b_2K_2+3b_1K_3+4K_4)L+(\tfrac{3}{2}b_1^2 + 3b_2+7b_1K_2+6K_3)L+(\tfrac{13}{3}b_1+4K_2)L^3 + L^4, \tag{91}$$

where $b_i=\beta_i/\beta_0$ and $L=\beta_0\ln\xi$. The factor $\xi=s_0/s$ in Eq. (90) represents the arbitrary renormalization scale ambiguity of which the Adler function (86) is independent. The ξ dependence of the $K_i(\xi)$ coefficients is determined by inserting the expansion (81) into Eq. (90), and equating the two series obtained for $\xi=1$ and arbitrary ξ at each order in a_s.[14] The coefficients K_n are known up to third order in α_s^3. For $n\geqslant 2$ they depend on the renormalization scheme used, while the first two coefficients are universal

$$K_0=1,\quad K_1=1,\quad K_2(\overline{\mathrm{MS}})=F_3(\overline{\mathrm{MS}}),$$

$$K_3(\overline{\mathrm{MS}})=F_4(\overline{\mathrm{MS}})+\tfrac{1}{3}\pi^2\beta_0^2, \tag{92}$$

where $F_3(\overline{\mathrm{MS}})=1.9857-0.1153n_f$ and $F_4(\overline{\mathrm{MS}})=-6.6368-1.2001n_f-0.0052n_f^2$ are the coefficients of the perturbative series of $R_{e^+e^-}$. For $n_f=3$ one has $K_2=1.640$ and $K_3=6.371$. With the series (90), inserted into the right-hand side of Eq. (89), one obtains the perturbative expansion

$$\delta^{(0)}=\sum_{n=1}^{5}\tilde{K}_n(\xi)A^{(n)}(a_s), \tag{93}$$

with the functions

$$A^{(n)}(a_s)=\frac{1}{2\pi i}\oint_{|s|=s_0}\frac{ds}{s}\left[1-2\frac{s}{s_0}+2\left(\frac{s}{s_0}\right)^3 - \left(\frac{s}{s_0}\right)^4\right]a_s^n(-\xi s)$$
$$=\frac{1}{2\pi}\int_{-\pi}^{\pi}d\varphi[1+2e^{i\varphi} - 2e^{i3\varphi}-e^{i4\varphi}]a_s^n(\xi s_0 e^{i\varphi}), \tag{94}$$

where $s=-s_0e^{i\varphi}$ has been substituted in the second line and the integral path proceeds according to Fig. 17.

2. Fixed-order perturbation theory

Inserting the series (81) into Eq. (93), evaluating the contour integral, and collecting the terms with equal powers in a_s leads to the familiar expression (Le Diberder and Pich, 1992a)

$$\delta^{(0)}=\sum_n[\tilde{K}_n(\xi)+g_n(\xi)]\left(\frac{\alpha_s(\xi s_0)}{\pi}\right)^n, \tag{95}$$

where g_n are functions of $\tilde{K}_{m<n}$ and $\beta_{m<n-1}$ and of elementary integrals with logarithms of power $m<n$ in the integrand. Setting $\xi=1$ and replacing all known β_i and K_i coefficients by their numerical values, Eq. (95) simplifies to

$$\delta^{(0)}=a_s(s_0)+(1.6398+3.5625)a_s^2(s_0)+(6.371 + 19.995)a_s^3(s_0)+(K_4+78.003)a_s^4(s_0)+(K_5 + 14.250K_4-391.54)a_s^5(s_0)+(K_6+17.813K_5 + 45.112K_4+1.583\,33\beta_4-8062.1)a_s^6(s_0), \tag{96}$$

where for the purpose of later studies we have kept terms up to sixth order. When only two numbers are given in the parentheses, the first number corresponds to K_n and the second to g_n.

The fixed-order perturbation theory (FOPT) series is truncated at given order despite the fact that parts of the higher coefficients $g_{n>4}(\xi)$ are known to all orders and could be resummed. These known parts are higher- (up to infinite-) order terms of the expansion (81) that are functions of $\beta_{n\leqslant 3}$ and $K_{n\leqslant 3}$ only. In effect, beyond the use of the perturbative expansion of the Adler function (90), two approximations have been used to obtain the FOPT series (96): (i) the RGE (75) has been Taylor expanded and terms higher than the given FOPT order have been truncated, and (ii) this Taylor expansion is used to predict $a_s(-s)$ on the entire $|s|=s_0$ contour.

3. Contour-improved fixed-order perturbation theory

A more promising approach to the solution of the contour integral (94) is to perform a direct numerical

[14]Note that this procedure corresponds to a fixed-order perturbation theory rule since known higher-order pieces of the expansion (81) are neglected when solving

$$\frac{\partial}{\partial\xi}\sum_{n=0}^{N}\tilde{K}_n(\xi)a_s^n(-\xi s)=\frac{\beta[a_s^n(-\xi s)]}{\xi}\sum_{n=0}^{N}(n+1)\tilde{K}_n(\xi)a_s^n(-\xi s) + \sum_{n=0}^{N}a_s^{n+1}(-\xi s)\frac{\partial\tilde{K}_n(\xi)}{\partial\xi}\sim\mathcal{O}(a_s^{N+1}),$$

for a truncated series with maximum known order N. A resummation of the subleading logarithms has been proposed by Dams and Kleiss (2005).

evaluation by means of single-step integration and using the solution of the RGE to four loops as input for the running $a_s(-\xi s)$ at each integration step (Pivovarov, 1991, 1992; Le Diberder and Pich, 1992a). It implicitly provides a partial resummation of the (known) higher-order logarithmic integrals and improves the convergence of the perturbative series. While, for instance, the third-order term in the expansion (96) contributes some 17% to the total (truncated) perturbative prediction, the corresponding term of the numerical solution amounts only to 6% [assuming $\alpha_s(m_\tau^2)=0.35$]. This numerical solution of Eq. (93) will be referred to as contour-improved fixed-order perturbation theory (CIPT) in the following.

Single-step integration also avoids the Taylor approximation of the RGE on the entire contour, since a_s is iteratively computed from the previous step using the full known RGE.[15] Figure 18 shows the comparison between the iteratively evolved $\alpha_s(m_\tau^2 e^{i\varphi})$ (referred to as the exact solution) and fourth-order Taylor expansion (81) on the circle $\varphi=-\pi,\ldots,\pi$ (Menke, 1998). The differences appear to be significant far away from the reference value at $\varphi=0$. However, as shown below, the numerical effect of this discrepancy on the contour integral is small compared to the main difference between FOPT and CIPT, which is the truncation of the perturbative series after integration.

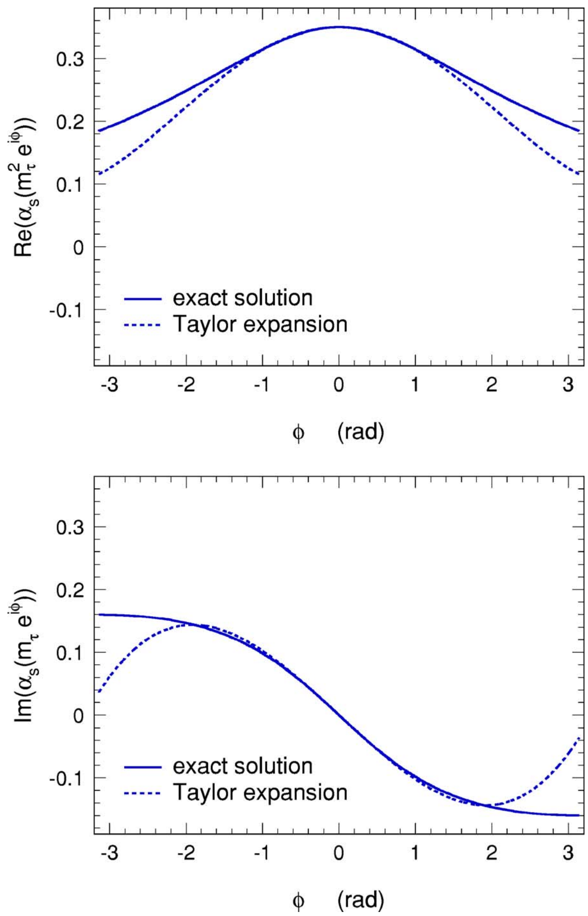

FIG. 18. (Color online) Comparison between the iteratively evolved $\alpha_s(m_\tau^2 e^{i\varphi})$ (exact solution) and fourth-order Taylor expansion (81) on the circle $\varphi=-\pi,\ldots,\pi$ (Menke, 1998). This example uses $\alpha_s(m_\tau^2)=0.35$.

4. Effective charge perturbation theory

Inspired by the pioneering work of Grunberg (1980); Stevenson (1981); Dhar (1983); Dhar and Gupta (1983, 1984), and the use of effective charges to approach the perturbative prediction of R_τ has become popular recently (Maxwell and Tonge, 1996, 1998; Raczka, 1998; Körner *et al.*, 2001a). The advocated advantage of this technique is that the perturbative prediction of the effective charge is renormalization scheme (RS) and scale invariant since it is a physical observable. The effective τ charge is defined by

$$a_\tau = \delta^{(0)}, \tag{97}$$

and obeys the RGE

$$\frac{da_\tau}{d\ln s} = \beta_\tau(a_\tau) = -a_\tau^2 \sum_{n=0}^{\infty} \beta_{\tau,n} a_\tau^n. \tag{98}$$

The first two terms in the expansion of β_τ are universal (i.e., RS independent), while higher-order terms must be computed using perturbation theory. The prescription for this computation is obtained from the relation between the renormalization scheme and scale used to obtain the FOPT coefficients in the series (95), and the requirement of RS and scale invariance. Since a_τ is scheme and scale invariant, its evolution coefficients $\beta_{\tau,i}$ have the same property. "Another way of looking at this is to say that the method of effective charges involves a specific choice of renormalization scheme and scale (…), so that the energy evolution of the observable is identical to the beta-function evolution of the coupling" (Dinsdale and Maxwell, 2005).

The function β_τ is obtained from

$$\frac{da_\tau}{da_s} = \frac{d\beta_\tau(a_\tau)}{d\beta(a_s)}, \tag{99}$$

which, setting $\xi=1$, can be rewritten in the form

$$\beta_\tau(a_\tau) = \frac{da_\tau}{d\ln s} = \frac{da_\tau}{da_s}\frac{da_s}{d\ln s}\bigg|_{a_s=a_s(a_\tau)} = \frac{da_\tau}{da_s}\beta(a_s)\bigg|_{a_s=a_s(a_\tau)}. \tag{100}$$

Inserting Eq. (95) for a_τ on the left-hand side and right-hand side of Eq. (100), and equating the coefficients for

[15]It has been tested that the single-step integration, i.e., $a_s(\xi s_0 e^{i(\varphi+\Delta\varphi)})$ is computed from $a_s(\xi s_0 e^{i\varphi})$, using a modified Euler method (that is, a Taylor expansion of a_s in each integration step), or using explicit fourth-order Runge-Kutta integration, leads to the same result, as far as the step size is chosen to be small enough (1000 integration steps on the contour are found to be largely sufficient).

each order in a_s leads to the coefficients[16]

$$\beta_{\tau,2} = \beta_2 - \beta_1 c_2 + \beta_0(-c_2^2 + c_3), \tag{101}$$

$$\beta_{\tau,3} = \beta_3 - 2\beta_2 c_2 + \beta_1 c_2^2 + 2\beta_0(2c_2^3 - 3c_2c_3 + c_4), \tag{102}$$

$$\beta_{\tau,4} = \beta_4 - 3\beta_3 c_2 + \beta_2(4c_2^2 - c_3) + \beta_1(-2c_2c_3 + c_4) + \beta_0(-14c_2^4 + 28c_2^2c_3 - 5c_3^2 - 12c_2c_4 + 3c_5), \tag{103}$$

where $c_i = K_i + g_i(1)$ [cf. Eq. (95)] and $\beta_{\tau,0} = \beta_0$, $\beta_{\tau,1} = \beta_1$ because $K_0 = K_1 = 1$. Inserting the known β_i and c_i coefficients, one finds (Körner *et al.*, 2001a)

$$\beta_{\tau,2} = -12.320,$$

$$\beta_{\tau,3} = -182.72 + 4.5K_4,$$

$$\beta_{\tau,4} = -236.2 + \beta_4 - 40.27K_4 + 6.75K_5,$$

$$\beta_{\tau,5} = 16427 - 20.80\beta_4 + \beta_5 - 521.6K_4 - 65.79K_5 + 9K_6, \tag{104}$$

with a noticeable sign alteration for $\beta_{\tau,2}$ (and also for $\beta_{\tau,3}$ if $K_4 < 40$). Neglecting nonperturbative contributions, one has

$$a_\tau(s_0) = R_{\tau,V+A}(s_0)/(3|V_{ud}|^2) - 1, \tag{105}$$

which using Eq. (22) and the $|V_{ud}|$ value given in Sec. IV yields $a_\tau(m_\tau^2) = 0.2219 \pm 0.0055$.

5. Estimating unknown higher-order perturbative coefficients

Compared with the $\overline{\text{MS}}$ RGE (75) the $\beta_\tau(a_\tau)$ series is significantly less convergent, taking into account that $a_\tau(m_\tau^2) \simeq 1.8a_s(m_\tau^2)$. This property has been used in the past to estimate an effective K_4^{eff} coefficient, which was found to be $K_4^{\text{eff}} \sim 27$ (Kataev and Starshenko, 1995). It approximates the true value of K_4 in the limit of vanishing higher-order contributions. In effect, the derivative of $a_\tau(m_\tau^2)$ with respect to K_4 is large[17]

$$\left.\frac{da_\tau(m_\tau^2)}{dK_4}\right|_{a_\tau(m_\tau^2)=0.22, K_4=25} \simeq 0.0020, \tag{106}$$

so that the precise experimental error on $a_\tau(m_\tau^2)$ allows us to predict K_4 with an accuracy of a few units, if we assume that subleading contributions can be neglected. However, this assumption is unfounded since, taking naively the unknown higher-order coefficients to grow like a geometric series, i.e., $z_n \sim z_{n-1}^2/z_{n-2}$, with $z = \beta, K$, and using the estimate $K_4 = 25$ so that $K_5 \sim 98$, $\beta_{\tau,4} \sim -360$ (with $\beta_4 \sim 222$), one finds

$$\left.\frac{da_\tau(m_\tau^2)}{dK_5}\right|_{a_\tau(m_\tau^2), K_4, K_5, \beta_4 \dots} \simeq 0.0004, \tag{107}$$

which is not small with respect to Eq. (106), in particular considering the coarseness of the assumptions that went into the estimate (107). It is found that even the sixth-order coefficient is not negligible. Assuming the same geometric growth, one would expect $K_6 \sim 395$ with a derivative of $da_\tau(m_\tau^2)/dK_6 \sim 5 \times 10^{-5}$, which appears small. However, considering that the uncertainty on K_6 is at least of the same size as its estimated value (which is probably still optimistic) generates an uncertainty in $a_\tau(m_\tau^2)$ that is equivalent to $\sigma(K_4) \sim 10$. Taking correspondingly the fifth-order uncertainty of the estimated value of K_5, we conclude that the systematic uncertainty on K_4 obtained with the effective charge scheme is at least of the order of $\sigma(K_4) \sim 23$.

Another method to estimate K_4^{eff} has been suggested by Le Diberder (1995). It consists of increasing the sensitivity of the CIPT prediction of $\delta^{(0)}$ on K_4 by reducing the renormalization scale ξ in Eq. (93). The result 27 ± 5 is consistent with the one obtained from ECPT. However, these methods are not independent as can be seen in the following. Using the integral (79), and taking $s \to \infty$ so that $a_\tau, a_s \to 0$, we can write (Stevenson, 1981)

$$\ln \frac{s}{\Lambda^2} - \ln \frac{s}{\Lambda_\tau^2} = 2 \ln \frac{\Lambda_\tau}{\Lambda} = \frac{1}{\beta_0 a_s(s)} - \frac{1}{\beta_0 a_\tau(s)} + \mathcal{O}(a_s) = c_2 + \mathcal{O}(a_s), \tag{108}$$

$$\Leftrightarrow \Lambda_\tau \simeq \Lambda e^{c_2/\beta_0} \approx 3.2\Lambda. \tag{109}$$

Since the asymptotic scale parameters are reciprocal to the scale, transforming FOPT into ECPT is equivalent to reducing the renormalization scale, at lowest order.

In terms of the measurement of $\alpha_s(m_\tau^2)$ the three perturbative methods FOPT, CIPT, and ECPT use similar information. However, their dependence on the unknown higher-order coefficients $K_{n\geqslant 4}$ can be dramatically different. Figure 19 shows the evolution of $a_\tau(s_0)$ for FOPT, CIPT, with renormalization scales $\xi = 1$ and $\xi = 0.4$, and ECPT, all normalized to $a_\tau(m_\tau^2) = 0.22$. The solid lines correspond to fifth-order perturbation theory with assumed $K_4 = 25$, $K_5 = 98$, and for variations of these (dashed and dotted lines). One observes relatively small dependence for FOPT and CIPT with $\xi = 1$, while large and very large effects are found with CIPT ($\xi = 0.4$) and

[16]For completeness we also give the sixth-order coefficient, which is later needed for extrapolation tests

$$\beta_{\tau,5} = \beta_5 - 4\beta_4 c_2 + 2\beta_3(4c_2^2 - c_3) + 4\beta_2(-2c_2^3 + c_2c_3) + \beta_1(-6c_2^4 + 16c_2^2c_3 - 3c_3^2 - 8c_2c_4 + 2c_5) + 4\beta_0(12c_2^5 - 30c_2^3c_3 + 12c_2c_3^2 + 14c_2^2c_4 - 4c_3c_4 - 5c_2c_5 + c_6).$$

[17]One can obtain the solution for $a_\tau(m_\tau^2)$ as a function of β_τ coefficients without explicitly integrating the RGE (98), by using a fixed point of the differential equation with the one-loop solution at $s \to \infty$, $\Lambda^2 = s e^{-1/\beta_0 a_\tau(s)}$, so that the four-loop $a_\tau(\infty \to m_\tau^2)$ evolution reproduces the experimental value. This gives $\Lambda = 0.41$ GeV.

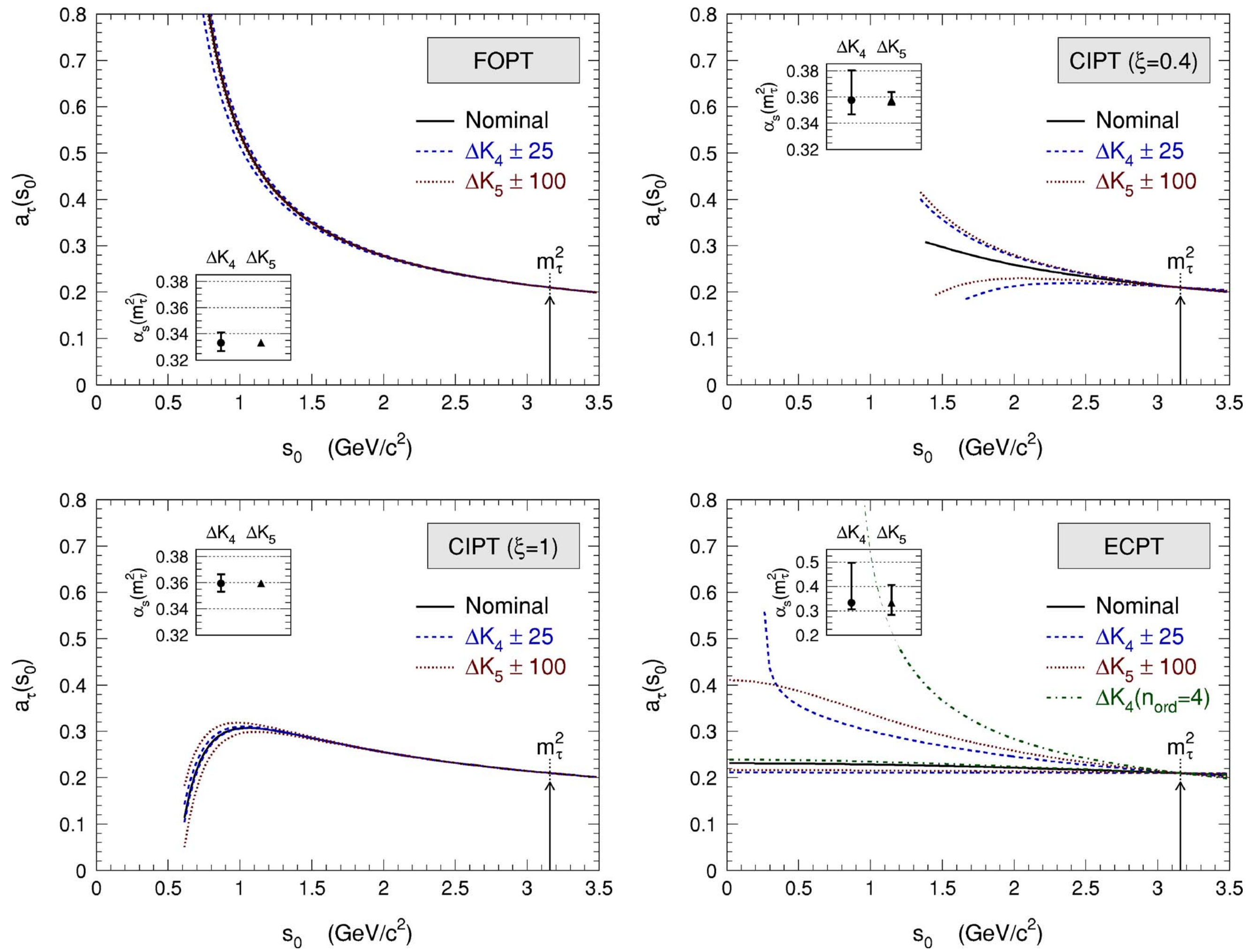

FIG. 19. (Color online) Evolution of $a_\tau(s_0)$ for different perturbative methods, and for variations of the unknown higher-order perturbative coefficients K_4 (dashed) and K_5 (dotted). All methods are normalized to $a_\tau(m_\tau^2)=0.22$. The inseted frames give the $\alpha_s(m_\tau^2)$ values derived from this a_τ value in the respective methods. The error bars show uncertainties, added in quadrature, from the K_4 and K_5 variations quoted on the plots.

ECPT. The latter effect provides sensitivity to estimate the unknown coefficients. To better analyze this sensitivity, we have compared the ΔK_4 variation in fifth-order ECPT to the fourth-order effect (dash-dotted line in the lower right-hand plot of Fig. 19). Including the bold estimate for the next order significantly reduces the dependence on the K_4 term. This cancellation becomes obvious when looking at the numerical expansion (104): the K_4 coefficient enters $\beta_{\tau,3}$ and $\beta_{\tau,4}$ with different signs, and with a larger coefficient at fifth order to compensate for the a_τ suppression. Similar behavior is observed for K_5 when turning on the sixth-order term. We conclude that for the K_4 term the strong K_5 dependence observed in ECPT is (by part) an artifact of the truncation of the perturbative series, and it is therefore dangerous to use it for an estimate of the unknown coefficients.

The embedded frames in Fig. 19 give the $\alpha_s(m_\tau^2)$ values derived from the given a_τ value in the respective methods. The error bars indicate the uncertainty, added in quadrature, from the K_4 and K_5 variations as quoted. One observes that the difference in α_s between FOPT and CIPT is not covered by the uncertainties on K_4 and K_5. This is because the main contribution to the difference in these methods is due to the truncation of the *known* higher-order terms of the Taylor expansion after the contour integration, rather than due to the unknown coefficients. Due to the good convergence of these series, the dependence on the K_5 coefficient is marginal.

It should be mentioned that a large computational effort is underway with the goal to calculate the K_4 coefficient. The large number of five-loop diagrams needed to calculate the two-point current correlator at this order is somewhat discouraging, however, the results on two gauge-invariant subsets are already available. The subset of order $\mathcal{O}(\alpha_s^4 n_f^3)$ was evaluated long ago through the summation of renormalon chains (Beneke, 1993), while the much harder subset $\mathcal{O}(\alpha_s^4 n_f^2)$ was recently calculated (Baikov *et al.*, 2002). The known parts amount to about half of the expected K_4 coefficient assuming a geometric growth. Using the results of Kataev and Starshenko (1995) for different n_f obtained with the effective charge method, it is possible to compare the n_f^2 estimated term at the α_s^4 order of the Adler function expansion ($3.64n_f^2$) with the newly computed one ($1.875n_f^2$). The difference provides a conservative estimate for the uncertainty of the ECPT procedure to predict the full K_4 term, as one could expect the sum of all $\alpha_s^4 n_f^i$ terms to be closer to the true value than the term-by-term comparison. A successful test of the procedure has been performed for K_3, where all $\alpha_s^3 n_f^i$ terms are exactly known. The two unknown remaining terms $\mathcal{O}(\alpha_s^4 n_f^1)$ and $\mathcal{O}(\alpha_s^4 n_f^0)$, the direct calculation of which is prevented by the present computing power available to this project, have been estimated (Baikov *et al.*, 2003) to be

$$K_4 = -0.010\,09n_f^3 + 1.875n_f^2 - 31.8n_f + 105.7, \qquad (110)$$

where the first two terms are known exactly. The calculation for $n_f=3$ yields $K_4 \simeq 27$ with an uncertainty estimated to ± 16 (Baikov *et al.*, 2003).

6. Infrared behavior of the effective charge

In the effective charge scheme, the physical coupling should have a finite infrared behavior and hence must not suffer from the Landau pole that lets $\overline{\text{MS}}$ (but also momentum subtraction schemes) break down below a scale $\sqrt{s} \sim 1$ GeV. The universal two-loop function $\beta_\tau(a_\tau)$ does, however, suffer from a singularity at $\sqrt{s} \sim 1.1$ GeV [for $a_\tau(m_\tau^2)=0.22$]. Only adding the negative three-loop coefficient regularizes $\beta_\tau(a_\tau)$ and leads to a freezing $a_\tau(s\to 0) \simeq 0.62$. Adding higher orders does not qualitatively alter this behavior, however, the freezing value is unstable against variations of the unknown coefficients (which again exhibits the mediocre convergence of the ECPT series). The lower right-hand plot of Fig. 19 shows the evolution of $a_\tau(s)$ for different orders and assumptions upon the unknown higher-order coefficients [cf. the discussion by Brodsky *et al.* (2002)].

7. Renormalons and the large-β_0 expansion

The perturbative series in quantum field theory[18]

$$R_N = \sum_{n=0}^{N} r_n \alpha^{n+1}, \qquad (111)$$

be they Abelian or not, are divergent at $N\to\infty$ for any value of α. Because the number of Feynman graphs increases at each order n, one expects a factorial growth of the perturbative coefficients of the corresponding S-matrix series

[18]The suppression of the constant term in the definition of Eq. (111) is convenient to avoid $1/\alpha$ terms in the definition of the Borel integral (115). It is without consequence for the following discussion.

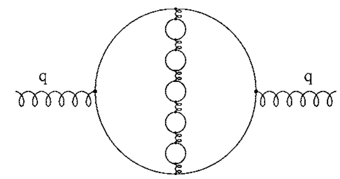

FIG. 20. Multifermion loop insertion (renormalons) into a fermion-antifermion vacuum-polarization diagram.

$$r_n \sim K a^n n! n^\gamma, \qquad (112)$$

with constant K, a, γ. The divergent behavior of perturbative expansions often has physical significance: it indicates the nonperturbative structure of the vacuum and its excitations. To be a useful approximation of the true value R, the series (111) must be *asymptotic to* R for given α, i.e., it exists a number K_N so that[19] $|R-R_N| < K_{N+1}\alpha^{N+2}$. If $r_n \sim K_n$, the best approximation of R is achieved when the series is truncated at its minimal (absolute) term and the truncation error can be roughly estimated by the size of the minimal term. The accuracy in the point of minimal sensitivity depends on the strength of the perturbative expansion parameter (the coupling). The larger it is, the lower the order when minimal sensitivity is reached, and the worse is the approximation. Note that as long as the computed order is below the order of minimal sensitivity, there is no actual difference between a divergent or a convergent series.

A convenient way to deal with this divergence is to consider the Borel transform

$$B[R](t) \equiv \sum_{n=0}^{\infty} \frac{r_n}{n!} t^n, \qquad (113)$$

which is believed to have a finite radius of convergence in the t plane (Mueller, 1992). The nth fixed-order perturbation coefficient is then generated by the nth derivative

$$r_n = \left. \frac{d^n B[R](t)}{dt^n} \right|_{t=0}. \qquad (114)$$

The explicit factor $n!$ in the denominator of $B[R](t)$ makes the Borel-transformed series much better behaved. Summing up all orders leads to the integral representation[20]

[19]Our discussion of renormalons has greatly benefited from the comprehensive review given by Beneke (1999).

[20]The Borel integral is easily derived using the integral representation $n! = \int_0^\infty dv \exp(-v) v^n$, and exchanging summation and integration in Eq. (111) [see, e.g., Lovett-Turner and Maxwell (1994)]. Note, however, that this interchange is formally not justified in presence of the Landau pole for the coupling constant.

$$R(\alpha) = \int_0^\infty dt e^{-t/\alpha} B[R](t). \tag{115}$$

If the integral exists, it gives the Borel sum of the original divergent series. Existence requires that $B[R](t)$ has no singularities in the integration range. However, for a factorial behavior akin to Eq. (112) (nonalternating series), the Borel transform is given by $B[R](t) \propto (1-at)^{-1-\gamma}$. Hence if γ is positive there exists a singularity $t=1/a$ so that the integral (115) does not exist. Indeed, "the divergent behavior of the original series is encoded in the singularities of its Borel transform" (Beneke, 1999). One notices that the larger a, i.e., the faster diverging the series is, the singularity moves closer to zero.

Let us consider a renormalized fermion-loop insertion into a quark-antiquark vacuum-polarization diagram (cf. one bubble in Fig. 20). Assuming dominance of the $[\beta_0 a_s(-s)]^n$ term (denoted as the *large-β_0 expansion*), one can resum this chain with a large number of n bubbles. If one neglects higher-order terms of the β function, it is thus possible to derive estimates for the FOPT coefficients of a given perturbative series at all orders. This assumption is supported empirically by the observation that the β_0 term dominates second-order radiative corrections for many observables in the $\overline{\text{MS}}$ scheme (Ball *et al.*, 1995). (We shall, however, anticipate here that the accuracy of these estimates is insufficient for the purpose of a precise perturbative prediction of R_τ, and difficult to control.) The procedure provides a *naive non-Abelianization* of the theory since lowest-order radiative corrections do not include gluon self-coupling.

Following this line, the Adler function can be expanded as (Beneke and Braun, 1999)

$$D(s) = 1 + a_s \sum_{n=0}^{N} a_s^n (d_n \beta_0^n + \delta_n), \tag{116}$$

where the coefficients d_n are computed in terms of fermion bubble diagrams[21] (see Fig. 20). The $\overline{\text{MS}}$ Borel transform of Eq. (116) is given by (Beneke, 1993; Broadhurst, 1993)

[21]One identifies the coefficients d_n in Eq. (116) with their leading-n_f pieces $d_n^{[n]}$ in $d_n = d_n^{[n]} n_f^k + \cdots + d_k^{[0]}$. It has been shown by Broadhurst (1993) that the $d_n^{[n]}$ in $\overline{\text{MS}}$ are given by ($s=\mu^2$)

$$d_n^{[n]} = 2^{1-n} n! \sum_{k=0}^{n} \left(-\frac{5}{9}\right)^k \frac{\Psi_{n+2-k}^{[n+2-k]}}{k!(n-k)!},$$

with the generating function

$$\Psi_m^{[m]} = \frac{3^{2-m}}{2} \left(\frac{d}{dx}\right)^{m-2} P(x)\bigg|_{x=1}, \quad \text{and}$$

$$P(x) = \frac{32}{3(1+x)} \sum_{k=2}^{\infty} \frac{(-1)^k k}{(k^2-x^2)^2}.$$

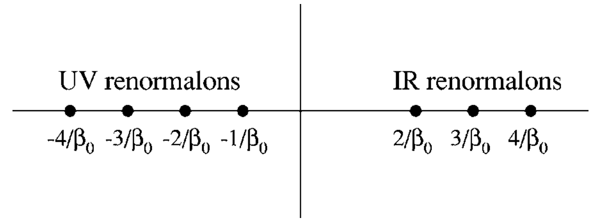

FIG. 21. Ultraviolet (UV) and infrared (IR) renormalons in the Borel plane of the Adler function.

$$B[D](u) = \frac{32\pi}{3} e^{5/3u} \frac{u}{1-(1-u)^2} \sum_{k=2}^{\infty} \frac{(-1)^k k}{[k^2-(1-u)^2]^2}, \tag{117}$$

where $u=-\beta_0 t$, and where we have chosen the renormalization scale to be equal to the momentum scale. Neglecting corrections δ_n, the series (116) leads to the large-β_0 expansion of $D(s)$. The first elements of the series are

$$d_0 = 1, \quad d_1\beta_0 = 0.496, \quad d_2\beta_0^2 = 15.71,$$
$$d_3\beta_0^3 = 24.83, \quad d_4\beta_0^4 = 787.8, \quad d_5\beta_0^5 = -1991, \tag{118}$$

which compare only coarsely with the exact terms (92) where these are known. The Borel transform $B[D](u)$ has singularities on the real axis, which can be distinguished in infrared (IR renormalons) for small virtuality, and ultraviolet singularities (UV renormalons) for high virtuality of the exchanged gluon. One finds an infinite sequence of IR (UV) renormalons at positive (negative) integer u, with the exception of $u=1$ (see Fig. 21).

The integral (115) may still be solvable in the presence of renormalons by acquiring an imaginary part from moving the integration contour above or below the real axis. The associated ambiguity is exponentially small in the expansion parameter α, and is therefore of nonperturbative origin. Correspondingly, the IR poles give rise to ambiguities when one uses the generators (114) to recompute $D(s)$ from its Borel transform. Using in first order

$$a_s(s) = \frac{1}{\beta_0 \ln(s/\Lambda^2)}, \tag{119}$$

one obtains for the associated ambiguity for $u=2,3,\ldots,$

$$\Delta D(s) \sim e^{-u/\beta_0 a_s} = \left(\frac{\Lambda^2}{s}\right)^u. \tag{120}$$

These IR renormalons proportional to $(\Lambda^2/s)^u$ are reabsorbed into the nonperturbative terms of the OPE. The absence of a $u=1$ IR renormalon is thereby related to the impossibility to build a gauge-invariant operator of dimension $D=2$, which is an important property that is exploited for the determination of α_s from R_τ. The lowest IR renormalon is hence of the order $(\Lambda^2/s)^2$. On the contrary to UV renormalons, this term is scale independent and cannot be decreased (Beneke and Zakharov, 1992). It should therefore have physical meaning and can be identified with the gluon condensate $\langle 0|G_{\mu\nu}G^{\mu\nu}|0\rangle$ as the leading infrared contribution to the Adler function. However, while IR renormalons lead to nonperturbative operators for power corrections, it does not necessarily contain all of them. For example, at $D=4$ one misses the quark condensate $\langle 0|q\bar{q}|0\rangle$, which is generated by chiral symmetry breaking that does not occur in perturbation theory.

Due to asymptotic freedom, governed by the negative sign in front of the RGE β function, UV renormalons arise on the negative real axis[22] (on the contrary to QED where they occur on the positive side) so that they are outside the integration range of Eq. (115) and insofar harmless, that is, Borel summable (Mueller, 1992). Let us return for a moment to the series (111) in the large-β_0 expansion. For large n, the factorial growth of the perturbation series is dominated by the contribution of the leading UV renormalon $k=-1$ with alternating coefficients $r_n \sim n! n^{\gamma}(-\beta_0)^n$. A guess at which order $N_{\min}$ minimal sensitivity is achieved can be obtained from the argument that the series is convergent, i.e., reliable at order $n+1$ if $\alpha(r_{n+1}/r_n<1)$. Considering leading IR and UV renormalons only, one finds from the asymptotic behavior $r_{n+1}/r_n \sim n\beta_0/2$ (IR) and $r_{n+1}/r_n \sim -n\beta_0$ (UV). Hence the breakdown of convergence is first caused by the UV renormalon and $N_{\min} \sim 1/\beta_0 a_s$ is of order 1. A series truncated at finite order brings an intrinsic limitation of accuracy along with it. The associated error is estimated with the magnitude of the order $N=N_{\min}$ term of the perturbative series. That gives using for the leading UV renormalon

$$|r_N| a_s^N \sim N! N^{\gamma}(-\beta_0 a_s)^N \sim \frac{\Lambda^2}{s} \times \text{logarithms}, \tag{121}$$

where the right-hand side is obtained with the use of the Stirling formula, and where we have fixed the renormalization scale at $\mu^2=s$. The truncation of the perturbative series is accompanied by an uncertainty which scales like $1/s$, i.e., with apparent dimension $D=2$. This contribution is, however, not to be confounded with nonperturbative IR renormalon ambiguities.[23] Similarly to Eq. (116) the R_τ FOPT series (95) can be written as

$$\delta^{(0)}(s) = 1 + a_s \sum_{n=0}^{N} a_s^n (d_n^\tau \beta_0^n + \delta_n^\tau), \tag{122}$$

where $d_n^\tau \beta_0^n + \delta_n^\tau = K_{n+1} + g_{n+1}(1)$. Inserting Eq. (117) into Eq. (89), and taking advantage of the factorized s dependence in the large-β_0 expansion, the Borel transform of Eq. (122) is (Beneke, 1993)

$$B[R_\tau](u) = B[D](u)\frac{\sin(\pi u)}{\pi}\left(\frac{1}{u} + \frac{2}{1-u} + \frac{3}{3-u}\frac{1}{4-u}\right). \tag{123}$$

The first elements of the series are

$$d_0^\tau = 1, \quad d_1^\tau \beta_0 = 5.119, \quad d_2^\tau \beta_0^2 = 28.78,$$

$$d_3^\tau \beta_0^3 = 156.6, \quad d_4^\tau \beta_0^4 = 900.9, \quad d_5^\tau \beta_0^5 = 4867. \tag{124}$$

They compare reasonably well with the exact terms (96) where these are known. In this approach, the unknown fixed-order fourth-order coefficient is estimated to be $K_4 \sim 79$, which is significantly larger than the estimate based on ECPT, and also larger than the one obtained from the large-β_0 expansion of the Adler function (118).

Apart from the conceptual interest in the study of renormalons, the main question regarding the concrete use of the large-β_0 expansion certainly is: How large are the uncertainties? From Eq. (124) we see that the series is positive and that minimal sensitivity is reached at $n \sim 5$. On the other hand, the resummation of the known $g_n(\xi)$ coefficients (96) shows that large negative coefficients occur at higher-order FOPT so that one would need a far larger than a geometric growth of the K_n coefficients to keep the series positive. A direct comparison between the large-β_0 expansion coefficients for the Adler function with the exact calculation (92) reveals an oscillating behavior of the large-β_0 series, i.e., small d_n coefficients for n even and large d_n for n odd. For example, the large-β_0 d_3 coefficient is overestimated. One also has to worry about important contributions from the d_5 term, which is found to be 788. As a consequence, our conclusion is that the uncertainties associated with the large-β_0 expansion are not under sufficient control to improve the perturbative prediction of R_τ. It is also an unreliable estimator of the uncertainty of the perturbative series.

8. Comparison of perturbative methods

Some comparisons between fixed-order perturbative methods have already been given for the discussion of estimating the unknown higher-order coefficients in Sec. VII.B.5. The slow convergence of ECPT (and CIPT at small renormalization scales, $\xi \ll 1$) has been pointed out in this respect. To further study the convergence of the perturbative series, we give in Table V contributions of the different orders in PT to $\delta^{(0)}$ for the various approaches and using $\alpha_s(m_\tau^2)=0.35$. We assumed here $K_4=25$ and a geometric growth of all other unknown PT and RGE coefficients. In the case of CIPT the results are given for the various techniques used to evolve $\alpha_s(s_0 e^{i\varphi})$: the truncated Taylor expansion (81), Runge-Kutta integration of the RGE with $\xi=1$, and Runge-Kutta integration with $\xi=0.4$.

As advocated by Le Diberder and Pich (1992a), faster convergence is observed for CIPT compared to FOPT yielding a significantly smaller error associated with the

[22]In QCD, the presence of IR renormalons implies that nonperturbative corrections should be added to define the theory unambiguously. The same is true for UV renormalons in QED. This corresponds to the observation of large coupling constants in the respective energy regimes.

[23]It has been shown iby Beneke and Zakharov (1992) that the truncation uncertainty at $N_{\min}$ scales as $\Lambda^2 s/\mu^4$ once the renormalization scheme dependence of Λ is taken into account.

TABLE V. Massless perturbative contribution to $R_\tau(m_\tau^2)$ for the various methods considered, and at orders $n\geqslant 1$ with $\alpha_s(m_\tau^2)=0.35$. The value of K_4 is set to 25, while all unknown higher-order $K_{n>4}$ and $\beta_{n>3}$ coefficients are assumed to follow a geometric growth.

Perturbative method	δ^0							
	$n=1$	$n=2$	$n=3$	$(n=4)$	$(n=5)$	$(n=6)$	$\sum_{n=1}^{4}$	$\sum_{n=1}^{6}$
FOPT ($\xi=1$)	0.1114	0.0646	0.0365	0.0159	0.0010	−0.0086	0.2283	0.2208
CIPT (Taylor RGE, $\xi=1$)	0.1573	0.0317	0.0126	0.0042	0.0011	0.0001	0.2058	0.2070
CIPT (full RGE, $\xi=1$)	0.1524	0.0311	0.0129	0.0046	0.0013	0.0002	0.2009	0.2025
CIPT (full RGE, $\xi=0.4$)	0.2166	−0.0133	0.0006	−0.0007	0.0010	−0.0007	0.2032	0.2048
ECPT	0.1442	0.2187	−0.1195	−0.0344	−0.0160	−0.0120	0.2090	0.1810
Large-β_0 expansion	0.1114	0.0635	0.0398	0.0241	0.0155	0.0093	0.2388	0.2636

renormalization scale ambiguity (while, somewhat counterintuitive, the uncertainty due to the unknown K_4 and higher-order coefficients is similar in both approaches). Our coarse extrapolation of higher-order coefficients could indicate that minimal sensitivity is reached at $n\sim 5$ for FOPT, while the series further converges for CIPT. Although the Taylor expansion in the CIPT integral exhibits significant deviations from the exact solution on the integration circle (cf. Fig. 18), the actual numerical effect from this on $\delta^{(0)}$ is small (cf. second and third columns in Table V). As discussed in Sec. VII.B.4, the convergence of the ECPT series is much worse than for FOPT and CIPT. Consequently, the difference between truncation at $n=4$ and $n=6$ is expected to be significant. Similar behavior is observed for the large-β_0 expansion.

The CIPT series is found better behaved than FOPT (as well as ECPT) and is therefore preferred for the numerical analysis of the τ hadronic width. As a matter of fact, the difference in the result observed when using a Taylor expansion and truncating the perturbative series after integrating along the contour (FOPT) with the exact result at given order (CIPT) is exhibiting the incompleteness of the perturbative series. However, it is even worse than that since large known coefficients are neglected in FOPT so that the difference between CIPT and FOPT is actually overstating the perturbative truncation uncertainty. This can be verified by studying the behavior of this difference for the various orders in perturbation theory given in Table V. The CIPT-vs-FOPT discrepancy increases with the addition of each order, up to order four where a maximum is reached. Adding the fifth order does not reduce the effect, and only beyond fifth order the two evaluations become asymptotic to each other. As a consequence varying the unknown higher-order coefficients *and* using the difference between FOPT and CIPT as indicator of the theoretical uncertainties overemphasizes the truncation effect.

9. Quark-mass and nonperturbative contributions

Following Shifman, Vainshtein, and Zakharov (Shifman *et al.*, 1979a 1979b, 1979c), the first contribution to R_τ beyond the $D=0$ perturbative expansion is the nondynamical quark mass correction of dimension[24] $D=2$, i.e., corrections in powers of $1/s_0$. The leading $D=2$ corrections induced by light-quark masses are computed using running quark masses evaluated at the two-loop level. Evaluation of the contour integral in FOPT leads to (Braaten *et al.*, 1992)

$$\delta^{(2\text{-mass})}_{ud,V/A} = -8\left(1+\frac{16}{3}a_s(s_0)\right)\frac{m_u^2(s_0)+m_d^2(s_0)}{s_0} \pm 4\left(1+\frac{25}{3}a_s(s_0)\right)\frac{m_u(s_0)m_d(s_0)}{s_0}, \tag{125}$$

where $m_i(s_0)$ are running quark masses evaluated at the scale s_0 using the RGE γ function (76). The following values are used by ALEPH for the renormalization-group invariant quark mass parameters $\hat{m}_i$ defined in Eq. (80):

$$\hat{m}_u = 8.7\pm 1.5\ \text{MeV},\quad \hat{m}_d = 15.4\pm 1.5\ \text{MeV},$$

$$\hat{m}_s = 270\pm 30\ \text{MeV}. \tag{126}$$

The dimension $D=4$ operators have dynamical contributions from the gluon condensate $\langle a_s GG\rangle$ and light u,d quark condensates $\langle m_i q_i q_j\rangle$, which are the matrix elements of the gluon field strength squared and the scalar quark densities, respectively. Remaining $D=4$ operators are running quark masses to the fourth power. Inserting the Wilson coefficients of these operators (Becchi *et al.*, 1981; Broadhurst, 1981; Chetyrkin *et al.*, 1985; Generalis, 1989) in the contour integral one obtains (Braaten *et al.*, 1992)

[24]Corrections of dimension $D=2$ refer to the mass dependence of the perturbative OPE coefficients of the unit operator.

$$
\begin{aligned}
\delta^{(4)}_{ud,V/A} = & \frac{11}{4}\pi^2 a_s^2(s_0)\frac{\langle a_s GG\rangle}{s_0^2} \\
& + 16\pi^2\left[1+\frac{9}{2}a_s^2(s_0)\right]\frac{\langle (m_u \mp m_d)(\bar{u}u \mp \bar{d}d)\rangle}{s_0^2} \\
& - 18\pi^2 a_s^2(s_0)\left[\frac{\langle m_u\bar{u}u + m_d\bar{d}d\rangle}{s_0^2}\right. \\
& \left. + \frac{4}{9}\sum_{k=u,d,s}\frac{\langle m_k\bar{q}_k q_k\rangle}{s_0^2}\right] - \left[\frac{48}{7}\frac{1}{a_s(s_0)} - \frac{22}{7}\right] \\
& \times \frac{[m_u(s_0) \mp m_d(s_0)][m_u^3(s_0) \mp m_d^3(s_0)]}{s_0^2} \\
& \pm 6\frac{m_u(s_0)m_d(s_0)[m_u(s_0) \mp m_d(s_0)]^2}{s_0^2} \\
& + 36\frac{m_u^2(s_0)m_d^2(s_0)}{s_0^2}. \qquad (127)
\end{aligned}
$$

Where two signs are given the upper (lower) one is for V (A). The gluon condensate vanishes in first order $\alpha_s(s_0)$. However, there appear second-order terms in the Wilson coefficients due to the s dependence of a_s, which after integration becomes a_s^2.

The contributions from dimension $D=6$ operators are complex. The most important operators arise from four-quark dynamical effects of the form $\bar{q}_i\Gamma_1 q_j \bar{q}_k \Gamma_2 q_l$. Other operators, such as the triple gluon condensate whose Wilson coefficient vanishes at order α_s, or those which are suppressed by powers of quark masses, are neglected in the evaluation of the contour integrals performed by Braaten *et al.* (1992). The large number of independent operators of the four-quark type occurring in the $D=6$ term can be reduced by means of the *factorization* (or *vacuum saturation*) assumption (Shifman *et al.*, 1979a, 1979b, 1979c) to leading order α_s. The operators are then expressed as products of scale-dependent two-quark condensates $\alpha_s(\mu)\langle\bar{q}_i q_i(\mu)\rangle\langle\bar{q}_j q_j(\mu)\rangle$. To take into account possible deviations from the vacuum saturation assumption, one can introduce an effective scale-independent operator $\rho\alpha_s\langle\bar{q}q\rangle^2$ that replaces the above product. The effective $D=6$ term obtained in this way is (Braaten *et al.*, 1992)

$$
\delta^{(6)}_{ud,V/A} \simeq \begin{pmatrix} 7 \\ -11 \end{pmatrix} \frac{256\pi^4}{27}\frac{\rho\alpha_s\langle\bar{q}q\rangle^2}{s_0^3}, \qquad (128)
$$

predicting a different sign and hence a partial cancellation between vector and axial-vector contributions.[25]

The dimension $D=8$ contribution has a structure of nontrivial quark-quark, quark-gluon, and four-gluon condensates whose explicit form has been given by Broadhurst and Generalis (1985). For the theoretical prediction of R_τ it is custom to absorb the complete long- and short-distance parts into the scale-invariant phenomenological $D=8$ operator $\langle\mathcal{O}_8\rangle$, which is fit simultaneously with α_s and other unknown nonperturbative operators to date.

Higher-order contributions from $D\geq 10$ operators are expected to be small as, equivalent to the gluon condensate, constant terms and terms in leading order α_s vanish in Eq. (83) after integrating over the contour.

[25] It has been pointed out by Chetyrkin and Kwiatkowski (1993) that Eq. (128) assumes that the same ρ parameter can be used for both vector and axial-vector contributions.

C. Results

It was shown by Le Diberder and Pich (1992b) that one can exploit the shape of spectral functions to obtain additional constraints on $\alpha_s(s_0)$ and—more importantly—on nonperturbative effective operators. The τ *spectral moments* at $s_0=m_\tau^2$ are defined by

$$
R^{k\ell}_{\tau,V/A} = \int_0^{m_\tau^2} ds\left(1-\frac{s}{m_\tau^2}\right)^k\left(\frac{s}{m_\tau^2}\right)^\ell \frac{dR_{\tau,V/A}}{ds}, \qquad (129)
$$

where $R^{00}_{\tau,V/A}=R_{\tau,V/A}$. The factor $(1-s/m_\tau^2)^k$ suppresses the integrand at the crossing of the positive real axis where the validity of the OPE less certain (Braten, 1998) and the experimental accuracy is statistically limited. Its counterpart $(s/m_\tau^2)^\ell$ projects upon higher energies. The spectral information is used to fit simultaneously $\alpha_s(m_\tau^2)$ and the effective operators $\langle a_s GG\rangle$, $\rho\alpha_s\langle\bar{q}q\rangle^2$, and $\langle\mathcal{O}_D\rangle$ for dimension $D=4$, 6, and 8, respectively. Due to the intrinsic experimental correlations only five moments are used as input to the fit.

In analogy to R_τ, contributions to the moments originating from perturbative and nonperturbative QCD are decomposed through the OPE,

$$
\begin{aligned}
R^{k\ell}_{\tau,V/A} = & \tfrac{3}{2}|V_{ud}|^2 S_{\rm EW}\Big(1+\delta^{(0,k\ell)}+\delta'_{\rm EW}+\delta^{(\text{2-mass},k\ell)}_{ud,V/A} \\
& + \sum_{D=4,6,\ldots}\delta^{(D,k\ell)}_{ud,V/A}\Big). \qquad (130)
\end{aligned}
$$

The prediction of the perturbative contribution takes the form

$$
\delta^{(0,k\ell)} = \sum_{n=1}^{3}\tilde{K}_n(\xi)A^{(n,k\ell)}(a_s), \qquad (131)
$$

with the functions

$$
\begin{aligned}
A^{(n,k\ell)}(a_s) = & \frac{1}{2\pi i}\oint_{|s|=m_\tau^2}\frac{ds}{s}\left[2\Gamma(3+k)\left(\frac{\Gamma(1+\ell)}{\Gamma(4+k+\ell)}\right.\right. \\
& \left. + 2\frac{\Gamma(2+\ell)}{\Gamma(5+k+\ell)}\right) - I\left(\frac{s}{s_0},1+\ell,3+k\right) \\
& \left. - 2I\left(\frac{s}{s_0},2+\ell,3+k\right)\right]a_s^n(-\xi s), \qquad (132)
\end{aligned}
$$

which make use of the elementary integrals $I(\gamma,a,b) = \int_0^\gamma t^{a-1}(1-t)^{b-1}dt$. The contour integrals are numerically solved for the running $a_s(-\xi s)$ (CIPT).

In the chiral limit and neglecting the small logarithmic s dependence of the Wilson coefficients, the dimension D nonperturbative contributions in Eq. (130) read

$$\delta^{(D,k\ell)}_{ud,V/A} = 8\pi^2 \begin{pmatrix} (D=2) & (D=4) & (D=6) & (D=8) & (D=10) & (k,\ell) \\ 1 & 0 & -3 & -2 & 0 & (0,0) \\ 1 & 1 & -3 & -5 & -2 & (1,0) \\ 0 & -1 & -1 & 3 & 5 & (1,1) \\ 0 & 0 & 1 & 1 & -3 & (1,2) \\ 0 & 0 & 0 & -1 & -1 & (1,3) \end{pmatrix} \sum_{\dim \mathcal{O}=D} C^{(1+0)}(\mu)\frac{\langle \mathcal{O}_D(\mu)\rangle_{V/A}}{m_\tau^D}, \qquad (133)$$

where the matrix is defined by the choice of coefficients for moments $k=1$, $\ell=0,1,2,3$ and the corresponding dimension D.[26] For completeness, we also give the coefficients for dimension $D=10$, which is not considered by experiments since they do not contribute to $R^{00}_{\tau,V/A}$ at leading order. With increasing weight ℓ contributions from low dimensional operators vanish. For example, the only nonperturbative contribution to the moment $R^{13}_{\tau,V/A}$ stems from dimension $D=8$ and beyond. Hence in a fit using spectral moments $D=8$ will be determined by $R^{13}_{\tau,V/A}$. This observation is in some sense a "paradox," as higher moments project upon higher masses on the contrary to R_τ and the spirit of the OPE, where the higher dimension terms are enhanced at small s_0.

For practical purpose it is more convenient to define moments that are normalized to the corresponding $R_{\tau,V/A}$ in order to decouple the normalization from the shape of the τ spectral functions

$$D^{k\ell}_{\tau,V/A} = \frac{R^{k\ell}_{\tau,V/A}}{R_{\tau,V/A}}. \qquad (134)$$

The two sets of experimentally almost uncorrelated observables—$R_{\tau,V/A}$, on one hand, and the spectral moments, on the other hand—yield independent constraints on $\alpha_s(m_\tau^2)$ and thus provide an important test of consistency. The correlation between these observables is completely negligible in the $V+A$ case where $R_{\tau,V+A}$ is calculated from the difference $R_\tau - R_{\tau,S}$, which has no correlation with the hadronic invariant mass spectrum. One experimentally obtains $D^{k\ell}_{\tau,V/A}$ by integrating the weighed normalized invariant mass-squared spectrum. The corresponding theoretical predictions are easily modified.

[26]In the chiral limit, vector and axial-vector currents are conserved so that $s\Pi^{(0)}_V = s\Pi^{(0)}_A = 0$.

1. The ALEPH determination of $\alpha_s(m_\tau^2)$ and nonperturbative contributions

Combined fits to experimental spectral moments and extraction of $\alpha_s(m_\tau^2)$ together with the leading nonperturbative operators have been performed by ALEPH, CLEO, and OPAL (Buskulic *et al.*, 1993; Coan *et al.*, 1995; Barate *et al.*, 1998c; Ackerstaff *et al.*, 1999a; Schael *et al.*, 2005) using similar strategies and inputs. Let us follow the most recent analysis performed by the ALEPH Collaboration (Schael *et al.*, 2005).

Since the determination of α_s should be model independent, experiments proceed by fitting simultaneously nonperturbative operators, which is possible since correlations between these and α_s turn out to be small enough. The theoretical framework and its intrinsic uncertainties were the subject of the previous section. Minor additional contributions originate from the CKM matrix element $|V_{ud}|$, the electroweak radiative correction factor $S_{\rm EW}$, the light quark masses $m_{u,d}$, and quark condensates (Sec. VII.B.9). The largest contributions have their origin in the truncation of the perturbative expansion. Although it introduces some double counting for the systematic error, the procedure used by Schael *et al.* (2005) considers separate variations of the unknown higher-order coefficient K_4 and renormalization scale. The renormalization scale is varied around m_τ from 1.1 to 2.5 GeV with the variation over half of the range taken as systematic uncertainty. Taking advantage of the new theoretical developments discussed above, the value $K_4=25\pm 25$ has been used by Schael *et al.* (2005).

The fit minimizes the χ^2 of the differences between measured and adjusted quantities contracted with the inverse of the sum of the experimental and theoretical covariance matrices. The results of Schael *et al.* (2005) are listed in Table VI. The precision of $\alpha_s(m_\tau^2)$ obtained with the two perturbative methods employed is comparable, however, their central values differ by 0.01–0.02, which is larger than the theoretical errors assigned. The $\delta^{(2)}$ term is theoretical only with quark masses varying within their allowed ranges (126). The quark condensates in the $\delta^{(4)}$ term are obtained from

TABLE VI. Fit results (Schael *et al.*, 2005) for $\alpha_s(m_\tau^2)$ and the nonperturbative contributions for vector, axial-vector, and $V+A$ combined fits using the corresponding experimental spectral moments as input parameters. Where two errors are given the first is experimental and the second theoretical. The $\delta^{(2)}$ term is theoretical only with quark masses varying within their allowed ranges (see text). The quark condensates in the $\delta^{(4)}$ term are obtained from PCAC, while the gluon condensate is determined by the fit. The total nonperturbative contribution is the sum $\delta_{\rm NP}=\delta^{(4)}+\delta^{(6)}+\delta^{(8)}$. Full results are listed only for the CIPT perturbative prescriptions, except for $\alpha_s(m_\tau^2)$ where both CIPT and FOPT results are given.

Parameter	Vector (V)	Axial vector (A)	$V+A$
$\alpha_s(m_\tau^2)$ (CIPT)	$0.355\pm0.008\pm0.009$	$0.333\pm0.009\pm0.009$	$0.350\pm0.005\pm0.009$
$\alpha_s(m_\tau^2)$ (FOPT)	$0.331\pm0.006\pm0.012$	$0.327\pm0.007\pm0.012$	$0.331\pm0.004\pm0.012$
$\delta^{(2)}$ (CIPT)	$(-3.3\pm3.0)\times10^{-4}$	$(-5.1\pm3.0)\times10^{-4}$	$(-4.4\pm2.0)\times10^{-4}$
$\langle a_sGG\rangle$ (GeV^4) (CIPT)	$(0.4\pm0.3)\times10^{-2}$	$(-1.3\pm0.4)\times10^{-2}$	$(-0.5\pm0.3)\times10^{-2}$
$\delta^{(4)}$ (CIPT)	$(4.1\pm1.2)\times10^{-4}$	$(-5.7\pm0.1)\times10^{-3}$	$(-2.7\pm0.1)\times10^{-3}$
$\delta^{(6)}$ (CIPT)	$(2.85\pm0.22)\times10^{-2}$	$(-3.23\pm0.26)\times10^{-2}$	$(-2.1\pm2.2)\times10^{-3}$
$\delta^{(8)}$ (CIPT)	$(-9.0\pm0.5)\times10^{-3}$	$(8.9\pm0.6)\times10^{-3}$	$(-0.3\pm4.8)\times10^{-4}$
Total $\delta_{\rm NP}$ (CIPT)	$(1.99\pm0.27)\times10^{-2}$	$(-2.91\pm0.20)\times10^{-2}$	$(-4.8\pm1.7)\times10^{-3}$
χ^2/DF (CIPT)	0.52	4.97	3.66

PCAC, while the gluon condensate is determined by the fit. The main contributions to the theoretical uncertainty on $\alpha_s(m_\tau^2)$ are listed in Table VII. The fact that the χ^2 value of the axial-vector fit is better with FOPT than with CIPT should not affect the conclusion in favor of the latter method, reached in Sec. VII.B.8 and VII.B.3 on the basis of a better perturbative behavior, but may require further studies.

The final result on $\alpha_s(m_\tau^2)$ given by Schael *et al.* (2005) is taken as the arithmetic average of the CIPT and FOPT values given in Table VI, with half of their difference added as additional theoretical error $\alpha_s(m_\tau^2)=0.340\pm0.005_{\rm exp}\pm0.014_{\rm th}$. The first error accounts for the experimental uncertainty and the second error gives the uncertainty related to the theoretical prediction of the spectral moments including the ambiguity between CIPT and FOPT.

There is a remarkable agreement within statistical errors between the $\alpha_s(m_\tau^2)$ determinations using the vector and axial-vector data. This provides an important consistency check of the results, since the two corresponding spectral functions are experimentally independent and manifest a quite different resonant behavior.

The advantage of separating the vector and axial-vector channels and comparing to the inclusive $V+A$ fit becomes obvious in the adjustment of the leading nonperturbative contributions of dimension $D=6$ and $D=8$, which approximately cancel in the inclusive sum. This cancellation of nonperturbative terms increases the confidence in the $\alpha_s(m_\tau^2)$ determination from the inclusive $V+A$ observables. The gluon condensate is determined by the first $k=1$, $\ell=0,1$ moments, which receive lowest-order contributions. It is observed that the values obtained in the V and A fits are not consistent, which could indicate problems in the validity of the OPE approach used once nonperturbative terms become significant. Taking the value obtained in the $V+A$ fit, where nonperturbative effects are small, and adding as systematic uncertainties half of the difference between the vector and axial-vector fits as well as between the CIPT and FOPT results, ALEPH measures the gluon condensate to be

$$\langle a_sGG\rangle = 0.001 \pm 0.012\ \mathrm{GeV}^4. \qquad (135)$$

This result does not provide evidence for a nonzero gluon condensate, but it is consistent with and has comparable accuracy to the independent value obtained using charmonium sum rules and e^+e^- data in the charm region, $(0.011\pm0.009)\,\mathrm{GeV}^4$ in a combined determination with the c quark mass (Ioffe and Zyablyuk, 2003).

The $D=6,8$ nonperturbative contributions are obtained after averaging the FOPT and CIPT values:

$$\delta_V^{(6)} = (2.8 \pm 0.3) \times 10^{-2}, \quad \delta_V^{(8)} = (-\,8.8 \pm 0.6) \times 10^{-3},$$

$$\delta_A^{(6)} = (-\,3.1 \pm 0.3) \times 10^{-2}, \quad \delta_A^{(8)} = (8.7 \pm 0.6) \times 10^{-3},$$

$$\delta_{V+A}^{(6)} = (-\,1.8 \pm 2.4) \times 10^{-3},$$

$$\delta_{V+A}^{(8)} = (0.5 \pm 5.1) \times 10^{-4}. \qquad (136)$$

The remarkable feature is the approximate cancellation of these contributions in the $V+A$ case, for both $D=6$ and $D=8$. This property was predicted (Braaten *et al.*, 1992) for $D=6$ using the simplifying assumption of vacuum saturation for the matrix elements of four-quark operators, yielding $\delta_V^{(6)}/\delta_A^{(6)}=-7/11=-0.64$, in fair agreement with the above results which reads -0.90 ± 0.18. The estimate (Braaten *et al.*, 1992) for $\delta_V^{(6)}=(2.5\pm1.3)\times10^{-2}$ agrees well with the experimental result.

TABLE VII. Sources of theoretical uncertainties and their impact on $R_{\tau,V+A}$ and $\alpha_s(m_\tau^2)$ (Schael *et al.*, 2005).

		$\Delta^{\text{th}} R_{\tau,V+A}$		$\Delta^{\text{th}}\alpha_s(m_\tau^2)$	
Error source	Value $\pm\Delta^{\text{th}}$	CIPT	FOPT	CIPT	FOPT
S_{EW}	1.0198 ± 0.0006	0.002		0.001	
$\lvert V_{ud}\rvert$	0.9745 ± 0.0004	0.002		0.001	
K_4	25 ± 25	0.015	0.009	0.007	0.003
R-scale μ	$m_\tau^2\pm2$ GeV^2	0.012	0.035	0.006	0.011
Total errors		0.019	0.036	0.009	0.012

The total nonperturbative $V+A$ correction, $\delta_{\text{NP},V+A}=(-4.3\pm1.9)\times10^{-3}$, is an order of magnitude smaller than the corresponding values in the V and A components, $\delta_{\text{NP},V}=(2.0\pm0.3)\times10^{-2}$ and $\delta_{\text{NP},A}=(-2.8\pm0.3)\times10^{-2}$.

2. OPAL results

The OPAL analysis (Ackerstaff *et al.*, 1999a) makes use of the spectral functions shown in Fig. 4 and also provides a complete description in terms of QCD of their vector and axial-vector data. It proceeds along very similar lines as the ALEPH analysis, with the difference that OPAL has chosen to quote their results separately for three prescriptions for the perturbative expansion, CIPT, FOPT, and with renormalon chains, respectively, i.e.,

$$\alpha_s(m_\tau^2)=\begin{cases}0.348\pm0.009_{\text{exp}}\pm0.019_{\text{th}}, & \text{CIPT}\\ 0.324\pm0.006_{\text{exp}}\pm0.013_{\text{th}}, & \text{FOPT}\\ 0.306\pm0.005_{\text{exp}}\pm0.011_{\text{th}}, & \text{renormalon.}\end{cases} \tag{137}$$

The OPAL results using CIPT and FOPT agree with those from ALEPH. The quoted theoretical uncertainties are consistently treated between the two analyses, with the important difference that the more recent ALEPH analysis (Schael *et al.*, 2005) uses a reduced uncertainty range for the K_4 parameter ($K_4=25\pm25$) as compared to $K_4=50\pm50$ in the 1998 analysis (Barate *et al.*, 1998c) and $K_4=25\pm50$ in OPAL. The justification of the smaller K_4 uncertainty was provided in Sec. VII.B.1. As for the value obtained with the renormalon chains, we refer the reader to our discussion in Secs. VII.B.7 and VII.B.8 where we concluded that however interesting this approach is, its performance for a reliable and precise determination of $\alpha_s(m_\tau^2)$ is not adequate. OPAL also derives values for the gluon condensate: Averaging the results of the CIPT and FOPT analyses, one obtains $\langle a_s GG\rangle=0.005\pm0.017$ GeV^4, in agreement with ALEPH.

3. Running of $\alpha_s(s)$ below m_τ^2

Using the spectral functions, one can simulate the physics of a hypothetical τ lepton with a mass $\sqrt{s_0}$ smaller than m_τ through Eq. (82). Assuming quark-hadron duality, the evolution of $R_\tau(s_0)$ provides a direct test of the running of $\alpha_s(s_0)$, governed by the RGE β function. On the other hand, it is also a test of the stability of the OPE approach in τ decays. Studies performed in this section employ only CIPT. Results obtained with FOPT are similar[27] and differ mostly in the central $\alpha_s(m_\tau^2)$ value.

The functional dependence of $R_{\tau,V+A}(s_0)$ is plotted on the upper plot of Fig. 22 together with the theoretical prediction using the results of Table VI. The spreads due to uncertainties are shown as error bands. Correlations between two adjacent points in s_0 are large as the only new information is provided by the small mass difference between the two points and the slightly modified weight functions. Moreover, they are reinforced by the original experimental and theoretical correlations. Below 1 GeV^2 the error of the theoretical prediction of $R_{\tau,V+A}(s_0)$ starts to blow up due to the increasing uncertainty from the unknown K_4 perturbative term; errors of the nonperturbative contributions are *not* contained in the theoretical error band. Figure 22 (lower) shows the plot corresponding to Fig. 22 (upper), translated into the running of $\alpha_s(s_0)$, i.e., the experimental value for $\alpha_s(s_0)$ has been individually determined at every s_0 from the comparison of data and theory. Also plotted is the four-loop RGE evolution using three-quark flavors.

It is remarkable that the theoretical prediction using the parameters determined at the τ mass and $R_{\tau,V+A}(s_0)$ extracted from the measured $V+A$ spectral function agree down to $s_0\sim0.8$ GeV^2. The agreement is good to about 2% at 1 GeV^2. This result, even more directly illustrated by the lower plot of Fig. 22, demonstrates the validity of the perturbative approach down to masses around 1 GeV, well below the τ mass scale. The agreement with the expected scale evolution between 1 and 1.8 GeV is an interesting result, considering the relatively low mass range, where α_s is seen to decrease by a factor of 1.6 and reaches rather large values ~0.55 at the lowest masses. This behavior provides confidence that

[27]As already indicated by the smaller χ^2 value of the spectral moments fit (see Table VI), the agreement between the FOPT evolution computation and data is better than it is when using CIPT.

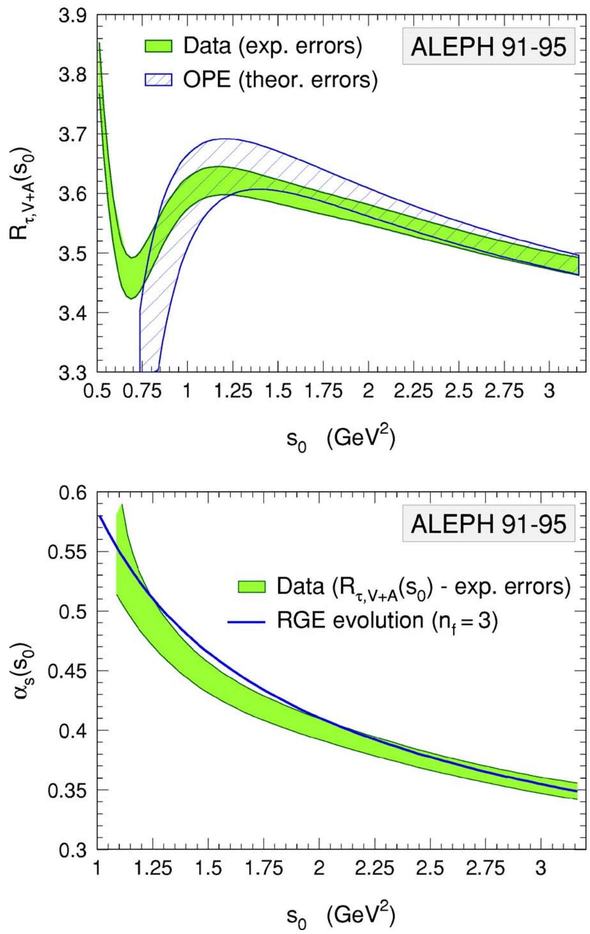

FIG. 22. (Color online) Upper: The ratio $R_{\tau,V+A}$ versus the square "τ mass" s_0. Curves are plotted as error bands to emphasize their strong point-to-point correlations in s_0. Also shown is the theoretical prediction using CIPT and results for $R_{\tau,V+A}$ and nonperturbative terms from Table VI. Lower: The running of $\alpha_s(s_0)$ obtained from the fit of the theoretical prediction to $R_{\tau,V+A}(s_0)$ using CIPT. The shaded band shows data including only experimental errors. The curve gives the four-loop RGE evolution for three flavors.

the $\alpha_s(m_\tau^2)$ measurement is on solid phenomenological ground.

4. Final assessment on the $\alpha_s(m_\tau^2)$ determination

Although the recent ALEPH evaluation of $\alpha_s(m_\tau^2)$ represents the state of the art, several remarks can be made:

- The analysis is based on the ALEPH spectral functions and branching fractions, ensuring a good consistency between all observables, but not exploiting the experimental information currently available from other experiments. Since the result on $\alpha_s(m_\tau^2)$ is limited by theoretical uncertainties, one should expect only a small improvement of the final error in this way, however it can influence the central value.
- One example is the evaluation of the strange component. Some discrepancy is observed between the ALEPH measurement of the $(K\pi\pi)^-\nu$ mode and the CLEO and OPAL results, as discussed in Sec. III.C. Although this could still be the result of a statistical fluctuation, their average provides a significant shift in the central value compared to using the ALEPH number alone. Another improvement is the substitution of the measured branching fraction for the $K^-\nu$ mode by the more precise value predicted from $\tau-\mu$ universality [see Eq. (16)]. Both operations have the effect to increase the strange $R_{\tau,S}$ ratio from 0.1603 ± 0.0064, as obtained by ALEPH, to 0.1686 ± 0.0047 for the world average.
- One can likewise substitute the world average value for the universality-consolidated value of the electronic branching fraction given in Eq. (13), $\mathcal{B}_e^{\text{uni}}=(17.818\pm0.032)\%$, to the corresponding ALEPH result, $\mathcal{B}_e=(17.810\pm0.039)\%$, with little effect on the central value, but some improvement in the precision.
- Most of the theoretical uncertainty originates from limited knowledge of the perturbative expansion, only predicted to third order. This problem was discussed in detail in Sec. VII.B.1 and, among the standard FOPT and CIPT approaches, arguments have been presented in favor of the latter one. We therefore take the result from the CIPT expansion, not introducing any additional uncertainty spanning the difference between FOPT and CIPT results. The dominant theoretical errors are from the uncertainty in K_4 and from the renormalization scale dependence, both covering the effect of truncating the series after the estimated fourth order.

From this analysis, one finds the new value for the nonstrange ratio,

$$\begin{aligned} R_{\tau,V+A} &= R_\tau - R_{\tau,S} \\ &= (3.640 \pm 0.010) - (0.1686 \pm 0.0047) \\ &= 3.471 \pm 0.011, \end{aligned} \tag{138}$$

to be compared to the ALEPH value of 3.482 ± 0.014. The result (138) translates into an updated determination of $\alpha_s(m_\tau^2)$ from the inclusive $V+A$ component using the CIPT approach

$$\alpha_s(m_\tau^2) = 0.345 \pm 0.004_{\text{exp}} \pm 0.009_{\text{th}}, \tag{139}$$

with improved experimental and theoretical precision over the ALEPH result.

5. Evolution to M_Z^2

It is customary to compare α_s values, obtained at different renormalization scales, at the scale of the Z-boson mass. To do this, one evolves the α_s result using the RGE (75). A difficulty arises from the quark thresholds: In the MS scheme, or any of its modifications such as $\overline{\text{MS}}$, the beta function governing the running of the strong-coupling constant is independent of quark masses. This simplifies the calculation of QCD corrections beyond the one-loop level. On the other hand, decoupling of heavy quarks (Appelquist and Carazzone, 1975) is not manifest in each order of perturbation theory (Bernreuther, 1983). A heavy quark decoupling is realized in momentum-space dependent renormalization schemes (MO). The RGE in an MO scheme involves the scaling function $\beta_{\rm MO}=\beta(\alpha_s',m_i',a')$ that depends on the coupling $\alpha_s'(\mu^2)$, the quark masses $m_i'(\mu^2)$, and a gauge parameter $a'(\mu^2)$, where the primes stand for the scheme dependence of the parameters. Quark-loop calculations in this scheme appear rather complicated, however, the mass dependence of the β function provides a suppression of heavy-quark effects at scales much smaller than the masses of these quarks, i.e., it decouples heavy quarks from the light-particle Green's function to each order in perturbation theory.

To obtain decoupling in $\overline{\rm MS}$ schemes, one builds in the decoupling region $\mu \ll \bar{m}_q^{(n_f)}(\mu^2)$, where $\bar{m}^{(n_f)}(\mu^2)$ is the running $\overline{\rm MS}$ mass of the heavy quark with flavor f, an effective field theory that behaves as if only light quarks up to flavor n_f-1 were present. Matching conditions connect the parameters of the low-energy effective Lagrangian to the full theory. The coupling constant of the effective theory can then be developed in a power series of the coupling constant of the full theory with coefficients that depend on $x=\ln(\mu^2/\bar{m}_q^2)$. Doing so one obtains for the matching of a_s and light quark masses between the "light" flavor n_f-1 and the heavy-quark flavor n_f (Bernreuther and Wetzel, 1982; Wetzel, 1982; Chetyrkin, Kniehl, and Steinhauser, 1997, 1998; van Ritbergen *et al.*, 1997a; Rodrigo *et al.*, 1998)

$$a_s^{(n_f)}(\mu^2) = a_s^{(n_f-1)}(\mu^2)\left[1+\sum_{k=1}^{\infty} C_k(x)[a_s^{(n_f-1)}(\mu^2)]^k\right],$$

$$\bar{m}_q^{(n_f)}(\mu^2) = \bar{m}_q^{(n_f-1)}(\mu^2)\left[1+\sum_{k=1}^{\infty} H_k(x)[a_s^{(n_f-1)}(\mu^2)]^k\right]. \tag{140}$$

There is no straightforward choice of the matching scale μ. However, to acquire good convergence of the perturbative expansion, one should satisfy $\mu/\bar{m}_q \sim \mathcal{O}(1)$. Since vacuum polarization of quark pairs modifies the coupling constant, we believe that the scale $\mu=2\bar{m}_q$ is quite meaningful. The effect from this scale ambiguity is part of the systematic error assigned to the RGE evolution (see below).

The functions $C_k(x)$ and $H_k(x)$ are derived by inserting the RGE-based Taylor expansions [Eq. (81) and the equivalent for quark masses] into Eq. (140), and solving for each order in $a_s^{(n_f-1)}$ the corresponding coupled differential equations (Rodrigo *et al.*, 1998)

$$C_1 = \frac{1}{6}x, \quad C_2 = c_{2,0} + \frac{19}{24}x + \frac{1}{36}x^2, \tag{141}$$

$$C_3 = c_{3,0} + \left[\frac{241}{54} + \frac{13}{4}c_{2,0} - \left(\frac{325}{1728} + \frac{1}{6}c_{2,0}\right)n_f\right]x + \frac{511}{576}x^2 + \frac{1}{216}x^3, \tag{142}$$

$$H_1 = 0, \quad H_2 = d_{2,0} + \frac{5}{36}x - \frac{1}{12}x^2, \tag{143}$$

$$H_3 = d_{3,0} + \left[\frac{1627}{1296} - c_{2,0} + \frac{35}{6}d_{2,0} + \left(\frac{35}{648} - \frac{1}{3}d_{2,0}\right)n_f + \frac{5}{6}\zeta_3\right]x - \frac{299}{432}x^2 - \left(\frac{37}{216} - \frac{1}{108}n_f\right)x^3, \tag{144}$$

where the integration coefficients $c_{i,0}$, $d_{i,0}$ are computed in the $\overline{\rm MS}$ scheme at the scale of the quark masses [i.e., $m_q=\bar{m}_q(m_q)$] (Bernreuther and Wetzel, 1982; Wetzel, 1982; Chetyrkin, Kniehl, and Steinhauser, 1997; Rodrigo *et al.*, 1998)

$$c_{1,0} = d_{1,0} = 0, \quad c_{2,0} = -\frac{11}{72},$$

$$c_{3,0} = \frac{82043}{27648}\zeta_3 - \frac{575263}{124416} + \frac{2633}{31104}n_f,$$

$$d_{2,0} = -\frac{89}{432}. \tag{145}$$

The evolution of the $\alpha_s(m_\tau^2)$ measurement from inclusive $V+A$ observables given in Eq. (139), based on Runge-Kutta integration of the RGE (75) to next-to—next-to—next-to leading order (N^{3}LO) (see Sec. VII.A), and three-loop quark-flavor matching (140), gives

$$\alpha_s(M_Z^2) = 0.1215 \pm 0.0004_{\rm exp} \pm 0.0010_{\rm th} \pm 0.0005_{\rm evol} = 0.1215 \pm 0.0012. \tag{146}$$

The first two errors originate from the $\alpha_s(m_\tau^2)$ determination given in Eq. (139) and the last error stands for ambiguities in the evolution due to uncertainties in the matching scales of the quark thresholds (Rodrigo *et al.*, 1998). This evolution error receives contributions from the uncertainties in the c-quark mass (0.000 20, m_c varied by ±0.1 GeV) and the b-quark mass (0.000 05, m_b varied by ±0.1 GeV), the matching scale (0.000 23, μ varied between $0.7m_q$ and $3.0m_q$), the three-loop truncation in the matching expansion (0.000 26), and the four-loop truncation in the RGE equation (0.000 31), where we used for the last two errors the size of the highest known perturbative term as systematic uncertainty. These errors have been added in quadrature. The result (146) is a determination of the strong coupling at the Z mass scale with a precision of 1%.

The evolution path of $\alpha_s(m_\tau^2)$ is shown in the upper plot of Fig. 23. The two discontinuities are due to thequark-flavor matching at $\mu=2\bar{m}_q$. One could prefer to avoid discontinuities by choosing $\mu=\bar{m}_q$ so that the logarithms in Eq. (140) vanish, and matching becomes

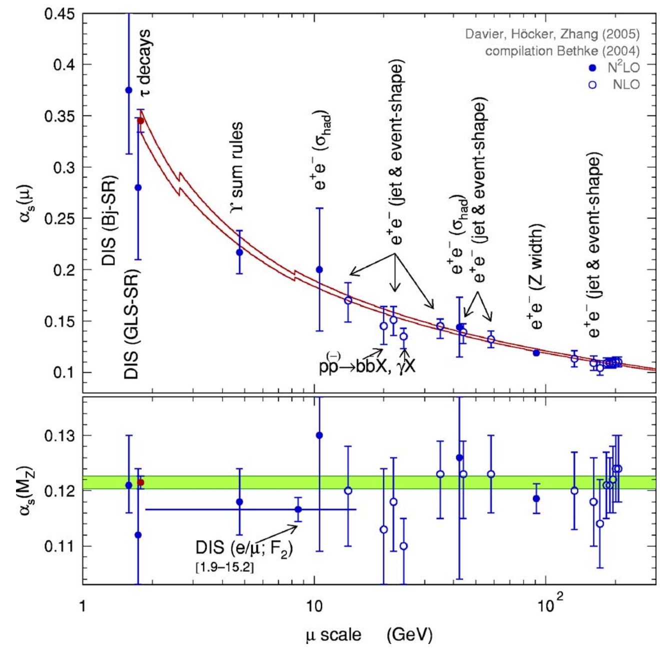

FIG. 23. (Color online) Top: The evolution of $\alpha_s(m_\tau^2)$, Eq. (139), to higher scales μ using the four-loop RGE and the three-loop matching conditions applied at heavy quark-pair thresholds (hence the discontinuities at $2m_c$ and $2m_b$). The evolution is compared with other independent measurements (see text) covering scales varying over more than two orders magnitude. Experimental values are discussed in the text; they are mostly taken from Bethke (2004). Bottom: The corresponding extrapolated α_s values at M_Z. The shaded band displays the τ decay result within errors.

(almost) smooth. However, in this case, one must first evolve from m_τ down to $\bar{m}_c$ to match the c-quark flavor, before evolving to $\bar{m}_b$. The effect on $\alpha_s(M_Z^2)$ from this ambiguity is within the assigned systematic uncertainty for the evolution.

6. Comparison with other determinations of $\alpha_s(M_Z^2)$

The evolution of $\alpha_s(m_\tau^2)$ in Fig. 23 is compared with other independent measurements compiled by Bethke (2004). Listed below are some outstanding measurements made over a large energy range in a variety of processes with different experimental and theoretical precisions.

DIS (Bj-SR): $\alpha_s(1.58\ \text{GeV}) = 0.375^{+0.062}_{-0.081}$ (Ellis and Karliner, 1995) was obtained using the polarized structure function data for protons $g_1^p(x)$ and neutrons $g_1^n(x)$ from the CERN SMC (Adams *et al.*, 1994) and SLAC E142 (Abe *et al.*, 1995) experiments, based on the Bjorken sum rule (Bjorken, 1970) at next-to—next-to leading order (N^2LO) (Larin and Vermaseren, 1991; Larin *et al.*, 1991)

$$\int_0^1 [g_1^p(x) - g_1^n(x)]dx = \frac{1}{3}\left|\frac{g_A}{g_V}\right|\left[1 - \frac{\alpha_s}{\pi} - 3.58\left(\frac{\alpha_s}{\pi}\right)^2 - 20.2\left(\frac{\alpha_s}{\pi}\right)^3\right]. \quad (147)$$

Here g_V and g_A are the vector and axial-vector coupling constants of the neutron decay, $|g_A/g_V| = -1.2573 \pm 0.0028$ (determined assuming CVC), and the last two coefficients are calculated for three active flavors. No explicit corrections for nonperturbative higher twist effects[28] were applied to derive this result. However, an estimate of the size of the perturbative $\mathcal{O}(\alpha_s^4)$ term was taken into account.

DIS (GLS-SR): $\alpha_s(1.73\ \text{GeV}) = 0.280 \pm 0.061_{\text{exp}}\ {}^{+0.035}_{-0.030}|_{\text{th}}$ is an update of the analysis using structure function F_3 data in the Q^2 range from 1 to 15.5 GeV^2 performed by the CCFR Collaboration (Kim *et al.*, 1998). It uses the Gross–Llewellyn-Smith (GLS) sum rule (Gross and Llewellyn-Smith, 1969) at N^2LO (Larin and Vermaseren, 1991; Larin *et al.*, 1991; Chýla and Kataev, 1992)

$$\int_0^1 F_3(x,Q^2)dx \equiv 3\left[1 - \frac{\alpha_s}{\pi} - 3.58\left(\frac{\alpha_s}{\pi}\right)^2 - 19.0\left(\frac{\alpha_s}{\pi}\right)^3\right], \quad (148)$$

given for three active flavors. The systematic uncertainty is dominated by the extrapolation of the GLS integral to the region $x < 0.01$ where no measurements exist, and to $x > 0.5$, which is substituted by the structure function F_2 from SLAC data (Withlow *et al.*, 1992). The theoretical error is dominated by uncertainties in the higher twist corrections.

Υ *sum rules*: $\alpha_s(m_b)|_{m_b=4.75\ \text{GeV}} = 0.217 \pm 0.021$ was found together with the bottom quark pole mass m_b from sum rules for the Υ system in N^2LO, resumming all $\mathcal{O}(\alpha_s^2, \alpha_s v, v^2)$ terms with v being the velocity of the heavy quark (Penin and Pivovarov, 1998). The precision of this result on $\alpha_s(m_b)$ was not confirmed by a similar analysis (Hoang, 1999), where the theoretical parameter space has been scanned, which leads to a more conservative estimate of the theory uncertainty.

$e^+e^-(\sigma_{had})$: $\alpha_s(10.52\ \text{GeV}) = 0.20 \pm 0.06$ was determined in N^2LO by CLEO (Ammar *et al.*, 1998) using the total e^+e^- hadronic cross section according to

$$R = \frac{\sigma(e^+e^- \to \text{hadrons})}{\sigma(e^+e^- \to \mu^+\mu^-)} = 3\sum_i Q_i^2\left[1 + \frac{\alpha_s}{\pi} + 1.52\left(\frac{\alpha_s}{\pi}\right)^2 - 11.5\left(\frac{\alpha_s}{\pi}\right)^3\right], \quad (149)$$

where Q_i are electric charges of quark flavors i that are produced at the center-of-mass energy just below the $\Upsilon(4S)$ resonance in the e^+e^- continuum. Another measurement $\alpha_s(42.4\ \text{GeV}) = 0.175 \pm 0.028$ was obtained with the use of data from PETRA and TRISTAN in the

[28]Interactions involving more than one parton, like secondary interactions of quarks with the target remnant, give rise to additional contributions to the structure functions. These "higher twist" terms are classified according to their Q^2 dependence $1/Q^{2n}$, where $n=0$ is leading twist (twist 2), $n=1$ is twist 4, etc.

center-of-mass energy range from 20 to 65 GeV (Haidt, 1995; Bethke, 2000).

e^+e^- *(jet & event shape)*: Using data from PETRA, TRISTAN, SLC, and LEP1,2 over a large energy range, several determinations of α_s were obtained based on the jet rate and event-shape variables that are sensitive to gluon radiation governed by the strong-coupling constant. The observables are calculated in resummed NLO (i.e., NLO matched with next-to-leading order logarithms). In all these determinations, the theoretical uncertainty from the renormalization scale uncertainty is the dominant error source. At low PETRA energy the hadronization uncertainty is also important. See references in the work of Bethke (2000).

$p\bar{p}\to b\bar{b}X$: $\alpha_s(20\ \text{GeV})=0.145\ ^{+0.012}_{-0.010}|_{\text{exp}}\ ^{+0.013}_{-0.016}|_{\text{th}}$ was obtained by UA1 (Albajar *et al.*, 1996) from a measurement of the $p\bar{p}\to b\bar{b}X$ cross section process for which NLO QCD predictions exist. The theoretical error includes uncertainties due to different sets of structure functions, renormalization/factorization scale uncertainties, and the b-quark mass.

$p\bar{p},pp\to\gamma X$: $\alpha_s(24.3\ \text{GeV})=0.135\pm0.006_{\text{exp}}\ ^{+0.011}_{-0.005}|_{\text{th}}$ was determined by UA6 (Werlen *et al.*, 1999) in NLO from a measurement of the cross-section difference $\sigma(p\bar{p}\to\gamma X)-\sigma(pp\to\gamma X)$ such that poorly known contributions of sea quarks and gluon distributions in the proton cancel. The theoretical error includes uncertainties from the scale choice and from the variation of parton distribution functions.

e^+e^- *(Z width)*: $\alpha_s(M_Z)_{Z\ \text{width}}=0.1186\pm0.0027$ was determined from the hadronic width at the Z^0 resonance by a global fit to all electroweak data in N^{2}LO (Abbaneo *et al.*, 2004).

A comparison is best achieved by extrapolating these measurements to M_Z as shown in the lower plot in Fig. 23. The most precise result at the M_Z scale stems from τ decays (146), which is a 1.1% determination limited in accuracy by theoretical uncertainties in the perturbative expansion. The significant improvement in precision compared to the previous ALEPH result (Barate *et al.*, 1998c), $0.1202\pm0.0008_{\text{exp}}\pm0.0024_{\text{th}}\pm0.0010_{\text{evol}}$, is due to higher statistics and more detailed experimental analysis, but mostly because of the smaller theory uncertainty assigned to the perturbative expansion and our conclusion to lift the ambiguity between CIPT and FOPT.

Another precise determination [DIS $(e/\mu;F_2)$ 1.9–15.2 GeV], $\alpha_s(M_Z^2)=0.1166\pm0.0009_{\text{stat}}\pm0.0020_{\text{syst}}$ (Santiago and Yndurain, 2001; Bethke, 2003), obtained using the structure function F_2 from deep inelastic electron (e) and muon (μ) scattering (DIS) data in the Q^2 range between 3.5 and 230 GeV^2 is also shown. The analyses use N^{2}LO calculations wherever available. The systematic error is mostly theoretical including higher twist effects and an estimate of the N^{3}LO corrections, and is doubled to account for missing contributions associated with the renormalization scale and scheme uncertainties.

In addition to the measurements shown in Fig. 23, there is now a precise determination from lattice QCD simulations (Davis *et al.*, 2004): $\alpha_s(M_Z^2)=0.121\pm0.003$. This is the first lattice determination with realistic quark vacuum polarization and an $\mathcal{O}(a^2)$ improved staggered-quark discretization of the light-quark action.

7. Measure of asymptotic freedom between m_τ^2 and M_Z^2

The τ decay and Z width determinations have comparable accuracies, which are, however, very different in nature. The τ value is dominated by theoretical uncertainties, whereas the determination at the Z resonance, benefiting from the much larger energy scale and correspondingly small uncertainties from the truncated perturbative expansion, is limited by the experimental precision on the electroweak observables, essentially the ratio of leptonic to hadronic peak cross sections. The consistency between the two results provides a powerful test of the strong interaction coupling, over a range of s spanning more than three orders of magnitude, as predicted by the non-Abelian nature of the QCD gauge theory. The difference between the extrapolated τ-decay value and the measurement at Z is

$$\alpha_s^\tau(M_Z^2)-\alpha_s^Z(M_Z^2)=0.0029\pm0.0010_\tau\pm0.0027_Z, \quad (150)$$

which agrees with zero with a relative precision of 2.4%.

In fact, the comparison of these two values is valuable since they are among the most precise single measurements and they are widely spaced in energy scale. Thus it allows one to perform an accurate test of asymptotic freedom. Let us consider the following evolution estimator (Abdallah *et al.*, 2004) for the inverse of $\alpha_s(s)$:

$$r(s_1,s_2)=2\frac{\alpha_s^{-1}(s_1)-\alpha_s^{-1}(s_2)}{\ln s_1-\ln s_2}, \quad (151)$$

which reduces to the logarithmic derivative of $\alpha_s^{-1}(s)$ when $s_1\to s_2$,

$$\frac{d\alpha_s^{-1}}{d\ln\sqrt{s}}=-\frac{2\pi\beta(s)}{\alpha_s^2}=\frac{2\beta_0}{\pi}\left(1+\frac{\beta_1}{\beta_0}\frac{\alpha_s}{\pi}+\cdots\right), \quad (152)$$

with the same notation used in Eq. (75). At first order, the logarithmic derivative is driven by β_0.

The τ and Z experimental determinations of $\alpha_s(s)$ yield the value

$$r_{\text{exp}}(m_\tau^2,M_Z^2)=1.405\pm0.053, \quad (153)$$

which agrees with the QCD prediction using the RGE to N^{3}LO, and three-loop quark-flavor matching (140), as discussed in Sec. VII.C.5,

$$r_{\text{QCD}}(m_\tau^2,M_Z^2)=1.353\pm0.006. \quad (154)$$

This is to our knowledge the most precise experimental test of the asymptotic freedom property of QCD at present. It can be compared to an independent determination (Abdallah *et al.*, 2004), using an analysis of event shape observables at LEP between the Z energy and 207 GeV, $r(M_Z^2,(207\text{GeV})^2)=1.11\pm0.21$, for a QCD expectation of 1.27.

VIII. SPECTRAL FUNCTIONS OF TAU FINAL STATES WITH STRANGENESS

Complete experimental studies of the Cabibbo-suppressed decays of the τ became available at LEP (Barate *et al.*, 1999b) allowing one to initiate systematic QCD studies (Davier, 1997; Höcker, 1997; Chen, 1998; Chen *et al.*, 1999; Davier *et al.*, 2001) of the effect induced by the strange quark mass in the τ decay width (Braaten *et al.*, 1992; Chetyrkin and Kwiatkowski, 1993; Chetyrkin, Gorishny, and Spiridonov, 1997; Chetyrkin and Kühn, 1997; Chetyrkin, Kniehl, and Steinhauser, 1998; Maltman, 1998a; Pich and Prades, 1998, 1999, 2000; Prades, 1999; Prades and Pich, 1999; Kambor and Maltman, 2000, 2001; Körner *et al.*, 2001b). Indeed, from the separate measurement of the strangeness $S=0$ and $S=-1$ τ decay widths, it is possible to pin down the SU(3) breaking effects and to obtain information on the strange quark mass. Recent experimental information (Richichi *et al.*, 1999; Abbiendi *et al.*, 2004) can now be included in addition to the ALEPH data. In this section the current situation on the physics of τ decays with net strangeness is reviewed, with emphasis on the determination of the strange quark mass and the CKM element $|V_{us}|$. We anticipate here that while the determination of $|V_{us}|$ through QCD sum rules is found to be robust, a reliable and competitive determination of the strange quark mass m_s is difficult because of poor convergence of the mass-dependent perturbative series, and lack of sufficient inclusiveness of the higher-order spectral moments that are most sensitive to m_s.

A. Strange spectral functions

The experimental determination of nonstrange and strange (subscript S) spectral functions has been discussed in Sec. IV. As shown in Sec. VII.C, one uses the spectral functions, or equivalently the fully corrected mass-squared distributions, to construct the spectral moments

$$R_{\tau,(S)}^{k\ell} = \int_0^{m_\tau^2} ds \left(1-\frac{s}{m_\tau^2}\right)^k \left(\frac{s}{m_\tau^2}\right)^\ell \frac{dR_{\tau,(S)}}{ds}, \tag{155}$$

where $R_{\tau,(S)}^{00}=R_{\tau,(S)}$.

To reduce theoretical uncertainties and emphasize the SU(3) breaking component originating from the larger s quark mass, it is convenient to consider the difference between nonstrange and strange spectral moments, properly normalized with their respective CKM matrix elements (Barate *et al.*, 1999b)

$$\delta R_\tau^{k\ell} = \frac{1}{|V_{ud}|^2} R_{\tau,S=0}^{k\ell} - \frac{1}{|V_{us}|^2} R_{\tau,S=-1}^{k\ell}, \tag{156}$$

for which the massless perturbative contribution vanishes. Contributions from the various decay modes to δR_τ^{00} are visualized in Fig. 24.

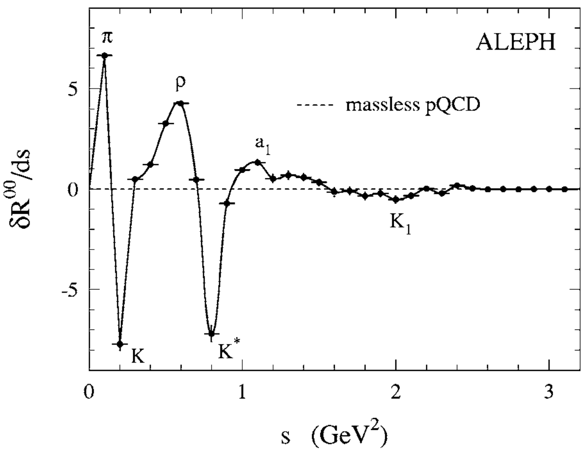

FIG. 24. Integrand of Eq. (155) with $(k=0,\ell=0)$ for the difference of the Cabibbo-corrected nonstrange and strange invariant mass spectra from Barate *et al.* (1999b). The contribution from massless perturbative QCD (pQCD) vanishes. To guide the eye, the solid line interpolates between the bins of constant 0.1 GeV^2 width.

B. Theoretical analysis of $R_{\tau,S}$

The inclusive τ decay ratio into strange hadronic final states,

$$R_{\tau,S} = \frac{\Gamma(\tau^- \to \text{hadrons}^-_{S=-1}\nu_\tau)}{\Gamma(\tau^- \to e^-\bar{\nu}_\tau)}, \tag{157}$$

can be used through the framework of the OPE to determine at the scale $s=m_\tau^2$ (Davier, 1997; Höcker, 1997; Chen, 1998; Chen *et al.*, 1999). However, the perturbative expansion computed for the mass term by Chetyrkin and Kwiatkowski (1993) was shown to be incorrect (Maltman, 1998a). After correction the series shows a problematic convergence behavior (Chetyrkin, Kühn, and Pivovarov, 1998; Maltman, 1998a; Pich and Prades, 1998; Prades, 1999; Prades and Pich, 1999), which is discussed in detail below.

Following Braaten *et al.* (1992) we recall the theoretical prediction for the inclusive vector plus axial-vector hadronic decay rate, given by

$$R_\tau(m_\tau^2) = 12\pi S_{\text{EW}} \int_0^{m_\tau^2} \frac{ds}{m_\tau^2}\left(1-\frac{s}{m_\tau^2}\right)^2 \left[\left(1+2\frac{s}{m_\tau^2}\right) \times \text{Im}\,\Pi^{(1+0)}(s+i\epsilon) - 2\frac{s}{m_\tau^2}\,\text{Im}\,\Pi^{(0)}(s+i\epsilon)\right], \tag{158}$$

with the two-point correlation functions $\Pi^{(J)} =|V_{ud}|^2\Pi^{(J)}_{ud,V+A}+|V_{us}|^2\Pi^{(J)}_{us,V+A}$ for the hadronic final state of spin J. The choice of the particular spin combination for the correlators taken in Eq. (158) has been justified by Braaten *et al.* (1992). Using the OPE (Shifman *et al.*, 1979a, 1979b, 1979c), Eq. (158) for the strange part can be decomposed as

$$R_{\tau,S} = 3|V_{us}|^2 S_{\rm EW}\left(1 + \delta^{(0)} + \delta'_{\rm EW} + \delta_S^{(2,m_q)} + \sum_{D=4,6,\ldots} \delta_S^{(D)}\right). \tag{159}$$

The $\delta^{(0)}$ term is the perturbative part of mass dimension $D=0$, known to third order in the expansion with $a_s = \alpha_s(m_\tau^2)/\pi$, and discussed in Sec. VII.B.1. The residual nonlogarithmic electroweak correction $\delta'_{\rm EW}\simeq 0.0010$ (Braaten and Li, 1990) is neglected in the following. Throughout this section, all QCD observables are expressed in the $\overline{\rm MS}$ renormalization scheme.

From the result obtained in Sec. VII.C.4 for the world average branching fraction for inclusive τ decays to strange hadronic final states (improved using lepton universality for the $K\nu$ mode), one obtains $R_{\tau,S} = 0.1686\pm 0.0047$ using the value for $\mathcal{B}_e^{\rm uni}$ given in Sec. III.B. This result can be compared with the QCD prediction for a massless strange quark neglecting nonperturbative contributions, $R_{\tau,S}^{(0)} = 3|V_{us}|^2 S_{\rm EW}(1+\delta^{(0)}) = 0.1847\pm 0.0029$, where the quoted error reflects the uncertainties on mostly $|V_{us}|$ and to a lesser extent $\alpha_s(m_\tau^2)$. The two values differ by 2.9σ, in the direction predicted for a nonzero m_s value.

The $\delta_S^{(2,m_q)}$ term in Eq. (159) is the mass contribution of dimension $D=2$, which is in practice only relevant for the strange quark mass. Fixed-order perturbation theory gives (Chetyrkin and Kwiatkowski, 1993; Maltman, 1998a)

$$\delta_S^{(2,m_s)} = -8\frac{m_s^2(m_\tau^2)}{m_\tau^2}\left[1 + \frac{16}{3}a_s + 46.00a_s^2 + \left(283.6 + \frac{3}{4}x_3^{(1+0)}\right)a_s^3 + \cdots\right]. \tag{160}$$

The third-order coefficient $x_3^{(1+0)}$ occurring in the expansion of the massive $J=1+0$ correlator has been recently calculated (Baikov *et al.*, 2004), while the $J=0$ correlator was already known up to third order. Previous analyses used an estimate for $x_3^{(1+0)}$, however, it turns out to be of minor numerical importance for the result on m_s. The true value (Baikov *et al.*, 2005) is $x_3^{(1+0)}=202.3$, while the naive estimate, assuming a geometric growth of the perturbative coefficients, gives $x_3^{(1+0)}\simeq x_2^{(1+0)}(x_2^{(1+0)}/x_1^{(1+0)}) \simeq 165$, which was taken with a 200% uncertainty. Setting $\alpha_s(m_\tau^2)=0.334$, one finds that Eq. (160) does not exhibit good convergence.

A contour-improved analysis (CIPT) for the dimension $D=2$ contribution has been used by Chetyrkin, Kühn, and Pivovarov (1998); Pich and Prades (1998); Prades (1999); and Prades and Pich (1999). It consists of direct numerical evaluation of the contour integral derived from Eq. (158), using the solution of the renormalization-group equation to four loops as input to the running $\alpha_s(s)$ and $m_s(s)$. This provides a resummation of all known higher-order logarithmic integrals and has been found to improve the convergence of the massless perturbative series. This is also the case for Eq. (160), however, not solving the convergence problem. Independently of whether FOPT or CIPT is used, the origin of the convergence problem is found in the $J=0$ component as defined in Eq. (158).

The phenomenological analysis is performed using the OPE framework including light quark masses and $D=4$ quark-mass corrections. Higher dimension terms are assumed to be numerically insignificant compared to the present experimental uncertainty so that for all practical purposes the strange quark mass can be obtained from

$$m_s^2(m_\tau^2) \simeq \frac{m_\tau^2}{\Delta_{k\ell}(a_s)}\left[\frac{\delta R_\tau^{k\ell}}{24S_{\rm EW}} + 2\pi^2\frac{\langle\delta O_4(m_\tau^2)\rangle}{m_\tau^4}Q_{k\ell}(a_s)\right], \tag{161}$$

where $\Delta_{k\ell}(a_s)$ and $Q_{k\ell}(a_s)$ are the pQCD series, defined by Pich and Prades (1999, 2000), associated with the $D=2$ and $D=4$ contributions to $\delta R_\tau^{k\ell}$, and

$$\langle\delta O_4(m_\tau^2)\rangle = \langle 0|m_s\bar{s}s - m_d\bar{d}d|0\rangle(m_\tau^2) \simeq -(1.5\pm 0.4)\times 10^{-3}\ {\rm GeV}^4. \tag{162}$$

As discussed above, the QCD series for $\Delta_{k\ell}=\Delta_{k\ell}^{(1+0)}+\Delta_{k\ell}^{(0)}$ are problematic, since they exhibit bad convergence originating from the longitudinal component ($\Delta_{k\ell}^{(0)}$) (Maltman, 1998a; Pich and Prades, 1998, 1999, 2000; Prades, 1999; Prades and Pich, 1999). The value of the strong-coupling constant is taken to be $\alpha_s(m_\tau^2) = 0.334\pm 0.022$, from the analyses of the nonstrange $V+A$ moments $R_\tau^{k\ell}$. Correlations between $\alpha_s(m_\tau^2)$ and the moments $\delta R_{k\ell}$ are negligible since the uncertainty on the former value is dominated by theory and on the latter one by the measurement of the strange component. Using these inputs, the pQCD series $\Delta_{k\ell}$ can be displayed up to third order using CIPT, separating the $(1+0)$ and (0) series ($a_s=0.106$):

$$\begin{aligned}
\Delta_{00}^{(1+0)}(a_s) &= 0.565 + 0.161 + 0.049 - 0.038 + \cdots,\\
\Delta_{10}^{(1+0)}(a_s) &= 0.684 + 0.251 + 0.144 + 0.042 + \cdots,\\
\Delta_{20}^{(1+0)}(a_s) &= 0.791 + 0.338 + 0.248 + 0.142 + \cdots,\\
\Delta_{30}^{(1+0)}(a_s) &= 0.893 + 0.428 + 0.363 + 0.264 + \cdots,\\
\Delta_{40}^{(1+0)}(a_s) &= 0.993 + 0.523 + 0.493 + 0.413 + \cdots,\\
\Delta_{00}^{(0)}(a_s) &= 0.408 + 0.320 + 0.323 + 0.375 + \cdots,\\
\Delta_{10}^{(0)}(a_s) &= 0.355 + 0.307 + 0.338 + 0.435 + \cdots,\\
\Delta_{20}^{(0)}(a_s) &= 0.324 + 0.305 + 0.360 + 0.505 + \cdots,\\
\Delta_{30}^{(0)}(a_s) &= 0.306 + 0.309 + 0.389 + 0.587 + \cdots,\\
\Delta_{40}^{(0)}(a_s) &= 0.295 + 0.317 + 0.421 + 0.680 + \cdots.
\end{aligned} \tag{163}$$

The exhibited behavior is that of an asymptotic series close to their point of minimum sensitivity and a prescription is needed to evaluate the expansions and to make a reasonable estimate of their uncertainties.

C. Several approaches

The bad convergence properties of the perturbative QCD expansion can be alleviated in several ways. For instance, one could try to work with the full series up to the highest known order (third), observing that terms in the overall expansion show a reasonable rate of decrease, at least in the CIPT approach. Fourth-order coefficients can be estimated using for instance the principle of minimal sensitivity (Stevenson, 1981) or the simplistic geometric growth rule. The latter method was used in early analyses (Davier, 1997; Höcker, 1997; Chen, 1998; Chen *et al.*, 1999).

Examination of examples of asymptotic series suggests that a reasonable procedure is to truncate the expansion where the terms reach their minimum value. The precise prescription—cutting at the minimum, or one order before or after, including the full last term or only a fraction of it—is arbitrary and this ambiguity must be reflected by a specific uncertainty attached to the procedure. Chen *et al.* (2001) and Davier *et al.* (2001) adopted the rule to keep all terms up to (and including) the minimal one and to assign as a systematic uncertainty the value of the last term retained. It follows that the Δ_{k0} series are summed up to third order for $k=0,1$, second order for $k=2$, and first order for $k=3,4$.

Since the culprit is the longitudinal expansion, it could be wise to remove the longitudinal piece beforehand from the inclusive data and to apply the QCD analysis only to the well-behaved $(1+0)$ part.[29] This method was already used by Barate *et al.* (1999b), where it was noted that the dominant contribution to the strange $J=0$ component is given by the kaon pole. Other longitudinal contributions can be identified and estimated, giving

$$R^{(0)}_{\tau,S}(K) = -0.006\,15 \pm 0.000\,26, \tag{164}$$

$$R^{(0)}_{\tau,S}(\text{other } 0^-,0^+) = -0.0015 \pm 0.0015, \tag{165}$$

leading to the result

$$\delta R^{00}_{\tau}(J=0) = 0.147 \pm 0.031, \tag{166}$$

where the $J=0$ contributions in the nonstrange part are assumed to be saturated by the pion pole and have been computed to be -0.0078. Similarly, one estimates the $J=0$ contributions for all (k,ℓ) moments and subtracts them from the measured moments.

More recent analyses rely on phenomenological parametrizations of the additional scalar and pseudoscalar contributions (Jamin *et al.*, 2002; Maltman and Kambor, 2002). The $0^{\pm}$ spectral functions constructed in this way rely on not so well-established resonances with poorly known couplings, however, they probably provide a realistic level for these contributions. Even with their intrinsically large uncertainties they are an order of magnitude more precise than the experimental estimate from ALEPH [Eq. (165)]. In the analysis of Gámiz *et al.* (2003) the corresponding contribution to $R_{\tau,s}$ yields

$$\delta R^{00}_{\tau}(J=0,\text{ph}) = 0.155 \pm 0.005, \tag{167}$$

where "ph" stands for phenomenological parametrizations. The quoted uncertainty in this method is clearly much smaller than in Eq. (166). It reflects the fact that pieces of the spin-0 spectral functions can be reconstructed using known resonances.

1. Verifying the stability of the results

As shown in the analysis of nonstrange τ decays by Barate *et al.* (1998c), one can test the validity of the QCD analysis by simulating the physics of a hypothetical τ lepton of lower mass, $\sqrt{s_0} \leq m_\tau$. This is obtained by replacing m_τ^2 by s_0 everywhere in Eqs. (155) and (158), and correcting the latter equation for the modified kinematic factor. Under the assumption of quark-hadron duality, the evaluation of the observables as function of s_0 represents a test of the OPE approach, since the energy dependence of theoretical predictions is determined once the parameters of the theory are fixed. The results of this exercise are given in Fig. 25, showing the variation with s_0 of the first four δR^{k0}_τ moments, and the value for $m_s(s_0)$ derived from each moment. The bands indicate the experimental and theoretical uncertainties. The agreement between data and theory, perfect at $s_0 = m_\tau^2$ by construction, remains acceptable for lower s_0 values, down to 1.6 GeV^2 (2.4 GeV^2) for $k=0$ ($k=4$). For the first three moments used in the final determination, the running observed in data follows the RGE evolution down to about 2 GeV^2. The validity of using higher moments thus appears more questionable.

2. Results and discussion

Several analyses of the ALEPH strange spectral function have been performed in order to extract $m_s(m_\tau^2)$. More recent analyses take advantage of new experimental input on the strange spectral function from Abbiendi *et al.* (2004) and improvements in branching fractions for some strange channels (see Table I).

- In the work of Barate *et al.* (1999b), a rather conservative road was followed, using only the $1+0$ part and a prudent estimate of the removed longitudinal part directly from data. A price was paid in the experimental sensitivity, leading to large errors. Also, the experimental moments were fit, not only to the strange quark mass, but also to the values of the nonperturbative operators $\langle \delta O_6 \rangle$ and $\langle \delta O_8 \rangle$. The value found by ALEPH is $m_s(m_\tau^2) = 176\, {}^{+37}_{-48}|_{\text{exp}}\, {}^{+24}_{-28}|_{\text{th}} \pm 14_{\text{meth}}$ MeV.
- Using the truncation method with $k=0,1,2$ moments (Chen *et al.*, 2001), the value $m_s(m_\tau^2) = 120 \pm 11_{\text{exp}} \pm 8_{|V_{us}|} \pm 19_{\text{th}}$ MeV is found.

[29] A drawback of this procedure is that it reduces inclusiveness of the data and hence makes the phenomenological analysis more vulnerable to quark-hadron duality violations.

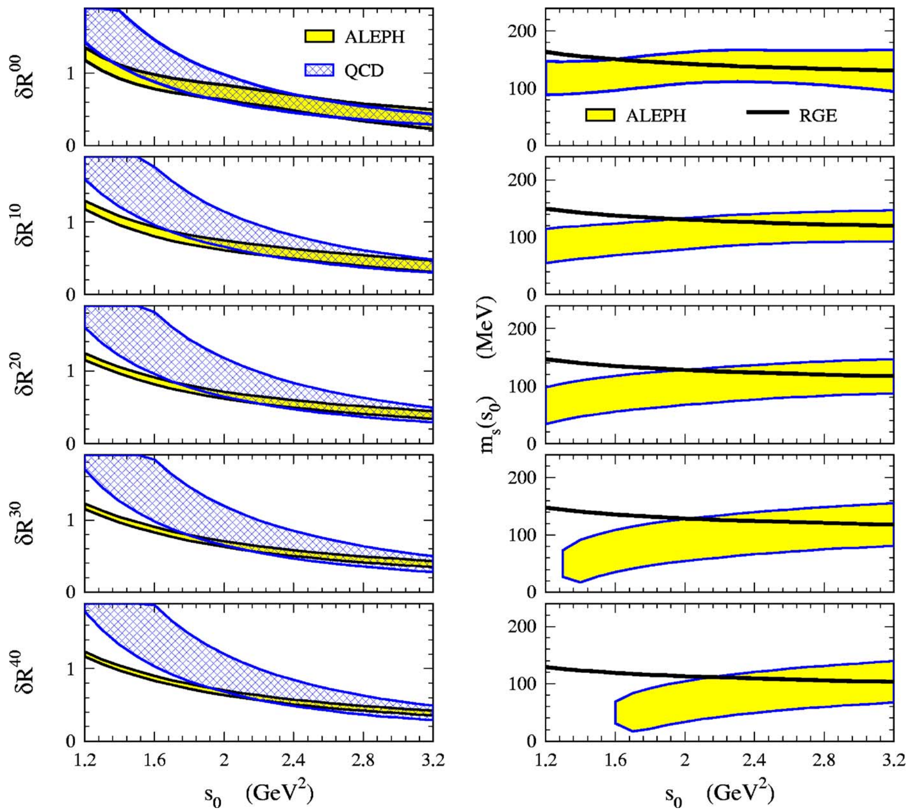

FIG. 25. (Color online) The observables $\delta R_\tau^{k0}(s_0)$ as a function of the τ mass squared s_0 confronted with the QCD predictions (left plots), and the derived $m_s(s_0)$ compared with the QCD RGE running (right plots). The bands correspond to the experimental and theoretical uncertainties (left plots), and experimental errors only (right plots). By construction, data and theory agree at $s_0 = m_\tau^2$. From Chen *et al.*, 2001.

- The analysis of Körner *et al.* (2001b) uses the ALEPH δR_τ^{00} moment and obtains $m_s(m_\tau^2) = 130 \pm 27_{\rm exp} \pm 9_{\rm th}$ MeV. It advocates contour-improved resummation and employs an effective charge as well as effective masses absorbing the higher perturbative terms. The small quoted theoretical uncertainty is not exhaustively motivated in their paper, and apparently no uncertainty is included from $|V_{us}|$, which should be of the order of ± 13 MeV.
- Another analysis (Kambor and Maltman, 2000, 2001) using the ALEPH data makes use of weight functions multiplying the correlators in Eq. (158). These weights are designed to improve the convergence of the perturbative series, while suppressing the less accurate high-mass part of the strange spectral function. This latter feature is similar to using higher moments in k and it is not entirely clear to what extent this procedure provides stable results and hence how reliable the answer is. Nevertheless, that result is in good agreement with other results, with a smaller theoretical uncertainty, but apparently not including the effect from the renormalization scale ambiguity.
- In the work of Gámiz *et al.* (2003), the longitudinal part is subtracted using a phenomenological prescription. The result $m_s(m_\tau^2) = 107 \pm 18$ MeV is obtained by taking the weighted average of the m_s values for $k = 0, \ldots, 4$ and $\ell = 0$ moments. This procedure is statistically hardly justified as the experimental moments are strongly correlated. The result is more precise than other determinations, however, a large systematic trend is observed for different k values: the m_s central values decrease monotonically from 151 MeV for $k=0$ to 91 MeV for $k=4$. No additional systematic uncertainty is included to account for this effect, which is larger than the final quoted error, dominated by the experimental error and the uncertainty on $|V_{us}|$. The updated value using the OPAL strange spectral function with world average branching ratios yields (Gámiz *et al.*, 2005) a value $m_s(m_\tau^2) = 84 \pm 23$ MeV.
- Another analysis (Baikov *et al.*, 2005) uses the full perturbative series for the $1+0$ correlator up to third order and an estimate of fourth-order contributions, while the longitudinal part is subtracted using the same phenomenological model as Gámiz *et al.* (2003). The result, based on the $k=3$, $\ell=0$ moment, is $m_s(m_\tau^2) = 100\ {}^{+5}_{-3}|_{\rm th}\ {}^{+17}_{-19}|_{\rm rest}$ MeV. Here the first (quite small) error shall cover uncertainties on the perturbative treatment, while the remaining error is dominated by the experimental and $|V_{us}|$ uncertainties. The same systematic trend is observed with $m_s(m_\tau^2)$ values ranging from 126 MeV for $k=2$ to 82 MeV for $k=4$.

Determinations of m_s from τ decays compare reasonably well to the results of analyses of the divergence of the vector and axial-vector current two-point function correlators (Becchi *et al.*, 1981; Gasser and Leutwyler, 1982; Kataev *et al.*, 1983; Dominguez and de Rafael, 1987; Narison, 1989; Dominguez *et al.*, 1991; Chetyrkin *et al.*, 1995; Jamin and Münz, 1995; Chetyrkin, Pirjol, and Schilcher, 1997; Colangelo *et al.*, 1997; Jamin, 1998).

In these approaches the phenomenological information on the associated scalar and pseudoscalar spectral functions is reconstructed from phase-shift resonance analyses, which are incomplete over the considered mass range and need to be supplemented by other assumed ingredients, in particular the description of the continuum.

Another approach (Narison, 1995) considers the difference between isovector and hypercharge vector current correlators as related to the $I=1$ and $I=0$ spectral functions accessible in e^+e^- annihilation into hadrons at low energy. Narison obtained $m_s(1\ \mathrm{GeV}^2)=198\pm29$ MeV. This approach was criticized by Maltman (1998b), pointing out the possibility of large isospin breaking leading to a significant deviation for the extracted m_s value. Subsequently in the work of Narison (1989), new SU(3)-breaking sum rules much less affected by SU(2) breaking were studied, with the result $m_s(1\ \mathrm{GeV}^2)=178\pm33$ MeV.

Finally, full lattice QCD calculations of m_s including dynamical quark actions have become available recently. A pioneering analysis using the so-called *staggered* fermion approach (Aubin *et al.*, 2004) finds in the $\overline{\mathrm{MS}}$ scheme $m_s(4\ \mathrm{GeV}^2)=76\pm8$ MeV. The quoted error is dominated by uncertainty in the perturbative theory, needed to obtain the $\overline{\mathrm{MS}}$ mass from the pole mass, itself calculated from the lattice bare mass. The included systematic uncertainty from the simulation on the lattice is quoted to be 3 MeV, while the statistical error is negligible. Other computations using $N_f=2$ Wilson fermions find significantly larger values of $m_s(4\ \mathrm{GeV}^2)=119\pm10$ MeV (Göckeler *et al.*, 2004) and $m_s(4\ \mathrm{GeV}^2)=116\pm6$ MeV (Becirevic *et al.*, 2004).

Available results on m_s are displayed in Fig. 26. They are scaled for convenience at a mass of 2 GeV, using the four-loop RGE γ function (Larin *et al.*, 1997). One observes a scatter among the values that exceeds the quoted uncertainties in some cases.

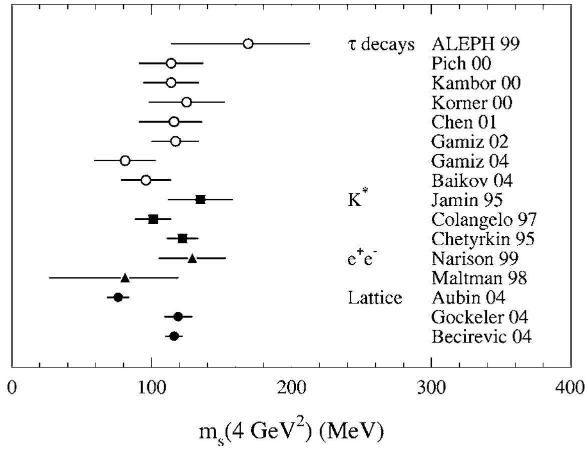

FIG. 26. Determinations of the $\overline{\mathrm{MS}}$ mass $\bar{m}_s(4\ \mathrm{GeV}^2)$ based on τ spectral functions and on other approaches: K^* and e^+e^- sum rules, lattice calculations.

D. Sensitivity to $|V_{us}|$ and concluding remarks on m_s determinations

Before concluding the discussion of strange τ decays, it is useful to combine available experimental information. Taking detector-corrected experimental mass spectra from Barate *et al.* (1999b), the world average branching fractions for the strange final states (Table I) and the value (16) for the $\tau^-\to K^-\nu_\tau$ branching ratio, an improved strange spectral function can be constructed. We use it in this last section.

Besides the strange quark mass, detailed analysis of the strange τ width can bring independent information on the CKM matrix element $|V_{us}|$. In fact, the present uncertainty on $|V_{us}|$ is a major contribution to the final error on m_s. One can turn the argument around and consider the possibility that data on strange τ decays could ultimately provide a powerful determination of $|V_{us}|$ (Gámiz *et al.*, 2003, 2005). Figure 27 illustrates the method: the bands show regions in the $|V_{us}|$-vs-$m_s(m_\tau^2)$ plane which are allowed by the different moments δR_τ^{k0} for $J=1+0$ (i.e., longitudinal part excluded) within their total (experimental and theoretical) errors. It is found that the various moments are sensitive to $|V_{us}|$ and m_s in a different way. While higher-k moments exhibit a strong m_s dependence, δR_τ^{00} is particularly sensitive to $|V_{us}|$, almost independently of m_s. This property can be exploited to achieve a determination of $|V_{us}|$ from τ decays. Since the τ SU(3) breaking relation (156) involves both $|V_{ud}|$ and $|V_{us}|$, unitarity of the CKM matrix is used ($|V_{ub}|$ being negligible) and only $|V_{us}|$ is kept as a variable.

Using as an independent determination the m_s value from recent lattice calculations (Aubin *et al.*, 2004) evolved to the τ scale, $m_s(m_\tau^2)=79\pm8$ MeV, one gets from δR_τ^{00} alone

$$|V_{us}| = 0.2204 \pm 0.0028_{\mathrm{exp}} \pm 0.0003_{\mathrm{th}} \pm 0.0001_{m_s}, \quad (168)$$

where the quoted errors are from the τ data (dominantly from strange channels), the theory at large (S_{EW}, δO_4, f_π, f_K, α_S, m_τ, the phenomenological longitudinal part), and m_s. The theoretical error is reduced because the $(1+0)$ expansion of the (0,0) moment is well behaved, in contrast to the higher moments. Thus the uncertainty on the result is dominated by the experimental error on the branching ratios for strange hadronic final states.

The present result is not yet competitive with the best determinations of $|V_{us}|$, but it is approaching these. Although it could be a statistical fluctuation, the fact that the result (168) is on the low side of recent results from $K_{\ell 3}$ and $K_{\mu 2}$ decays may be worrisome. It could indicate that not all τ strange final states have been identified. In this context it is important to revisit in particular the branching ratio for the $\nu_\tau K^-\pi^+\pi^-$ mode where the agreement is marginal between ALEPH on the low side and CLEO and OPAL on the high side (Sec. III.C).

One could forecast a significant improvement with the analyses of high statistics τ samples available at the B factories. The detectors at these facilities (*BABAR* and

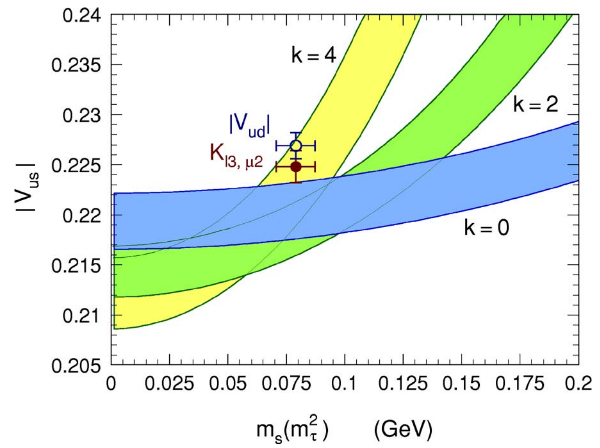

FIG. 27. (Color online) The values of $|V_{us}|$ and $m_s(m_\tau^2)$ derived from the experimental strange and nonstrange moments obtained from the ALEPH spectral functions normalized to world average branching ratios. The various curves correspond to the different $k,\ell=0$ moments with k from 0 to 4. The width of the bands indicates the present experimental accuracy. The longitudinal components are subtracted using K and π branching fractions together with τ-μ universality, and the phenomenological contributions estimated by Gámiz *et al.* (2003). Data points indicate the $|V_{us}|$ and $m_s(m_\tau^2)$ results from outside τ physics. The two $|V_{us}|$ values shown correspond to the average of the $K_{\ell 3}$ and $K_{\mu 2}$ results (full circle), and to the $\sqrt{1-|V_{ud}|^2}$ unitarity-based number (open circle) (Isidori, 2005).

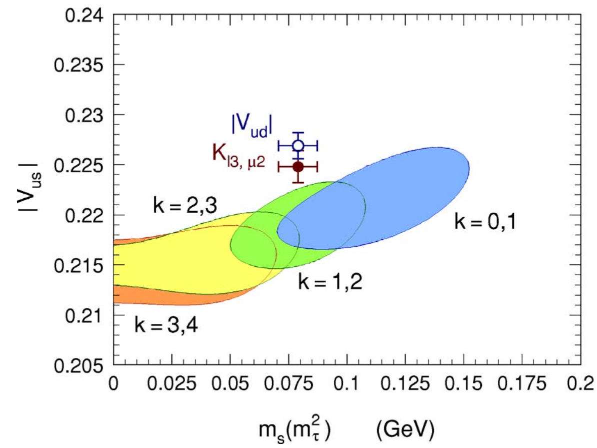

FIG. 28. (Color online) The 68% C.L. contours in the $|V_{us}|$-vs-$m_s(m_\tau^2)$ plane from the fit of different pairs of moments derived from the experimental strange and nonstrange ALEPH spectral functions normalized to world average branching ratios. The longitudinal components are subtracted using the τ-μ universality-improved K and π branching fractions, and phenomenological contributions estimated by Gámiz *et al.* (2003). The results exhibit a systematic trend with the orders of the pair chosen. Data points show the best present knowledge of $|V_{us}|$ (the open circle determined using unitarity) and $m_s(m_\tau^2)$ from outside τ physics. The two $|V_{us}|$ values shown correspond to the average of the $K_{\ell 3}$ and $K_{\mu 2}$ results (full circle), and to the $\sqrt{1-|V_{ud}|^2}$ unitarity-based number (open circle) (Isidori, 2005).

Belle) are equipped with powerful Cherenkov counters, well suited to separate kaons and pions in a large momentum domain, and one should expect significant improvement in the measurement of small, statistics-limited strange branching fractions. Then it is conceivable that a competitive determination of $|V_{us}|$ can be obtained.

We now turn back to the m_s determination. In fact, owing to the availability of the different moments, it is possible to fit them simultaneously and to derive both $|V_{us}|$ and m_s. In doing so it is mandatory to take into account strong correlations between the moments. With the present best data it seems not possible to achieve a consistent description of all five moments ($k=0$–4) with a unique solution for $|V_{us}|$ and m_s. The situation is best illustrated in Fig. 28 showing the 68% C.L. contours when only pairs of moments are considered in the fit. Typical examples are given with the following "adjacent" k pairs: going from $k=0,1$ to $k=3,4$ pairs clearly selects different regions in the plane. The situation is worse than it looks at first sight since moments are highly correlated. Indeed, the correlation coefficient ranges from 0.68 ($k=0$–4) to 0.99 ($k=2$–3, 3–4). A fit of the three $k=0,2,4$ moments (adding more does not extract any new information from the data) yields a χ^2 of 6.4 for 1 degree of freedom, corresponding to a goodness-of-fit probability of only 1%.

We are concerned that the pattern emerging from Fig. 28 undermines the reliability in the previous findings of m_s from τ decays, at least within their quoted errors. More recent determinations (Baikov *et al.*, 2005; Gámiz *et al.*, 2005) have focused on the higher $k=2,3,4$ moments [only the $k=3$ moment is used by Baikov *et al.* (2005)] since they are more sensitive to m_s and they used a world average value for $|V_{us}|$. However, Fig. 28 shows that the data prefer a lower value, not consistent with the world average. This might be the worse behavior result of the perturbative expansion of higher moments as detailed in Eq. (163), even for the $J=1+0$ part. Another sign of potential problems is found in the m_s running study as function of s_0 in Sec. VIII.C.1, where the stability of the results for higher moments could not be safely established.

It may be that some of these alarming features will disappear with better experimental data, especially if systematic deviations are found. More precise data from the B factories on multihadronic strange final states will certainly add valuable information to this problem. As for the moment, whereas the $|V_{us}|$ measurement from the $k=0$ SU(3) breaking moment appears reasonably safe, the m_s determination is unfortunately plagued with systematic effects and does not appear to be sufficiently robust for a precise and model-independent measurement.

IX. CHIRAL SYMMETRY AND QCD SUM RULES

In the limit of n_f massless quarks ($m_i=0$, $i=u,d,\ldots$), the QCD Lagrangian possesses a global $SU_L(n_f) \times SU_R(n_f)$ chiral symmetry between the left- and right-handed quarks in flavor space. The associated conserved Noether currents are the vector (V^μ) and axial-vector (A^μ) quark currents. The vector and axial-vector charges

$$Q_{V/A} = \int d^3x V^0/A^0(x), \tag{169}$$

are generators of the symmetry group. For a state $|\phi\rangle$, which is symmetric under $SU(3)_L \times SU(3)_R$, one then must have (Gasser and Leutwyler, 1982)[30]

$$\langle\phi|A^a_\mu(x)A^b_\mu(y)|\phi\rangle = \langle\phi|V^a_\mu(x)V^b_\mu(y)|\phi\rangle \quad (a,b=,1,\ldots,8), \tag{170}$$

which requires that for every contribution on the right-hand side of Eq. (170) ($J^P=0^+$ or 1^-) there exists a mass degenerate partner on the left-hand side ($J^P=0^-$ or 1^+). However, chiral symmetry, which should be a good symmetry for light u,d,s quarks, is not observed in low-energy hadronic spectra of e^+e^- annihilation or τ spectral functions. In order to be consistent with this experimental fact, the chiral flavor group $SU(3)_L \times SU(3)_R$ is assumed to be spontaneously broken down to $SU(3)_{L+R}$ where the vacuum expectation values are symmetric,

$$\langle\bar{u}u\rangle = \langle\bar{d}d\rangle = \langle\bar{s}s\rangle \neq 0. \tag{171}$$

The spontaneous breaking of axial charge symmetry generates an octet of massless pseudoscalar Goldstone mesons (Goldstone, 1961; Goldstone *et al.*, 1961; Nambu and Jona-Lasinio, 1961), which is identified with the eight lightest hadronic states: π^+, π^0, π^-, η, K^+, K^-, K^0, and $\bar{K}^0$. For nonzero quark masses the axial-vector current is not conserved and its divergence reads

$$\partial_\mu A^\mu_{ij} = (m_i + m_j)\bar{q}_i(i\gamma_5)q_j, \tag{172}$$

which is associated with the decay constant f_P of a pseudoscalar meson P with four-momentum q_μ, defined as

$$\langle 0|\partial_\mu A^\mu_P|P\rangle = \sqrt{2}f_P m_P^2 \text{ or } \langle 0|A^\mu_P|P\rangle = \sqrt{2}f_P q^\mu. \tag{173}$$

The nonvanishing physical masses of pseudoscalars reflect the fact that chiral symmetry is not exact in QCD. True zero u,d,s quark masses would generate massless pseudoscalar mesons. Explicit mass relations between pseudoscalars can be deduced from chiral perturbation theory (cf. Sec. IX.D). There is no indication of spontaneously breaking of the vector charge symmetry (the vector charge operators annihilate the vacuum): no light scalars have been found experimentally, and vector mesons can be classified in degenerate multiplets, which are $SU(3)_V$ representations. Hence the longitudinal part of the vector correlator in Eq. (38) vanishes in the chiral limit, $\Pi^{(0)}_{ij,V}(q^2)=0$.

[30]The conserved right- ($R=V+A$) and left-handed ($L=V-A$) currents under $SU(3)_L \times SU(3)_R$ transform like $(\underline{8},\underline{1})$ and $(\underline{1},\underline{8})$, respectively. If $|\phi\rangle$ is invariant then $\langle\phi|RL|\phi\rangle=0 \Rightarrow \langle\phi|V^2-A^2|\phi\rangle=0$, which is Eq. (170).

Reducing chiral symmetry to the nonstrange sector, i.e., to $SU(2)_L \times SU(2)_R$, one has the Lorentz-decomposed two-point correlation function

$$\begin{aligned}\Pi^{\mu\nu}_{\bar{u}d,LR}(q) &\equiv i\int d^4x e^{iqx}\langle 0|T[L^\mu(x)R^\nu(0)^\dagger]|0\rangle \\ &= (-g^{\mu\nu}q^2 + q^\mu q^\nu)\Pi^{(1)}_{ud,LR}(q^2) \\ &\quad + q^\mu q^\nu \Pi^{(0)}_{ud,LR}(q^2),\end{aligned} \tag{174}$$

where L^μ and R^μ are the left- and right-handed quark currents,

$$L^\mu = \bar{u}\gamma^\mu(1-\gamma_5)d, \quad R^\mu = \bar{u}\gamma^\mu(1+\gamma_5)d. \tag{175}$$

With Eqs. (174) and (175) and the correlators for vector and axial-vector currents (38) one finds

$$\Pi^{\mu\nu}_{\bar{u}d,LR}(q) = \Pi^{\mu\nu}_{\bar{u}d,V}(q) - \Pi^{\mu\nu}_{\bar{u}d,A}(q). \tag{176}$$

In the chiral limit and for $q^2\to\infty$, the correlator $\Pi^{\mu\nu}_{ud,LR}(q)$ vanishes [which again implies the degeneracy of Eq. (170)]. Using a dispersion relation and comparing $q^\mu q^\nu$ and q^2 terms in Eq. (174), one obtains the two Weinberg sum rules (WSRs) for u,d quark correlators (Weinberg, 1967)

$$\begin{aligned}\text{(1) WSR:} \int_0^{s_0\to\infty} ds\, \text{Im}[\Pi^{(1)}_{\bar{u}d,V}(s) - \Pi^{(1)}_{\bar{u}d,A}(s) + \Pi^{(0)}_{\bar{u}d,V}(s) \\ - \Pi^{(0)}_{\bar{u}d,A}(s)] = 0,\end{aligned} \tag{177}$$

$$\text{(2) WSR:} \int_0^{s_0\to\infty} ds s\, \text{Im}[\Pi^{(1)}_{\bar{u}d,V}(s) - \Pi^{(1)}_{\bar{u}d,A}(s)] = 0. \tag{178}$$

The upper integration bound s_0 is finite when integrating over experimental spectral functions, and the missing saturation of the integral at the cutoff is a source of systematic uncertainty. The first WSR can be simplified using the pion decay constant f_π defined in Eq. (173), which fixes the integral $\int ds \text{ Im } \Pi^{(0)}_{\bar{u}d,A}(s)=f_\pi^2$, and the fact the longitudinal vector correlator vanishes. Defining

$$\rho_{V-A}(s) = v_1(s) - a_1(s), \tag{179}$$

the two Weinberg sum rules read

$$\text{(1) WSR:} \frac{1}{4\pi^2}\int_0^{s_0\to\infty} ds \rho_{V-A}(s) = f_\pi^2, \tag{180}$$

$$\text{(2) WSR:} \frac{1}{4\pi^2}\int_0^{s_0\to\infty} ds s \rho_{V-A}(s) = 0. \tag{181}$$

In the presence of nonzero quark masses, only the first WSR remains valid while the second WSR breaks down due to contributions from the difference of nonconserved currents of order m_q^2/s, leading to a quadratic divergence of the integral (Floratos *et al.*, 1979). However, convergence can be recovered by considering a *Borel-transformed* (also denoted *Laplace-transformed*) version of the second WSR (see Sec. IX.C), where the result is expressed as a function of the Borel parameter M^2 and the u,d running quark masses at scale M^2 and quark condensates in powers of $1/M^0$, $1/M^2,\ldots$ (Floratos *et al.*, 1979; Shifman *et al.*, 1979a, 1979b, 1979c; Peccei and Solà, 1987).

Using a coarse narrow-width approximation for the resonances and a saturation of the corresponding vector and axial-vector spectral functions by π, $\rho(770)$, and $a_1(1260)$, Weinberg deduced from these sum rules the mass formula (Weinberg, 1967) $m_{a_1}/m_\rho \simeq 1.41$, which compares not too badly with the experimental value of 1.60 ± 0.05 (Eidelman *et al.*, 2004).

Das, Mathur, and Okubo (DMO) (1967) showed that the derivative of the vector minus axial-vector correlator $\Pi_{\bar{u}d,V-A}(q^2)$ taken at $q^2=0$ is connected with the radiative $\pi^-\to\ell^-\bar{\nu}_\ell\gamma$ decay axial-vector form factor F_A via[31]

$$\left.\frac{d(q^2\Pi_{\bar{u}d,V-A}(q^2))}{dq^2}\right|_{q^2=0} = \frac{1}{4\pi^2}\int_0^{s_0\to\infty} ds\frac{1}{s}\rho_{V-A}(s) = f_\pi^2\frac{\langle r_\pi^2\rangle}{3} - F_A, \tag{183}$$

with the pion charge radius squared $\langle r_\pi^2\rangle$ given in Eq. (66). Equation (183) has been used in the past to perform a finite-energy sum-rule determination of the electric polarizability[32] of the pion (Margvelashvili, 1988; Höcker, 1997; Kartvelishvili *et al.*, 1997; Menke, 1999). Equation (183) is an example for an *inverse moment spectral sum rule*. It is special because the integration kernel is singular at $s=0$ so that its residue is sensitive to chiral properties of the spectral functions (cf. Sec. IX.D).

The electromagnetic mass splitting between the charged and neutral pion has been calculated using current algebra techniques in chiral symmetry by Das *et al.* (1967). They derived the Das-Guralnik-Low-Mathur-Young (DGLMY) sum rule in the chiral limit

$$16\pi^2 i\int\frac{d^4q}{(2\pi)^4}\frac{1}{q^2}\int_0^{s_0\to\infty} dss\frac{\mathrm{Im}[\Pi^{(1)}_{\bar{u}d,V}(s)-\Pi^{(1)}_{\bar{u}d,A}(s)]}{q^2+s-i\epsilon} = \frac{1}{4\pi^2}\int_0^{s_0\to\infty} dss\ln\frac{s}{\Lambda^2}\rho_{V-A}(s) = -\frac{4\pi f_0^2}{3\alpha}(m_{\pi^\pm}^2-m_{\pi^0}^2), \tag{184}$$

where $f_0=f_\pi[1-13m_\pi^2/192\pi^2f_\pi^2-m_\pi^2\langle r_\pi^2\rangle/6+\mathcal{O}(m_\pi^4)] = 87.6\pm0.3$ MeV corresponds to $f_\pi=92.4\pm0.1\pm0.3$ MeV (Eidelman *et al.*, 2004), expressed in the chiral limit ($m_u=m_d=0$, $m_s\neq0$) (Moussallam, 1999). Making use of a relation from the work of Kawarabayashi and Suzuki (1966) and Riazzuddin and Fayazuddin (1966) and lowest resonance saturation, they obtained

$$m_{\pi^\pm}^2-m_{\pi^0}^2 = \frac{3\alpha m_\rho^2\ln 2}{4\pi m_\pi} = 5.1\ \text{MeV}, \tag{185}$$

in approximate agreement with the experimental value of 4.59 MeV (Eidelman *et al.*, 2004). Although apparently containing an arbitrary energy scale Λ, the sum rule (184) is actually independent of Λ by virtue of the second WSR. However, for finite s_0 a residual Λ dependence is maintained.

A. Chiral sum rules with τ spectral functions

The spectral integrals (177)–(184) are computed with variable upper integration bounds $s_0\leq m_\tau^2$ using the experimental τ hadronic spectral functions and their respective covariance matrices. The availability of covariance matrices allows one to perform a straightforward error propagation taking into account the strong bin-to-bin correlations of the spectral functions. The vector minus axial-vector τ spectral functions measured by ALEPH (Schael *et al.*, 2005) and OPAL (Ackerstaff *et al.*, 1999a) have been shown in the lower plot in Fig. 5. Local saturation of the spectral functions at the integral end point s_0 would require convergence of central values and all derivatives at zero. This is not yet achieved at $s_0=m_\tau^2$. We hence expect that the sum rules are not entirely satisfied for the τ spectral functions. The sum rules (177)–(184) versus the upper integration cutoff $s_0\leq m_\tau^2$ are plotted in Fig. 29 for the ALEPH spectral functions. The horizontal band depicts chiral predictions of the integrals, neglecting OPE power corrections. One observes that only for the DMO sum rule (lower left plot), where contributions from higher masses are suppressed, saturation at the τ mass is approximately satisfied within errors. The other sum rules are not saturated at m_τ^2, and no further conclusions can be drawn.

Many $V-A$ sum-rule analyses have been performed since the experimental spectral functions became available (Davier *et al.*, 1998; Bijnens *et al.*, 2001; Ioffe and Zyablyuk, 2001; Peris *et al.*, 2001; Cirigliano, Golowich, and Maltman, 2003; Cirigliano *et al.*, 2003; Ciulli *et al.*,

[31]In cases where the radiated photon is real the differential decay rate can be written as

$$d^2\Gamma_{\pi\to\ell\nu\gamma}/dE_\gamma dE_\ell = d^2(\Gamma_{\mathrm{IB}}+\Gamma_{\mathrm{SD}}+\Gamma_{\mathrm{INT}})/dE_\gamma dE_\ell, \tag{182}$$

where Γ_{IB}, Γ_{SD}, and Γ_{INT} are contributions from inner bremsstrahlung, structure-dependent radiation, and their interference. The structure-dependent term is parametrized using vector and axial-vector form factors $F_{V/A}$ (for the complete expression see Eidelman *et al.*, 2004).

[32]The electric polarizability α_E of a physical system can be classically understood as the proportionality constant that governs the induction of the dipole moment $\mathbf{p}$ of a system in presence of an external electric-field vector $\mathbf{E}$: $\mathbf{p}=\alpha_E\mathbf{E}$. The polarizability is an important quantity to characterize a particle, i.e., in probing its inner structure. In chiral perturbation theory, it can be shown (Teren'ev, 1973; Holstein, 1990) that the polarizability of the pion is given by $\alpha_E=\alpha F_A/m_\pi f_\pi^2$, which gives (Höcker, 1997) $\alpha_E=(2.86\pm0.33)\times10^{-4}$ fm^3. Using the value (66) for the pion charge radius squared, the analysis of a Borel-improved DMO sum rule yields (Höcker, 1997) $\alpha_E=(2.96\pm0.32)\times10^{-4}$ fm^3.

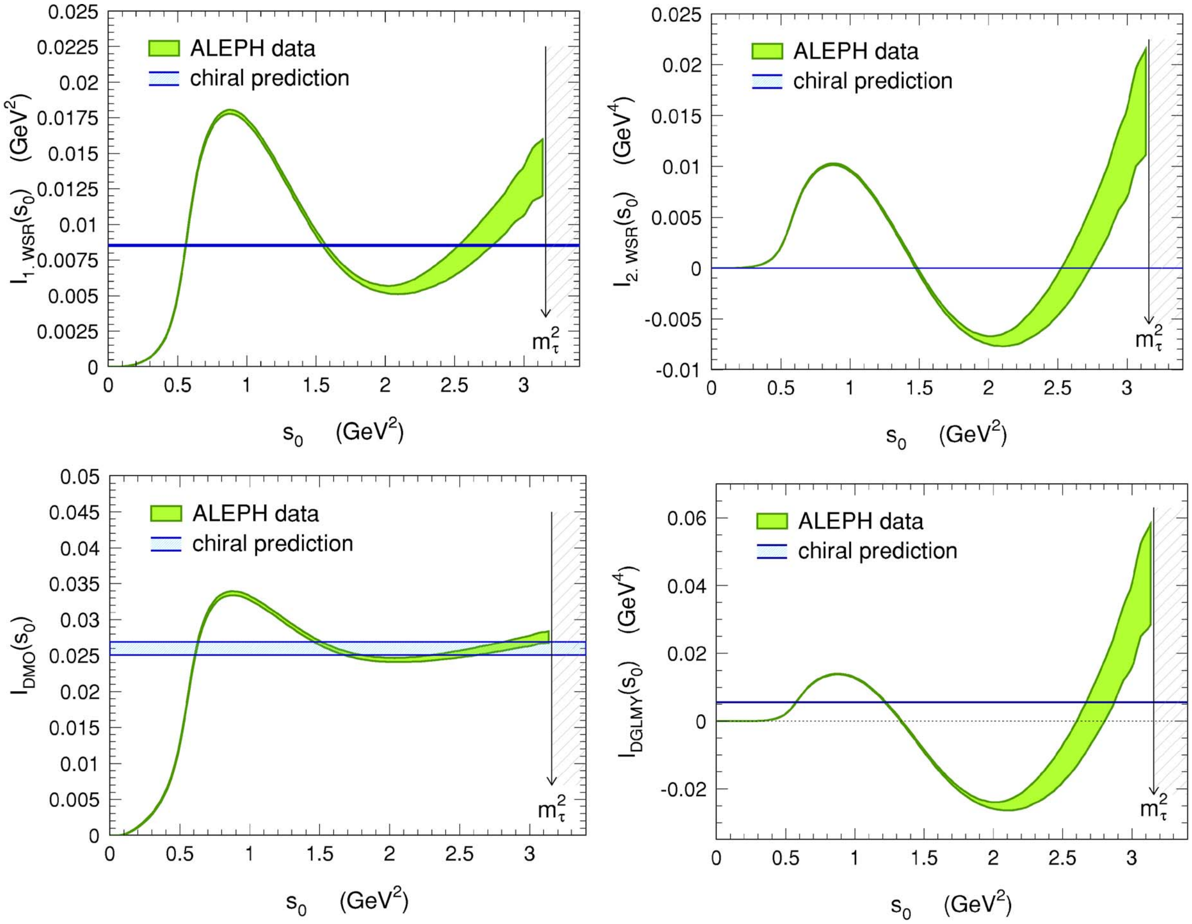

FIG. 29. (Color online) The first and second Weinberg sum rules (upper left and right), and the DMO and DGLMY sum rules (lower left and right) vs the upper integration cutoff (s_0). The horizontal bands indicate chiral predictions within errors, assuming full saturation of the integrals.

2004; Dominguez and Schilcher, 2004; Rojo and Latorre, 2004; Zyablyuk, 2004). Some results of these will be discussed in the following.

B. Operator product expansion

Nonperturbative effects give rise to nonperturbative OPE contributions to the $V-A$ correlation function

$$\Pi^{(1)}_{\bar{u}d,V}(s) - \Pi^{(1)}_{\bar{u}d,A}(s) = \sum_{D=2,4,6,\ldots} \frac{1}{(-s)^{D/2}} \sum_{\dim \mathcal{O}=D} C_{D,V-A}(s,\mu) \times \langle \mathcal{O}_D(\mu) \rangle_{V-A}, \tag{186}$$

where we shall omit the $V-A$ subscripts in the following. The dimension $D=0$ contribution is of pure perturbative origin and is degenerate in all orders of perturbation theory for vector and axial-vector currents. To NLO in QCD one has

$$C_D(s,\mu)\langle \mathcal{O}_D(\mu)\rangle = a_D(\mu) + b_D \ln\left(\frac{s}{\mu^2}\right). \tag{187}$$

The explicit logarithmic dependence of the Wilson coefficients (the b_D terms) is known for $D=2,4,6$, but not for higher dimensions. Useful relations between the OPE terms and spectral functions are obtained from projective sum rules (Kartvelishvili and Margvelashvili, 1992). When neglecting the logarithmic power terms in Eq. (187), one finds (Cirigliano *et al.*, 2003)

$$\frac{1}{4\pi^2}\int_0^{s_0} ds \left(\frac{s}{s_0}\right)^k \rho_{V-A}(s) = -\frac{1}{2\pi i}\oint_{|s|=s_0} ds \frac{a_D}{(-s)^{D/2}}\left(\frac{s}{s_0}\right)^k = (-1)^k \frac{a_D}{s_0^k}\delta_{k,(D/2)-1}, \tag{188}$$

where $\delta_{m,n}$ has the value 1 if $m=n$ and 0 elsewhere.

The validity of the OPE depends on the size of the cutoff scale s_0. Apart from the saturation of the spectral integral, this represents another source of systematic uncertainty related to the cutoff. The insertion of appropriate weight functions $w(s)$ under the spectral integral in Eq. (188) may help to reduce the impact of these systematics (see also the discussion by Cirigliano *et al.* (2003) and Cirigliano, Golowich, and Maltman (2003). While the impact of missing saturation can be reduced by suppressing the high-energy tail of the $V-A$ spectral function, the breakdown of the OPE due to quark-hadron duality violations is unavoidable to some extent. In practice, this duality violation is assumed to be absorbed by the OPE power operators that are fit phenomenologically to the spectral sum rules. The fit protects the physical observable (for instance, the strong-coupling constant as discussed in Sec. VII) that one is aiming to extract. If nonperturbative corrections are found to be large, this protection mechanism may not work sufficiently well anymore, and duality violations can entail systematic errors. Optimization between saturation of the integral, on one hand, and small duality violation, on the other hand, requires a compromise: If one aims at a minimum saturation loss, i.e., small residual modulations of the spectral function in the vicinity of the cutoff s_0, one has to apply a weight function that suppresses the high-energy tail.[33] However, the stronger the suppression, the larger the quark-hadron duality violation will be.

Using the formulas of Braaten *et al.* (1992) and Chetyrkin and Kwiatkowski (1993) for the nonperturbative power expansion of the correlators, one obtains for the $V-A$ correlators the OPE (Davier *et al.*, 1998)

$$\begin{aligned}\Pi^{(0+1)}_{\bar{u}d,V-A}(-s) = &-\frac{a_s(s)}{\pi^2}\frac{\hat{m}^2(s)}{s} + \left(\frac{8}{3}a_s(s) + \frac{59}{3}a_s^2(s)\right)\\ &\times\frac{\hat{m}\langle\bar{u}u+\bar{d}d\rangle}{s^2} - \frac{16}{7\pi^2}\frac{\hat{m}^4(s)}{s^2} - 8\pi^2 a_s(\mu^2)\\ &\times\left[1+\left(\frac{119}{24}-\frac{1}{2}L(s)\right)a_s(\mu^2)\right]\\ &\times\frac{\langle\mathcal{O}_6^1(\mu^2)\rangle}{s^3} + \frac{2\pi^2}{3}[3+4L(s)]\\ &\times a_s^2(\mu^2)\frac{\langle\mathcal{O}_6^2(\mu^2)\rangle}{s^3} + \frac{\langle\mathcal{O}_8\rangle}{s^4}, \end{aligned}\tag{189}$$

$$\begin{aligned}\Pi^{(0)}_{\bar{u}d,V-A}(-s) = &-\frac{3}{\pi^2}\left[2a_s^{-1}(s) - 5 + \left(-\frac{21373}{2448}\right.\right.\\ &\left.\left.+\frac{75}{17}\zeta(3)\right)a_s(s)\right]\frac{\hat{m}^2(s)}{s}\\ &-4\hat{C}(\mu^2)\frac{\hat{m}^2(\mu^2)}{s} - 2\frac{\hat{m}\langle\bar{u}u+\bar{d}d\rangle}{s^2}\\ &-\frac{1}{7\pi^2}\left[\frac{53}{2}-12a_s^{-1}(s)\right]\frac{\hat{m}^4(s)}{s^2},\end{aligned}\tag{190}$$

with $a_s(s)=\alpha_s(s)/\pi$, $L(s)=\ln(s/\mu^2)$, and the dimension $D=6$ operators

$$\begin{aligned}\mathcal{O}_6^1 &\equiv \bar{u}\gamma_\mu\gamma_5 T^a d\bar{d}\gamma^\mu\gamma_5 T^a u - \bar{u}\gamma_\mu T^a d\bar{d}\gamma^\mu T^a u,\\ \mathcal{O}_6^2 &\equiv \bar{u}\gamma_\mu\bar{d}d\gamma^\mu u - \bar{u}\gamma_\mu\gamma_5 d\bar{d}\gamma^\mu\gamma_5 u,\end{aligned}\tag{191}$$

and where the SU(3) generators T^a are normalized so that $\mathrm{tr}(T^aT^b)=\delta^{ab}/2$. The average mass $\hat{m}$ stands for $(m_u+m_d)/2$, i.e., SU(2) symmetry is assumed. The constant $\hat{C}(\mu^2)$ depends on the renormalization procedure and should not affect physical observables. Dimension $D=2$ mass terms are calculated perturbatively to order α_s^2, which suffices for light u,d, quarks. The coefficient functions of the dimension $D=4$ operators for vector and axial-vector currents have been calculated to subleading order by Chetyrkin *et al.* (1985) and Generalis (1989). Their vacuum expectation values are expressed in terms of the scale-invariant gluon and quark condensates. Since the Wilson coefficients of the gluon condensate are symmetric for vector and axial-vector currents, they vanish in the difference. The expectation values of the dimension $D=6$ operators (191) obey the inequalities $\langle\mathcal{O}_6^1(\mu^2)\rangle \geq 0$ and $\langle\mathcal{O}_6^2(\mu^2)\rangle \leq 0$, which can be derived from first principles. The corresponding coefficient functions were calculated in the chiral limit (Lanin *et al.*, 1986). Since $\langle\mathcal{O}_6^2(\mu^2)\rangle$ is subleading in $a_s(\mu^2)$, it is neglected in most phenomenological analyses. To leading order, one can use factorization of the matrix elements (that is, vacuum insertion) to rewrite $\langle\mathcal{O}_6^1\rangle$ in the form[34]

$$\langle\mathcal{O}_6^1\rangle \propto -\tfrac{64}{9}\pi^2 a_s\langle 0|\bar{u}u|0\rangle\langle 0|\bar{d}d|0\rangle. \tag{192}$$

For the dimension $D=8$ operators no higher-order calculations are available in the literature, so that it is customary in the QCD sum-rule analyses to neglect their logarithmic s dependence. Again, the $J=0$ contribution vanishes in the chiral limit. A factorization result similar to Eq. (192) can be derived, which now involves a five-dimensional quark-gluon mixed condensate (Grozin and Pinelis, 1986; Ioffe and Zyablyuk, 2001; Zyablyuk, 2004). Higher OPE dimensions are neglected [see Zyablyuk (2004) for an analysis that includes relevant $D=10$ operators].

C. Borel and pinched weight sum rules

Many ways have been explored to improve the saturation of the integrals at finite cutoff scale s_0, and to

[33]The suppression of the high-energy spectral function also reduces the experimental uncertainty on the integral since statistical errors are large at the kinematic end point of the τ phase space.

[34]Following Zyablyuk (2004), factorization for the $D=6$ operators can be written as $\langle(\bar{u}\lambda\Gamma_1 d)(\bar{d}\lambda\Gamma_2 u)\rangle = -(16/9)\mathrm{Tr}[\langle u\otimes\bar{u}\rangle\Gamma_1\langle d\otimes\bar{d}\rangle\Gamma_2]$, where Γ_i are Dirac matrices (acting on color, flavor, and Lorentz indices), the factor 16/8 includes the SU(3) color number, and the 4×4 matrix $\langle q\otimes\bar{q}\rangle$ is proportional to the quark condensate $\langle q\otimes\bar{q}\rangle = -(1/4)\langle 0|q\bar{q}|0\rangle$.

better control the validity of the OPE. In general, the approaches distinguish themselves by the definition of the weight $w(s)$ used under the integral

$$\frac{1}{4\pi^2}\int_0^{s_0} ds w(s)\rho_{V-A}(s). \qquad (193)$$

Since duality violations are expected to be largest in the vicinity of the timelike real axis (Poggio *et al.*, 1976), some authors suggest to use weights of the form $w_n(s) \propto (1-s/s_0)^n$ (Le Diberder and Pich, 1992b) (cf. Sec. VII.C). The class of functions that satisfy $w(s_0)=0$ is introduced as "pinched weights" by Cirigliano *et al.* (2003) and Cirigliano, Golowich, and Maltman (2003). As mentioned earlier, pinched weights improve the experimental accuracy of the sum rule but also reduce the effective inclusiveness of the spectrum, and hence make it more sensitive to duality violations.

Another way to improve the saturation of finite energy sum rules is to apply the Borel weight $w(s) = \exp(-s/M^2)$, emphasizing the lower resonances of the spectrum. Here, the OPE operators of dimension $D=n$ are suppressed as $\langle\mathcal{O}_{2n+2}\rangle/n!$, and all leading terms of the OPE vanish. The Borel-transformed sum rules give rise to nonperturbative corrections from quark condensates and nonvanishing quark masses that scale with the Borel parameter M^2 and with $\alpha_s(M^2)$. For example, the Borel-transformed first WSR reads (Floratos *et al.*, 1979; Narison, 1982; Pascual and de Rafael, 1982; Peccei and Solà, 1987)

$$\frac{1}{4\pi^2}\int_0^{s_0\to\infty} ds e^{-s/M^2}\rho_{V-A}(s) = f_\pi^2 + \frac{\alpha_s(M^2)}{2\pi}\left[-\frac{m_u(M^2)m_d(M^2)}{\pi^2} - \frac{8}{3}\frac{f_\pi^2 m_\pi^2}{M^2} - \frac{32\pi}{9}\frac{(\langle 0|\bar{q}q|0\rangle)^2}{M^4} + \cdots\right], \qquad (194)$$

where the lowest-order current algebra Gell-Mann-Oakes-Renner relation

$$f_\pi^2 m_\pi^2 = -(m_u + m_d)\langle 0|\bar{u}u|0\rangle, \qquad (195)$$

obtained from Eqs. (172) and (173), has been used (Gell-Mann *et al.*, 1978), and where $m_u(M^2)$ and $m_d(M^2)$ denote running light quark masses [see Jamin (2002) for a derivation of chiral corrections to Eq. (195), which are found to be of the order of −5%]. The Borel sum rule is plotted in Fig. 30 (upper) for $M=1$ GeV. Comparison with Fig. 29 (upper left-hand plot) exhibits gain in experimental precision and in the approach to the asymptotic regime. Inserting the experimental values for the parameters on the right-hand side of Eq. (194), and neglecting higher-order nonperturbative contributions $\mathcal{O}(M^{-6})$ and contributions other than quark condensates, one obtains $(8.44\pm0.17)\times10^{-3}$ GeV^2. From Fig. 30 we conclude that further nonperturbative power terms need to be added to satisfy the sum rule.

To reduce the correlation between the different operators, one can consider a Borel transformation in the complex plane of the Borel scale parameter, that is $M^2 \to M^2\exp[i(\pi-\phi)]$. Keeping only leading-order coefficients a_D in Eq. (187), one finds for the real and imaginary parts of the Borel transformation (Zyablyuk, 2004)

$$\frac{1}{4\pi^2}\int_0^{s_0\to\infty} e^{c_\phi}\cos(s_\phi)\rho_{V-A}(s) = f_\pi^2 + \sum_{k=1}^{\infty}(-1)^k\frac{\cos(k\phi)a_{2k+2}}{k!M^{2k}}, \qquad (196)$$

$$\frac{1}{4\pi^2 M^2}\int_0^{s_0\to\infty} e^{c_\phi}\sin(s_\phi)\rho_{V-A}(s) = \sum_{k=1}^{\infty}(-1)^k\frac{\sin(k\phi)a_{2k+2}}{k!M^{2k+2}}, \qquad (197)$$

with $s_\phi=(s/M^2)\sin\phi$ and $c_\phi=(s/M^2)\cos\phi$. If the sum rule is applied to the τ spectral functions, the argument of the cosine function must be negative to suppress the unknown $s_0>m_\tau^2$ tail of the spectrum. In the case of $\phi=\pi(2k-1)/2k$ $(k=2,3,\ldots)$ for the real part (196) and $\phi=\pi(k-1)/k$ $(k=3,4,\ldots)$ for the imaginary part (197), the sum rules become projective with vanishing leading operators of dimension $D=2k+2$. The real part for a particular working point chosen by Zyablyuk (2004) as a function of the cutoff s_0 is shown on the lower plot of Fig. 30. The chiral prediction given contains the pion pole, but no OPE power corrections. The sum rule is well saturated at $s_0=m_\tau^2$. The remaining discrepancy with the data is due to nonperturbative contributions. An update (Zyablyuk, 2004) of the numerical analysis performed by Ioffe and Zyablyuk (2001) finds for the leading $V-A$ operators using the ALEPH data (Barate *et al.*, 1998c)

$$a_6 = -(7.2\pm1.2)\times10^{-3}\ \text{GeV}^6, \qquad (198)$$

$$a_8 = (7.8\pm2.5)\times10^{-3}\ \text{GeV}^8. \qquad (199)$$

Zyablyuk also estimates the leading $D=10$ operator to be $a_{10}=-(4.4\pm2.8)\times10^{-3}$ GeV^{10}, without, however, reporting statistical correlations with a_6 and a_8. The imaginary part (197) of the Borel sum rule was used as input, as well as the angles $\phi=2\pi/3, 3\pi/4, 4\pi/5$ for which the operators a_8, a_{10}, a_{12} vanish, respectively. For the Borel parameter M^2 a range between 0.4 and 1.0 GeV^2 is used, which is integrated over to determine an average χ^2 estimator (Zyablyuk, 2004) that is minimized in the fit. The fit results for the real and imaginary parts of the sum rules (196) and (197), and for two working points in the parameter ϕ are shown in Fig. 31. The contribution from $D=10$ is significant here.

Recent theoretical developments match the $D=6$ operator, derived from the $V-A$ spectral sum rules, with the vacuum matrix elements $\langle\mathcal{O}_1\rangle_\mu$ and $\langle\mathcal{O}_8\rangle_\mu$, which are related to the electroweak penguin operator $\mathcal{Q}_8$ that contributes to $K\to\pi\pi$ decays [see, e.g., Bijnens *et al.* (2001) and Cirigliano, Golowich, and Maltman (2003)].

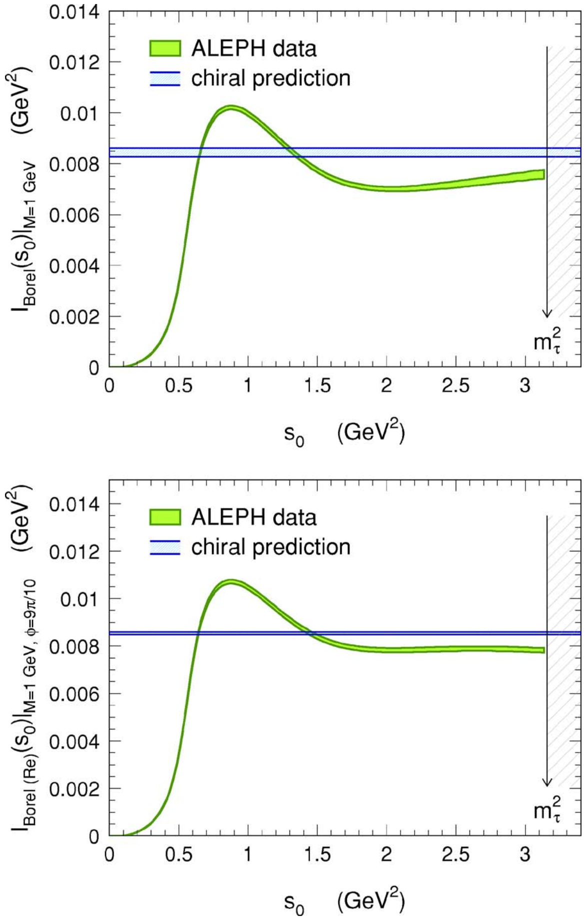

FIG. 30. (Color online) The Borel sum rule (194) (upper) and the real part of the complex Borel sum rule (196) for $\phi = 9\pi/10$ (lower), at $M=1$ GeV, and as a function of the integral cutoff s_0. The chiral prediction shown in the lower plot does not include OPE power corrections.

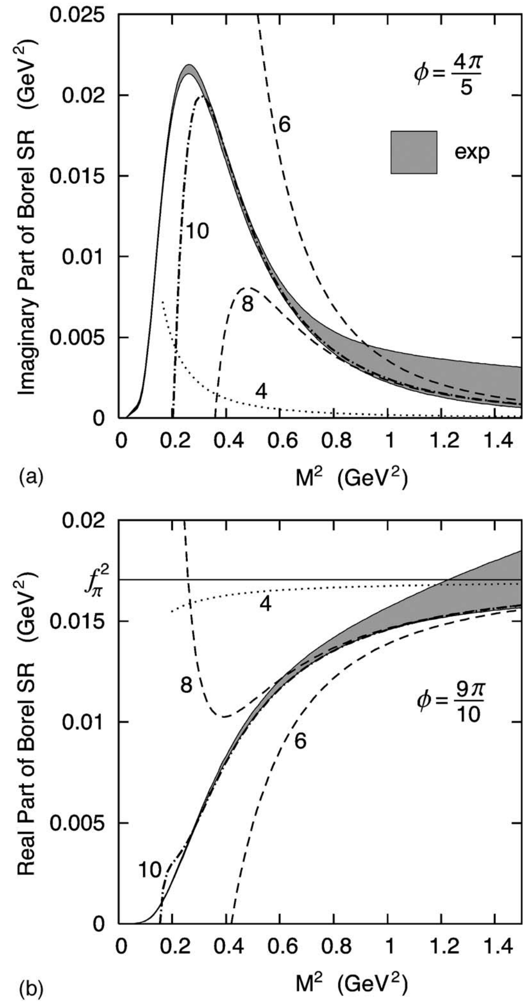

FIG. 31. Real part (196) of the Borel transformation for $\phi = 9\pi/10$ and its imaginary part (196) for $\phi = 4\pi/5$ as a function of the modulus M^2 of the Borel parameter. The leading order $D=12$ operator a_{12} vanishes in these sum rules. The shaded band shows the ALEPH data (Barate *et al.*, 1997b, 1998c), and lines display the leading-order operator series, i.e., neglecting all logarithmic terms. Numbers indicate the highest dimension considered in the operator sum. From Zyablyuk, 2004.

Together with the QCD penguin $\mathcal{Q}_6$, these operators generate direct *CP* violation in neutral kaon decays to two pions, the computation of which suffers from large uncertainties.

D. Inverse moment sum rules and chiral perturbation theory

We have seen that at sufficiently high energies nonperturbative effects are parametrized by vacuum condensates, following the OPE rules. A particular role is played by the condensates that are order parameters of the spontaneous breakdown of chiral symmetry (SBχS). They vanish at all orders of perturbation theory and control the high-energy behavior of chiral correlation functions, such as the difference of vector and axial-vector current two-point functions. On the other hand, at low energies, SBχS makes it possible to construct an effective theory of QCD, the chiral perturbation theory (χPT) (Weinberg, 1979; Gasser and Leutwyler, 1984), which uses Goldstone bosons as fundamental fields and provides a systematic expansion of QCD correlation functions in powers of momenta and quark masses. Any missing information is then parametrized by low-energy coupling constants, which can be determined phenomenologically in low-energy experiments involving pions and kaons. The fundamental parameters describing chiral symmetry breaking, the running quark masses, and the quark condensates appear in both low-energy χPT and the high-energy OPE expansion. For this reason it is useful to combine the two expansions in order to get a truly systematic approach to the chiral sum rules (Donoghue and Golowich, 1994). Such a combined approach has been illustrated by Davier *et al.* (1998) through determination of the L_{10} parameter of the chiral Lagrangian, including high-energy corrections coming from the OPE. The connection between the two domains is provided by the experimental τ spectral function $\rho V - A$.

At leading order χPT, L_{10} is obtained by the DMO sum rule (183)

$$\frac{1}{4\pi^2}\int_0^{s_0\to\infty} ds\frac{1}{s}\rho_{V-A}(s) \simeq -4L_{10}. \qquad (200)$$

As it stands the DMO sum rule (183) is subject to chiral corrections due to nonvanishing quark masses (Golowich and Kambor, 1997). On the other hand, the truncation of the integral at $s_0 \leq m_\tau^2$ introduces an error that competes with low-energy chiral corrections. Both types of corrections can be systematically included through (i) the high-energy expansion in $\alpha_s(s_0)$ and in inverse powers of s_0, and (ii) the low-energy expansion in powers of quark masses and of their logarithms.

In Sec. VII.C we have reviewed the simultaneous determination of the strong-coupling constant and the OPE operators using the spectral weights

$$w^{(k,\ell)}(s) = \left(1-\frac{s}{s_0}\right)^k\left(\frac{s}{s_0}\right)^\ell, \qquad (201)$$

for $k, \ell \geq 0$. Extension of the spectral moment analysis to negative integer values of ℓ [inverse moment sum rules (Golowich and Kambor, 1996)] requires, due to the pole at $s=0$, a modified contour of integration in the complex plane, as illustrated by Fig. 32. This is where χPT comes into play: Along the small circle C_2 placed at the production threshold $s_{\rm th}=4m_\pi^2$ one can use χPT predictions for the two-point correlators.

Generalizing the spectral moments (129) to inverse moment sum rules, one obtains for the Cauchy integral

$$R_{\tau,V/A}^{(k,\ell)} = 6\pi i|V_{ud}|^2 S_{\rm EW}\oint_C \frac{ds}{s_0} w^{(k,\ell)}(s)\left[\left(1+2\frac{s}{s_0}\right)\times\Pi_{V/A}^{(0+1)}(s) - 2\frac{s}{s_0}\Pi_A^{(0)}(s)\right], \qquad (202)$$

where $C=C_1+C_2$ for the inverse moments and $C=C_1$ for the positive moments (see Fig. 32).

The nonstrange correlators (38) are known up to two loops (Gasser and Leutwyler, 1984, 1985; Golowich and Kambor, 1995, 1998) in standard χPT.[35]

The analysis described by Davier *et al.* (1998) performs a fit of the OPE to the inverse moment sum rules $R_{\tau,V-A}^{(1,-1)}$ and the spectral moments (129). The inner integration circle C_2 occurring in $R_{\tau,V-A}^{(1,-1)}$ introduces sensitivity to the effective χPT parameter $L_{10}^{\rm eff}$, which is determined by the fit. This quantity is a well-defined observable that can be related to $L_{10}^r(\mu_{\chi\rm PT})$ at each loop in χPT.

[35] Davier *et al.* (1998) used generalized χPT [$G\chi$PT (Knecht and Stern, 1995)] to $\mathcal{O}(p^4)$ one-loop order only. Standard χPT assumes (Weinberg, 1977) the validity of Eq. (195) and $r \simeq 2m_K^2/m_\pi^2-1 \approx 25.9$, whereas $G\chi$PT admits lower values of these two quantities (Fuchs *et al.*, 1990, 1991; Knecht and Stern, 1995). Alterations of standard $\mathcal{O}(p^4)$ results for nonstrange correlators introduced by $G\chi$PT are marginal. They merely concern the symmetry-breaking $J=0$ component of the spectral functions and most of them are absorbed into the renormalization of f_π.

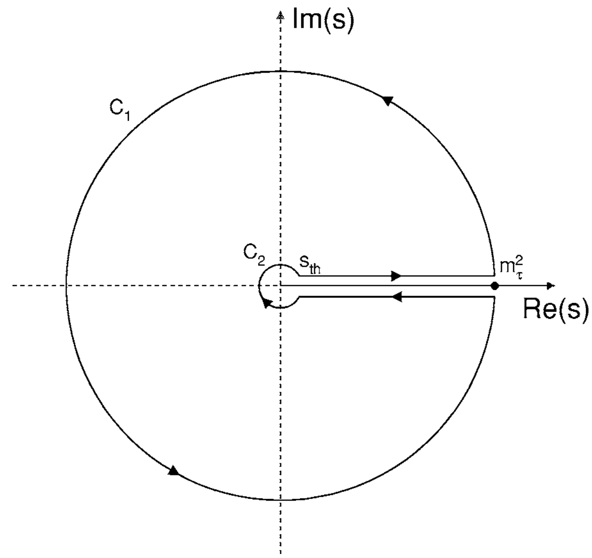

FIG. 32. Integration contour around the circles at $s=m_\tau^2$ and $s=s_{\rm th}$.

Spectral information is used to simultaneously determine $L_{10}^{\rm eff}$ and the nonperturbative phenomenological operators. For dimension $D=6$ the contribution from $\mathcal{O}_6^2$ is neglected since it is large N_C and α_s^2 suppressed. The results of the fit are reported as (Davier *et al.*, 1998)

$$L_{10}^{\rm eff} = -(6.36 \pm 0.09_{\rm exp} \pm 0.14_{\rm th} \pm 0.07_{\rm fit} \pm 0.06_{\rm OPE}) \times 10^{-3}, \qquad (203)$$

$$\langle\mathcal{O}_6\rangle = (5.0 \pm 0.5_{\rm exp} \pm 0.4_{\rm th} \pm 0.2_{\rm fit} \pm 1.1_{\rm OPE}) \times 10^{-4}\ {\rm GeV}^6, \qquad (204)$$

$$\langle\mathcal{O}_8\rangle = (8.7 \pm 1.0_{\rm exp} \pm 0.1_{\rm th} \pm 0.6_{\rm fit} \pm 2.1_{\rm OPE}) \times 10^{-3}\ {\rm GeV}^8, \qquad (205)$$

where $\mathcal{O}_6=\mathcal{O}_6^1(m_\tau^2)$. The fit errors are separated in experimental (first errors) and theoretical (second errors) parts, and systematic fit uncertainties (third errors) are added. The last errors estimate uncertainties due to the OPE breakdown (Barate *et al.*, 1998c). They are small for $L_{10}^{\rm eff}$ and dominant for nonperturbative operators. Correcting for the factor of about −13 between the definition of $\langle\mathcal{O}_6\rangle$ and a_6 of Eq. (198), the two estimates are in agreement. The results (204) and (205) have been confirmed by Ackerstaff *et al.* (1999a) using OPAL data. In general it is observed that while all available sum-rule analyses[36] agree on the value for the $D=6$ contribution to the $V-A$ correlator, the $D=8$ contribution, due to its smallness, is less stable. It exhibits a model dependence that exceeds the experimental error in Eq. (205).

[36] See also the detailed recent analysis (Catà *et al.*, 2005) on duality violations in $V-A$ sum rules, which came too late to be included in this review.

A stability test of the results (203)–(205) at m_τ^2 has been performed by Davier *et al.* (1998) fitting with variable "τ masses" $s_0 \leq m_\tau^2$ (Davier *et al.*, 1998). The resulting convergence was found satisfactory.

Expressing $L_{10}^{\rm eff}$ of Eq. (203) at the renormalization scale $\mu_{\chi\rm PT} = m_\rho \simeq 770$ MeV, one obtains (Davier *et al.*, 1998) $L_{10}^r(m_\rho) = -(5.13 \pm 0.19) \times 10^{-3}$, where experimental and theoretical errors of different sources have been added in quadrature. This result can be compared with the value of L_{10}^r that is obtained from the one-loop expression of the axial form factor F_A of $\pi^- \to e^- \bar{\nu}_e \gamma$ decays [see Bijnens and Talavera (1997) for notations]

$$F_A = \frac{4\sqrt{2} m_\pi}{f_\pi}(L_9 + L_{10}). \tag{206}$$

Using $L_9^r(m_\rho) = (6.78 \pm 0.15) \times 10^{-3}$ (Gasser and Leutwyler, 1985; Bijnens *et al.*, 1995; Davier *et al.*, 1998) and $F_A = 0.0116 \pm 0.0016$ (Eidelman *et al.*, 2004), one obtains $L_9 + L_{10} = (1.36 \pm 0.19) \times 10^{-3}$. This gives $L_{10}^r(m_\rho) = -(5.42 \pm 0.24) \times 10^{-3}$, in agreement with the τ result.

X. CONCLUSIONS AND PERSPECTIVES

The physics of hadronic τ decays has been the subject of much progress in the last decade, at both the experimental and theoretical level. Somewhat unexpectedly, hadronic τ decays provide one of the most powerful testing grounds for QCD. This situation results from a number of favorable conditions:

- The τ lepton is heavy enough to decay into a variety of hadrons, with net strangeness 0 and ± 1.
- τ leptons are copiously produced in pairs at e^+e^- colliders, leading to simple event topologies without extra background particles.
- The experimental study of τ decays could be done with large data samples: at LEP with high efficiency and small background; at the $\Upsilon(4S)$ energy with much increased statistics, but irreducible backgrounds. The two experimental setups offer complementary advantages.
- As a consequence, τ decays are experimentally known to great details and their rates measured with high precision.
- The theoretical description of hadronic τ decays is based on solid ground and found to be dominated by perturbative QCD, as the result of several lucky circumstances, which shall be briefly recalled below.

The τ decay rates into hadrons are expressed through spectral functions of different final states with specific quantum numbers. The spectral functions are the basic ingredients to the theoretical description of these decays, since they represent the probability to produce a given hadronic system from the vacuum, as a function of its invariant mass squared s. The spectral functions are dominated by known resonances at low mass, and tend to approach the quark-level asymptotic regime towards m_τ^2. They have been determined for individual hadronic modes, however, they are conveniently summed and separated into their inclusive vector and axial-vector components for the nonstrange part, while the Cabibbo-suppressed strange part cannot be fully separated at present due to the lack of necessary experimental information.

The nonstrange τ vector spectral functions can be compared to the corresponding quantities obtained in e^+e^- annihilation by virtue of isospin symmetry. The $\mathcal{O}(\%)$ precision reached makes it necessary to correct for isospin-symmetry breaking. Beyond superficial agreement, detailed comparison unveils discrepancies with some e^+e^- data sets. Since the vector spectral functions are the necessary ingredients to compute vacuum-polarization integrals, required for the evaluation of the running of $\alpha(s)$ or the anomalous magnetic moment of the muon a_μ, this disagreement leads to different results when using τ or e^+e^- spectral functions. While the e^+e^--based theoretical a_μ value disagrees with the measurement by 2.7 "standard deviations," possibly indicating a contribution from physics beyond the Standard Model, the τ-based calculation is consistent with experiment. Although the use of e^+e^- data is *a priori* more direct, the physics at stake is such that the present situation must evolve, requiring more experimental and theoretical cross-checks. Newest e^+e^- results already indicate better agreement with the τ data.

The observation that hadronic τ spectral functions can provide precision information on perturbative QCD is surprising, considering the moderate energy scale involved in these decays. Hence it is useful to recall briefly the reasons behind this success:

- The total semileptonic decay rate normalized to the leptonic width R_τ is obtained by integrating over s the total spectral function weighed by a known kinematic function originating from the $V-A$ leptonic tensor. This integral can be transformed to a complex contour integral over a circle at $|s| = m_\tau^2$, hence involving only large complex s values where perturbative QCD can be applied.
- One factor in the weight function, $(1 - s/m_\tau^2)^2$, chops off the integrand in the vicinity of the real axis where poles of the current correlator are located.
- The invariant-mass spectra in hadronic τ decays, dominated by resonances, are related to quark-level contributions expected at large mass. This global quark-hadron duality is expected to work best in more inclusive situations. In the case of hadronic τ decays, this condition is particularly well met with several resonance contributions in each of equal-importance vector and axial-vector components.
- The perturbative expansion of the spectral function is known to third order in α_s, with some estimates of the fourth-order coefficient.
- The perturbative and nonperturbative contributions can be treated systematically using the operator

product expansion, giving corrections organized in inverse powers D of m_τ.

- The *a priori* dominant nonperturbative term from the gluon condensate ($D=4$) is strongly suppressed by the second factor of the weight function $1+2s/m_\tau^2$. This accidental fact renders hadronic τ decays particularly favorable since nonperturbative effects are expected to be small.
- The next $D=6$ term is subject to a partial cancellation between the vector V and axial-vector A contributions, due to the $1-\gamma_5$ relative factor.

These fortunate circumstances explain why hadronic τ decays can be globally described by perturbative QCD with very small nonperturbative corrections. This behavior has been verified model independently using the measured spectral functions. From a simultaneous fit of the total hadronic rate, obtained with precision from the leptonic branching ratio and spectral moments that are weighted integrals of mass-squared distributions, the total nonperturbative contribution is found to be $\delta_{\mathrm{NP},V+A}=(-4.3\pm1.9)\times10^{-3}$ relative to the $V+A$ hadronic width. This is almost a factor of 50 smaller than the α_s-dependent perturbative correction to R_τ. The predicted near cancellation between the V and A contributions has been also observed as $\delta_{\mathrm{NP},V}=(2.0\pm0.3)\times10^{-2}$ and $\delta_{\mathrm{NP},A}=(-2.8\pm0.3)\times10^{-2}$.

Several approaches are available to treat the perturbative expansion of the τ hadronic width. In fixed-order perturbation theory (FOPT), all contributions beyond the known orders of the Adler function are neglected, even if some parts resulting from the running of α_s are calculable (and calculated). On the contrary, the contour-improved FOPT variant (CIPT) keeps all known terms. It has been shown that a faster convergence is achieved with CIPT and since the FOPT expansion represents an unnecessary approximation, the CIPT approach should be preferred. Analyses using ALEPH and OPAL spectral functions give $\alpha_s(m_\tau^2)$ values that are in agreement. The robustness of the result can be established by comparing results from separate fits based on the V or A spectral functions, which are less inclusive and include larger, yet still small, nonperturbative contributions: their results are in reasonable agreement. A further test is achieved by partial integration of the spectral function up to a variable hypothetical τ mass s_0 less than m_τ^2: the derived $\alpha_s(s_0)$ values are in agreement with the expected behavior from the QCD renormalization group down to s_0 values as low as 1 GeV^2, where the OPE begins to break down. Therefore the moderately high mass of the τ lepton is shown to be fully adequate for a precision measurement of α_s.

Using the final spectral functions from ALEPH, supplemented by the world average leptonic and total strange hadronic fractions, the most precise determination of the strong coupling at the τ mass scale gives

$$\alpha_s(m_\tau^2) = 0.345 \pm 0.004_{\mathrm{exp}} \pm 0.009_{\mathrm{th}}. \tag{207}$$

Evolving this value to the Z mass, and adding experimental and theoretical errors in quadrature, gives $\alpha_s(M_Z^2)_\tau=0.1215\pm0.0012$. Taken together with the measurement from the Z width at LEP, $\alpha_s(M_Z^2)_{Z\ \mathrm{width}}=0.1186\pm0.0027$, the $\alpha_s(m_\tau^2)$ determination provides a powerful test of the running of α_s as predicted by QCD. The property of asymptotic freedom can be conveniently tested using the estimator

$$r(s_1,s_2) = \frac{\Delta\alpha_s^{-1}}{\Delta \ln\sqrt{s}} = 1.405 \pm 0.053, \tag{208}$$

with $s_1=m_\tau^2$ and $s_2=M_Z^2$, while QCD predicts 1.353 ± 0.006.

Further progress in the QCD analyses of τ decays will have to wait for a full calculation of the fourth-order coefficient K_4 in the Adler function expansion. Such a program is underway and will succeed with the availability of improved computing power. When K_4 is known, we expect the perturbative uncertainty to become small: errors on $\alpha_s(m_\tau^2)$ from K_5, estimated assuming a geometric growth of the perturbative coefficients with 100% uncertainty, and from the renormalization scale will be 0.002 and 0.002, respectively. Using the existing data, the total error on $\alpha_s(m_\tau^2)$ will be reduced by a factor of 2 and reach a relative precision of 1.4%. Hence the calculation of K_4 will be highly rewarding.

Further progress can be considered with better quality data. Whereas ameliorating the precision on the branching ratios appears to be difficult, several areas could be improved with facilities such as B factories, affording very large statistics samples. Examples include studying the high mass part of the spectrum near the τ-mass end point, limited at the moment by statistics. This will improve knowledge of the spectral function in an interesting region and permit study of the approach to the asymptotic regime. Such topics can also be covered at a τ-charm factory operating near the τ threshold. Detailed physics simulations are required to quantitatively assess the potential of these measurements.

The strange component of the τ hadronic width gives access to the study of flavor-symmetry breaking induced by the massive s quark as compared to nearly massless u and d quarks. Although the expected shift in the strange hadronic width is found experimentally, it turns out that a competitive determination of the strange quark mass m_s is difficult because the poor convergence of the mass-dependent perturbative series and lack of sufficient inclusiveness in higher-order spectral moments that are sensitive to m_s. Thus various analyses have given somewhat different results, depending on the moments used. The situation might improve with a better determined strange spectral function. Contrary to the situation for m_s, the determination of the CKM matrix element $|V_{us}|$ from strange τ decays appears on safe grounds, since it relies directly on the nonweighted spectral function with maximum inclusiveness and a better control of the perturbative expansion. Present data yield

$$|V_{us}| = 0.2204 \pm 0.0028_{\rm exp} \pm 0.0003_{\rm th} \pm 0.0001_{m_s}, \quad (209)$$

where m_s has been taken from lattice calculations to be $m_s(m_\tau^2) = 79 \pm 8$ MeV.

The study of strange τ decays can benefit significantly from large statistical samples provided by B factories, complemented by the $K-\pi$ separation available with the *BABAR* and Belle detectors. The prospects are excellent for improving over the present situation. As discussed above, the determination of $|V_{us}|$ is limited by the experimental error, while the theoretical uncertainty would permit the best measurement of this quantity. We express our desire that these experiments measure the various strange decay channels in a systematic way towards achieving this goal. It could also occur that the present unsatisfactory situation on the determination of m_s will improve during this process. In any case, better strange spectral functions are needed.

Another active field of research is the study of finite-energy chiral sum rules, involving the nonstrange $V-A$ spectral function, which are of intrinsically nonperturbative nature. The analyses are divided into spectral moments that are weighted integrals over the $V-A$ spectral function with some high-mass damping function to reduce the systematic uncertainty due to the finite-energy integral cutoff and inverse moment sum rules, which, due to the singularity at $s=0$, give direct access to the chiral structure of the QCD Lagrangian. The former sum rules are useful to analyze the nonperturbative structure of the OPE, since it allows one to measure higher-dimensional operators of the expansion independently of perturbative contributions. Several analyses give similar results on the $D=6$ contribution, while the much smaller $D=8$ contribution exhibits some model dependence. Even $D=10$ has been considered and found to improve the fit, though not significantly. No sign of nonconvergence of the OPE has been detected at the τ-mass scale. Inverse moment sum rules have been traditionally used through the Das-Mathur-Okubo sum rule to determine the polarizability of the pion. In a more evolved later analysis the parameter L_{10} of the chiral Lagrangian has been determined, which at one loop and expressed at the chiral perturbation theory (χPT) renormalization scale $\mu_{\chi\rm PT} = m_\rho \simeq 770$ MeV, is found to be

$$L_{10}^r(m_\rho) = -(5.13 \pm 0.19) \times 10^{-3}, \quad (210)$$

where experimental and theoretical errors of different sources have been added in quadrature. This result is in agreement with, but more precise than, corresponding determinations from the axial form factor of $\pi^- \to e^- \bar{\nu}_e \gamma$ decays.

While the study of hadronic τ decays has achieved a high status thanks to precise and complete sets of measurements and development of the relevant theoretical framework, it is satisfying that advances are at hand at both the experimental and theoretical levels.

ACKNOWLEDGMENTS

We are indebted to all our experimental and theoretical colleagues who have provided valuable contributions to the field of τ physics. During this work we benefited from helpful discussions with Georges Grunberg, François Le Diberder, William Marciano, Sven Menke, Antonio Pich, Joachim Prades, Jan Stern, and Konstantin Zyablyuk. We thank Konstantin Chetyrkin, Matthias Jamin, Sven Menke, Antonio Pich, Achim Stahl, and Arkady Vainshtein for critically reading the document and providing helpful comments. Special thanks go to Shaomin Chen and Changzheng Yuan for the fruitful collaboration on spectral function measurements.

REFERENCES

Abbaneo, D., *et al.* (The LEP Electroweak Working Group), 2002, LEPEWWG/2002-01.
Abbaneo, D., *et al.* (The LEP Electroweak Working Group), 2004, LEPEWWG/2004-01, CERN-PH-EP/2004-069, e-print hep-ex/0412015.
Abbiendi, G., *et al.* (OPAL Collaboration), 1999, Phys. Lett. B **447**, 134.
Abbiendi, G., *et al.* (OPAL Collaboration), 2003, Phys. Lett. B **551**, 35.
Abbiendi, G., *et al.* (OPAL Collaboration), 2004, Eur. Phys. J. C **35**, 437.
Abe, K., *et al.* (E143 Collaboration), 1995, Phys. Rev. Lett. **74**, 346.
Abe, T., *et al.*, 2001, *Linear Collider Physics Resource Book for Snowmass 2001*, SLAC-R-570, e-print hep-ex/0106057.
Abdallah, J., *et al.* (DELPHI Collaboration), 2004, Eur. Phys. J. C **37**, 1.
Abreu, P., *et al.* (DELPHI Collaboration), 1998, Phys. Lett. B **426**, 411.
Abreu, P., *et al.* (DELPHI Collaboration), 1999, Eur. Phys. J. C **10**, 201.
Abreu, P., *et al.* (DELPHI Collaboration), 2001, Eur. Phys. J. C **20**, 617.
Acciarri, M., *et al.* (L3 Collaboration), 2001, Phys. Lett. B **507**, 47.
Achasov, M. N., *et al.* (SND Collaboration), 2005, J. Exp. Theor. Phys. **101**, 1053.
Achasov, M., *et al.*, 2006, e-print hep-ph/0604052.
Ackerstaff, K., *et al.* (OPAL Collaboration), 1998, Eur. Phys. J. C **4**, 193.
Ackerstaff, K., *et al.* (OPAL Collaboration), 1999a, Eur. Phys. J. C **7**, 571.
Ackerstaff, K., *et al.* (OPAL Collaboration), 1999b, Eur. Phys. J. C **8**, 183.
Adams, D., *et al.*, 1994, Phys. Lett. B **329**, 399.
Adler, S., 1974, Phys. Rev. D **10**, 3714.
Akers, R., *et al.* (OPAL Collaboration), 1995, Z. Phys. C **67**, 45.
Akers, R., *et al.* (OPAL Collaboration), 1997, Z. Phys. C **75**, 593.
Akhmetshin, R. R., *et al.* (CMD-2 Collaboration), 2004, Phys. Lett. B **578**, 285.
Albajar, C., *et al.* (UA1 Collaboration), 1996, Phys. Lett. B **369**, 46.
Albrecht, H., *et al.* (ARGUS Collaboration), 1988, Phys. Lett. B **202**, 149.

Albrecht, H., *et al.* (ARGUS Collaboration), 1993, Phys. Lett. B **316**, 608.

Alemany, R., M. Davier, and A. Höcker, 1998, Eur. Phys. J. C **2**, 123.

Aloisio, A., *et al.* (KLOE Collaboration), 2005, Phys. Lett. B **606**, 12.

Altarelli, G., P. Nason, and G. Ridolfi, 1995, Z. Phys. C **68**, 257.

Amendolia, S. R., *et al.* (NA7 Collaboration), 1986, Nucl. Phys. B **277**, 168.

Ammar, R., *et al.* (CLEO Collaboration), 1998, Phys. Rev. D **57**, 1350.

Anastassov, A., *et al.* (CLEO Collaboration), 1997, Phys. Rev. D **55**, 2559.

Anderson, S., *et al.* (CLEO Collaboration), 2000, Phys. Rev. D **61**, 112002.

Appelquist, T., and J. Carazzone, 1975, Phys. Rev. D **11**, 2856.

Arms, K., *et al.* (CLEO Collaboration), 2005, Phys. Rev. Lett. **94**, 241802.

Artuso, M., *et al.* (CLEO Collaboration), 1992, Phys. Rev. Lett. **69**, 3278.

Artuso, M., *et al.* (CLEO Collaboration), 1994, Phys. Rev. Lett. **72**, 3762.

Asner, D., *et al.* (CLEO Collaboration), 2000, Phys. Rev. D **61**, 012002.

Aubert, B., *et al.* (BABAR Collaboration), 2004, Phys. Rev. D **70**, 072004.

Aubert, B., *et al.* (BABAR Collaboration), 2005a, Phys. Rev. D **71**, 052001.

Aubert, B., *et al.* (BABAR Collaboration), 2005b, Phys. Rev. D **72**, 072001.

Aubin, C., *et al.* (HPQCD, MILC, and UKQCD Collaborations), 2004, Phys. Rev. D **70**, 031504(R).

Bai, J. Z., *et al.* (BES Collaboration), 2002, Phys. Rev. Lett. **88**, 101802.

Baikov, P. A., K. G. Chetyrkin, and J. H. Kühn, 2002, Phys. Rev. Lett. **88**, 012001.

Baikov, P. A., K. G. Chetyrkin, and J. H. Kühn, 2003, Phys. Rev. D **67**, 074026.

Baikov, P. A., K. G. Chetyrkin, and J. H. Kühn, 2005, Phys. Rev. Lett. **95**, 012003.

Bailey, J., *et al.*, 1977, Phys. Lett. **68B**, 191.

Balest, R., *et al.* (CLEO Collaboration, 1995, Phys. Rev. Lett. **75**, 3809.

Ball, P., M. Beneke, and V. M. Braun, 1995, Nucl. Phys. B **452**, 563.

Barate, R., *et al.* (ALEPH Collaboration), 1997a, Z. Phys. C **74**, 263.

Barate, R., *et al.* (ALEPH Collaboration), 1997b, Z. Phys. C **76**, 15.

Barate, R., *et al.* (ALEPH Collaboration), 1998a, Eur. Phys. J. C **1**, 65.

Barate, R., *et al.* (ALEPH Collaboration), 1998b, Eur. Phys. J. C **4**, 29.

Barate, R., *et al.* (ALEPH Collaboration), 1998c, Eur. Phys. J. C **4**, 409.

Barate, R., *et al.* (ALEPH Collaboration), 1999a, Eur. Phys. J. C **10**, 1.

Barate, R., *et al.* (ALEPH Collaboration), 1999b, Eur. Phys. J. C **11**, 599.

Bardeen, W. A., A. J. Buras, D. W. Duke, and T. Muta, 1978, Phys. Rev. D **18**, 3998.

Barkov, L. M., *et al.* (OLYA and CMD Collaborations), 1985, Nucl. Phys. B **256**, 365.

Bartelt, J., *et al.* (CLEO Collaboration), 1996, Phys. Rev. Lett. **76**, 4119.

Becchi, C., S. Narison, E. de Rafael, and F. J. Yndurain, 1981, Z. Phys. C **8**, 335.

Becirevic, D., *et al.*, 2004, Nucl. Phys. B (Proc. Suppl.) **140**, 246.

Behrend, H. J., *et al.* (CELLO Collaboration), 1990, Z. Phys. C **46**, 537.

Beneke, M., 1993, Nucl. Phys. B **405**, 424.

Beneke, M., 1999, Phys. Rep. **317**, 1.

Beneke, M., and V. M. Braun, 1999, Phys. Lett. B **348**, 513.

Beneke, M., and V. I. Zakharov, 1992, Phys. Rev. Lett. **69**, 2472.

Bennett, G. W., *et al.* [Muon $(g-2)$ Collaboration], 2004, Phys. Rev. Lett. **92**, 161802.

Bergfeld, T., *et al.* (CLEO Collaboration), 1997, Phys. Rev. Lett. **79**, 2406.

Bernreuther, W., 1983, Ann. Phys. (N.Y.) **151**, 127.

Bernreuther, W., and W. Wetzel, 1982, Nucl. Phys. B **197**, 228; 1982, Nucl. Phys. B **513**, 758(E).

Bethke, S., 2000, J. Phys. G **26**, R27.

Bethke, S., 2003, Nucl. Phys. B (Proc. Suppl.) **121**, 74.

Bethke, S., 2004, Nucl. Phys. B (Proc. Suppl.) **135**, 345.

Bijnens, J., G. Ecker, and J. Gasser, 1995, in *The Second* DAΦNE *Physics Handbook*, edited by L. Maiani, G. Pancheri, and N. Paver (INFN, Frascati), Vol. I, p. 125.

Bijnens, J., E. Gàmiz, and J. Prades, 2001, J. High Energy Phys. 10009.

Bijnens, J., and P. Gosdzinsky, 1996, Phys. Lett. B **388**, 203.

Bijnens, J., E. Pallante, and J. Prades, 1996, Nucl. Phys. B **474**, 379.

Bijnens, J., E. Pallante, and J. Prades, 2002, Nucl. Phys. B **626**, 410.

Bijnens, J., and P. Talavera, 1997, Nucl. Phys. B **489**, 387.

Binner, S., J. H. Kühn, and K. Melnikov, 1999, Phys. Lett. B **459**, 279.

Bisello, D., *et al.* (DM2 Collaboration), 1989, Phys. Lett. B **220**, 321.

Bishai, M., *et al.* (CLEO Collaboration), 1999, Phys. Rev. Lett. **82**, 281.

Bjorken, J., 1970, Phys. Rev. D **1**, 1376.

Blobel, V., 1984, Report No. DESY-84/118.

Blok, B., M. A. Shifman, and D.-X. Zhang, 1998, Phys. Rev. D **57**, 2691; **59**, 019901(E) (1998).

Blokland, I., A. Czarnecki, and K. Melnikov, 2002, Phys. Rev. Lett. **88**, 071803.

Blum, T., 2003, Phys. Rev. Lett. **91**, 052001.

Bortoletto, D., *et al.* (CLEO Collaboration), 1993a, Phys. Rev. Lett. **71**, 1791.

Bortoletto, D., *et al.* (CLEO Collaboration), 1993b, Phys. Rev. Lett. **71**, 3762.

Bouchiat, C., and L. Michel, 1961, J. Phys. Radium **22**, 121.

Braaten, E., 1988, Phys. Rev. Lett. **60**, 1606.

Braaten, E., 1989, Phys. Rev. D **39**, 1458.

Braaten, E., and C. S. Li, 1990, Phys. Rev. D **42**, 3888.

Braaten, E., S. Narison, and A. Pich, 1992, Nucl. Phys. B **373**, 581.

Brambilla, N., *et al.* (The Quarkonium Working Group), 2004, e-print hep-ph/0412158, p. 399.

Briere, R. A., *et al.* (CLEO Collaboration), 2003, Phys. Rev. Lett. **90**, 181802.

Broadhurst, D. J., 1981, Phys. Lett. **101B**, 423.

Broadhurst, D. J., 1993, Z. Phys. C **58**, 339.

Broadhurst, D. J., and S. C. Generalis, 1985, Phys. Lett. **165B**,

175.
Brodsky, S. J., and E. de Rafael, 1968, Phys. Rev. **168**, 1620.
Brodsky, S. J., S. Menke, C. Merino, and J. Rathsman, 2002, Phys. Rev. D **67**, 055008.
Browder, T. E., *et al.* (CLEO Collaboration), 2000, Phys. Rev. D **61**, 052004.
Buskulic, D., *et al.* (ALEPH Collaboration), 1993, Phys. Lett. B **307**, 209.
Buskulic, D., *et al.* (ALEPH Collaboration), 1996a, Z. Phys. C **70**, 561.
Buskulic, D., *et al.* (ALEPH Collaboration), 1996b, Z. Phys. C **70**, 579.
Bylsma, B., *et al.* (HRS Collaboration), 1987, Phys. Rev. D **35**, 2269.
Cabibbo, N., and R. Gatto, 1960, Phys. Rev. Lett. **4**, 313.
Cabibbo, N., and R. Gatto, 1961, Phys. Rev. **124**, 1577.
Catà, O., M. Golterman, and S. Peris, 2005, J. High Energy Phys. **0508**, 076.
Celmaster, W., and R. J. Gonsalves, 1980, Phys. Rev. Lett. **44**, 560.
Chen, S., 1998, Nucl. Phys. B (Proc. Suppl.) **64**, 256.
Chen, S., M. Davier, and A. Höcker, 1999, Nucl. Phys. B (Proc. Suppl.) **76**, 369.
Chen, S., *et al.*, 2001, Eur. Phys. J. C **22**, 31.
Chetyrkin, K. G., C. A. Dominguez, D. Pirjol, and K. Schilcher, 1995, Phys. Rev. D **51**, 5090.
Chetyrkin, K. G., S. G. Gorishny, and V. P. Spiridonov, 1985, Phys. Lett. **160B**, 149.
Chetyrkin, K. G., S. G. Gorishny, and V. P. Spiridonov, 1997, Phys. Lett. B **390**, 309.
Chetyrkin, K. G., A. L. Kataev, and F. V. Tkachov, 1979, Phys. Lett. **85**, 277.
Chetyrkin, K. G., B. A. Kniehl, and M. Steinhauser, 1997, Phys. Rev. Lett. **79**, 2184.
Chetyrkin, K. G., B. A. Kniehl, and M. Steinhauser, 1998, Nucl. Phys. B **510**, 61.
Chetyrkin, K. G., and J. H. Kühn, 1997, Phys. Lett. B **406**, 102.
Chetyrkin, K. G., J. H. Kühn, and A. A. Pivovarov, 1998, Nucl. Phys. B **533**, 473.
Chetyrkin, K. G., J. H. Kühn, and M. Steinhauser, 1996, Nucl. Phys. B **482**, 213.
Chetyrkin, K. G., and A. Kwiatkowski, 1993, Z. Phys. C **59**, 525.
Chetyrkin, K. G., D. Pirjol, and K. Schilcher, 1997, Phys. Lett. B **404**, 337.
Chýla, J., and A. L. Kataev, 1992, Phys. Lett. B **297**, 385.
Cirigliano, V., J. F. Donoghue, E. Golowich, and K. Maltman, 2003, Phys. Lett. B **555**, 71.
Cirigliano, V., G. Ecker, and H. Neufeld, 2001, Phys. Lett. B **513**, 361.
Cirigliano, V., G. Ecker, and H. Neufeld, 2002, J. High Energy Phys. 08002.
Cirigliano, V., E. Golowich, and K. Maltman, 2003, Phys. Rev. D **68**, 054013.
Ciulli, C., S. Sebu, K. Schilcher, and H. Spiesberger, 2004, Phys. Lett. B **595**, 359.
Coan, T., *et al.* (CLEO Collaboration), 1995, Phys. Lett. B **356**, 580.
Coan, T. E., *et al.* (CLEO Collaboration), 2004, Phys. Rev. Lett. **92**, 232001.
Colangelo, G., F. De Fazio, G. Nardulli, and N. Paver, 1997, Phys. Lett. B **408**, 340.
Colangelo, G., M. Finkemeier, and R. Urech, 1996, Phys. Rev. D **54**, 4403.
Czarnecki, A., and W. J. Marciano, 1999, Nucl. Phys. B (Proc. Suppl.) **76**, 245.
Czarnecki, A., and W. Marciano, 2001, Phys. Rev. D **64**, 013014.
Czarnecki, A., W. J. Marciano, and A. Vainshtein, 2003, Phys. Rev. D **67**, 073006; see references to the earlier works therein.
Czyż, H., and J. H. Kühn, 2001, Eur. Phys. J. C **18**, 497.
Czyż, H., J. H. Kühn, G. Rodrigo, and M. Szopa, 2002, Eur. Phys. J. C **24**, 71; see also the later publications on the subject from these authors and collaborators.
Dams, C., and R. Kleiss, 2005, Nucl. Phys. B **716**, 421.
Das, T., V. S. Mathur, and S. Okubo, 1967, Phys. Rev. Lett. **19**, 859.
Das, T., *et al.* 1967, Phys. Rev. Lett. **18**, 759.
Davier, M., 1997, Nucl. Phys. B (Proc. Suppl.) **55C**, 395.
Davier, M., 2003, in *Proceedings of the Workshop on Hadronic Cross-Section at Low-Energy (SIGHAD03)*, Pisa, Italy, 2003, e-print hep-ex/0312065.
Davier, M., S. Eidelman, A. Höcker, and Z. Zhang, 2003a, Eur. Phys. J. C **27**, 497.
Davier, M., S. Eidelman, A. Höcker, and Z. Zhang, 2003b, Eur. Phys. J. C **31**, 503.
Davier, M., L. Girlanda, A. Höcker, and J. Stern, 1998, Phys. Rev. D **58**, 096014.
Davier, M., and A. Höcker, 1998a, Phys. Lett. B **419**, 419.
Davier, M., and A. Höcker, 1998b, Phys. Lett. B **435**, 427.
Davier, M., and W. J. Marciano, 2004, Annu. Rev. Nucl. Part. Sci. **54**, 115.
Davier, M., *et al.* 2001, Nucl. Phys. B (Proc. Suppl.) **B98**, 319.
Davis, C. T. H., *et al.*, 2004, Phys. Rev. Lett. **92**, 022001.
Decamp, D., *et al.* (ALEPH Collaboration), 1992, Z. Phys. C **54**, 211.
Decker, R., and M. Finkemeier, 1993, Phys. Rev. D **48**, 4203.
Decker, R., and E. Mirkes, 1993, Phys. Rev. D **47**, 4012.
de Troconiz, J. F., and F. J. Yndurain, 2005, Phys. Rev. D **71**, 073008.
Dhar, A., 1983, Phys. Lett. **128B**, 407.
Dhar, A., and V. Gupta, 1983, Phys. Rev. D **29**, 2822.
Dine, M., and J. J. Sapirstein, 1979, Phys. Rev. Lett. **43**, 668.
Dinsdale, M. J., and C. J. Maxwell, 2005, Nucl. Phys. B **713**, 465.
Dirac, P. A. M., 1928, Proc. R. Soc. London, Ser. A **117**, 610.
Dominguez, C. A., and E. de Rafael, 1987, Ann. Phys. (N.Y.) **174**, 372.
Dominguez, C. A., and K. Schilcher, 2004, Phys. Lett. B **581**, 193.
Dominguez, C. A., C. Van Gend, and N. Paver, 1991, Phys. Lett. B **253**, 241.
Donoghue, J. F., and E. Golowich, 1994, Phys. Rev. D **49**, 1513.
Edwards, K., *et al.* (CLEO Collaboration), 1997, Phys. Rev. D **56**, R5297.
Edwards, K. W., *et al.* (CLEO Collaboration), 2000, Phys. Rev. D **61**, 072003.
Eidelman, S., and F. Jegerlehner, 1995, Z. Phys. C **67**, 585.
Eidelman, S., *et al.* (Particle Data Group), 2004, Phys. Lett. B **592**, 1.
Ellis, J., and M. Karliner, 1995, Phys. Lett. B **341**, 397.
Erler, J., 1999, Phys. Rev. D **59**, 054008.
Farley, F. J. M., and E. Picasso, 1990, in *The Muon (g-2) Experiments Advanced Series on Directions in High Energy Physics*, Vol. 7, *Quantum Electrodynamics*, edited by T. Kinoshita (World Scientific, Singapore).

Floratos, E., S. Narison, and E. de Rafael, 1979, Nucl. Phys. B **155**, 115.
Fuchs, N. H., H. Sazdjian, and J. Stern, 1990, Phys. Lett. B **238**, 380.
Fuchs, N. H., H. Sazdjian, and J. Stern, 1991, Phys. Lett. B **269**, 183.
Gabrielse, G., and J. Tan, 1994, in *Cavity Quantum Electrodynamics*, edited by P. Berman (Academic, San Diego), p. 267.
Gámiz, E., *et al.*, 2003, J. High Energy Phys. 01060.
Gámiz, E., *et al.* 2005, Phys. Rev. Lett. **94**, 011803.
Gasser, J., and H. Leutwyler, 1982, Phys. Rep. **87**, 77.
Gasser, J., and H. Leutwyler, 1984, Ann. Phys. (N.Y.) **158**, 142.
Gasser, J., and H. Leutwyler, 1985, Nucl. Phys. B **250**, 465.
Gell-Mann, M., R. J. Oakes, and B. Renner, 1968, Phys. Rev. **175**, 2195.
Generalis, S. C., 1989, J. Phys. G **15**, L225.
Ghozzi, S., and F. Jegerlehner, 2004, Phys. Lett. B **583**, 222.
Gibaut, O., *et al.* (CLEO Collaboration), 1994, Phys. Rev. Lett. **73**, 934.
Göckeler, N., *et al.*, 2004, e-print hep-ph/0409312.
Goldstone, J., 1961, Nuovo Cimento **19**, 154.
Goldstone, J., A. Salam, and S. Weinberg, 1961, Phys. Rev. **127**, 965.
Golowich, E., and J. Kambor, 1995, Nucl. Phys. B **447**, 373.
Golowich, E., and J. Kambor, 1996, Phys. Rev. D **53**, 2651.
Golowich, E., and J. Kambor, 1997, Phys. Lett. B **421**, 319.
Golowich, E., and J. Kambor, 1998, Phys. Rev. D **58**, 036004.
Gómez Dumm, D., A. Pich, and J. Portolés, 2000, Phys. Rev. D **62**, 054014.
Gorishnii, S. G., K. L. Kataev, and S. A. Larin, 1991, Phys. Lett. B **259**, 144.
Gounaris, G. J., and J. J. Sakurai, 1968, Phys. Rev. Lett. **21**, 244.
Gourdin, M., and E. de Rafael, 1969, Nucl. Phys. B **10**, 667.
Groote, S., J. G. Körner, K. Schilcher, and N. F. Nasrallah, 1998, Phys. Lett. B **440**, 375.
Gross, D., and C. Llewellyn-Smith, 1969, Nucl. Phys. B **14**, 337.
Grozin, A., and Y. Pinelis, 1986, Phys. Lett. **166B**, 429.
Grunberg, G., 1980, Phys. Lett. **95B**, 70.
Grunberg, G., 1984, Phys. Rev. D **29**, 2315.
Guerrero, F., and A. Pich, 1997, Phys. Lett. B **412**, 382.
Hagiwara, K., A. D. Martin, D. Nomura, and T. Teubner, 2004, Phys. Rev. D **69**, 093003.
Haidt, D., 1995, in *Direction in High Energy Physics Vol. 14, Precision Tests of the Standard Electroweak Model*, edited by P. Langacker (World Scientific, Singapore).
Hayakawa, M., and T. Kinoshita, 1998, Phys. Rev. D **57**, 465; **66**, 019902(E) (1998).
Hayakawa, M., T. Kinoshita, and A. I. Sanda, 1996, Phys. Rev. D **54**, 3137.
Hertzog, D. W., 2005, Nucl. Phys. B, Proc. Suppl. **144**, 191.
Hoang, A. H., 1999, Phys. Rev. D **59**, 014039.
Höcker, A., 1997, Nucl. Phys. B (Proc. Suppl.) **55C**, 379.
Höcker, A., 2004, in *Proceedings of the 32nd International Conference on High-Energy Physics (ICHEP'04)*, Beijing, China, 2004, e-print hep-ph/0410081.
Höcker, A., and V. Kartvelishvili, 1996, Nucl. Instrum. Methods Phys. Res. A **372**, 469.
Holstein, B. R., 1990, Comments Nucl. Part. Phys. **19**, 221.
Hughes, V. W., and T. Kinoshita, 1999, Rev. Mod. Phys. **71**, S133.
Ioffe, B. L., and K. N. Zyablyuk, 2001, Nucl. Phys. A **687**, 437.
Ioffe, B. L., and K. N. Zyablyuk, 2003, Eur. Phys. J. C **27**, 229.
Isidori, G., 2005, in *CKM 2005 Workshop, 2005*, San Diego, California.
Jadach, S., B. F. L. Ward, and Z. Was, 1994, Comput. Phys. Commun. **79**, 503.
Jamin, M., 1998, Nucl. Phys. B (Proc. Suppl.) **B64**, 250.
Jamin, M., 2002, Phys. Lett. B **538**, 71.
Jamin, M., and M. Münz, 1995, Z. Phys. C **66**, 633.
Jamin, M., J. A. Oller, and A. Pich, 2002, Eur. Phys. J. C **24**, 237.
Jegerlehner, F., 2004, Nucl. Phys. B, Proc. Suppl. **131**, 213.
Kambor, J., and K. Maltman, 2000, Nucl. Phys. A **680**, 155.
Kambor, J., and K. Maltman, 2001, Nucl. Phys. B (Proc. Suppl.) **B98**, 314.
Kartvelishvili, V. G., and M. V. Margvelashvili, 1992, Z. Phys. C **55**, 83.
Kartvelishvili, V., M. Margvelashvili, and G. Shaw, 1997, Nucl. Phys. B (Proc. Suppl.) **54A**, 309.
Kataev, A. L., N. V. Krasnikov, and A. A. Pivovarov, 1983, Nuovo Cimento Soc. Ital. Fis., A **76A**, 723.
Kataev, A. L., and V. V. Starshenko, 1995, Mod. Phys. Lett. A **10**, 235.
Kawarabayashi, K., and M. Suzuki, 1966, Phys. Rev. Lett. **16**, 225.
Kim, J. H., *et al.* (CCFR Collaboration), 1998, Phys. Rev. Lett. **81**, 3595.
Kinoshita, T., and M. Nio, 2004, Phys. Rev. D **70**, 113001.
Knecht, M., and A. Nyffeler, 2002, Phys. Rev. D **65**, 073034.
Knecht, M., and J. Stern, 1995, in *The Second* DAΦNE *Physics Handbook*, edited by L. Maiani, G. Pancheri, and N. Paver (INFN, Frascati), Vol. 1, 169.
Knecht, M., *et al.*, 2002, Phys. Rev. Lett. **88**, 071802.
Körner, J. G., F. Krajewski, and A. A. Pivovarov, 2001a, Phys. Rev. D **63**, 036001.
Körner, J. G., F. Krajewski, and A. A. Pivovarov, 2001b, Eur. Phys. J. C **20**, 259.
Krause, B., 1997, Phys. Lett. B **390**, 392.
Kühn, J. H., and E. Mirkes, 1992, Z. Phys. C **56**, 661.
Kühn, J. H., and A. Santamaria, 1990, Z. Phys. C **48**, 445.
Kühn, J. H., and M. Steinhauser, 1998, Phys. Lett. B **437**, 425.
Lanin, L. V., V. P. Spiridonov, and K. G. Chetyrkin, 1986, Yad. Fiz. **44**, 1372 [Sov. J. Nucl. Phys. **44**, 892, (1986)].
Larin, S. A., F. V. Tkachov, and J. A. M. Vermaseren, 1991, Phys. Rev. Lett. **66**, 862.
Larin, S. A., T. van Ritbergen, and J. A. M. Vermaseren, 1997, Phys. Lett. B **404**, 153.
Larin, S. A., and J. A. M. Vermaseren, 1991, Phys. Lett. B **259**, 345.
Le Diberder, F., 1995, Nucl. Phys. B (Proc. Suppl.) **B39**, 318.
Le Diberder, F., and A. Pich, 1992a, Phys. Lett. B **286**, 147.
Le Diberder, F., and A. Pich, 1992b, Phys. Lett. B **289**, 165.
Lovett-Turner, C. N., and C. J. Maxwell, 1994, Nucl. Phys. B **432**, 147.
Maltman, K., 1998a, Phys. Rev. D **58**, 093015.
Maltman, K., 1998b, Phys. Lett. B **428**, 179.
Maltman, K., 2006, Phys. Lett. B **633**, 512.
Maltman, K., and J. Kambor, 2002, Phys. Rev. D **65**, 074013.
Marciano, W., 1996, in *Particle Theory and Phenomenology*, edited by K. Lassila *et al.* (World Scientific, Singapore), p. 22.
Marciano, W., and A. Sirlin, 1988, Phys. Rev. Lett. **61**, 1815.
Marciano, W. J., 2005, in *CKM 2005 Workshop, 2005*, San Diego, California.
Margvelashvili, M. V., 1988, Phys. Lett. B **215**, 763.
Martin, A. D., and D. Zeppenfeld, 1995, Phys. Lett. B **345**, 558.

Maxwell, C. J., and D. G. Tonge, 1996, Nucl. Phys. B **481**, 681.
Maxwell, C. J., and D. G. Tonge, 1998, Nucl. Phys. B **535**, 19.
Melnikov, K., and A. Vainshtein, 2004, Phys. Rev. D **70**, 113006.
Menke, S., 1998, Ph.D. thesis.
Menke, S., 1999, Nucl. Phys. B **76**, 299.
Menke, S., 2001, eConf C010430 M09, e-print hep-ex/0106011.
Moussallam, B., 1999, Eur. Phys. J. C **6**, 681.
Mueller, A. H., 1992, "The QCD Perturbation Series," in *QCD-20 Years Later*, Aachen, 1992, edited by P. Zerwas and H. A. Kastrup (World Scientific, Singapore), p. 162.
Nagle, J., R. Julian, and J. Zacharias, 1947, Phys. Rev. **72**, 971.
Nagle, J., E. Nelson, and I. Rabi, 1947, Phys. Rev. **71**, 914.
Nambu, Y., and G. Jona-Lasinio, 1961, Phys. Rev. **122**, 345.
Narison, S., 1982, Z. Phys. C **14**, 263.
Narison, S., 1989, Phys. Lett. B **216**, 191.
Narison, S., 1995, Phys. Lett. B **358**, 113.
Narison, S., 1999, Phys. Lett. B **466**, 345.
Narison, S., and A. Pich, 1988, Phys. Lett. B **211**, 183.
Neubert, M., 1996, Nucl. Phys. B **463**, 511.
Pascual, P., and E. de Rafael, 1982, Z. Phys. C **12**, 127.
Peccei, R. D., and J. Solà, 1987, Nucl. Phys. B **281**, 1.
Penin, A. A., and A. A. Pivovarov, 1998, Phys. Lett. B **435**, 413.
Peris, S., B. Phily, and E. de Rafael, 2001, Phys. Rev. Lett. **86**, 14.
Pich, A., 1987, Phys. Lett. B **196**, 561.
Pich, A., and J. Prades, 1998, J. High Energy Phys. 06013.
Pich, A., and J. Prades, 1999, J. High Energy Phys. 10004.
Pich, A., and J. Prades, 2000, Nucl. Phys. B (Proc. Suppl.) **86**, 236.
Pivovarov, A. A., 1991, Sov. J. Nucl. Phys. **54**, 676.
Pivovarov, A. A., 1992, Z. Phys. C **53**, 461.
Poggio, E., H. Quinn, and S. Weinberg, 1976, Phys. Rev. D **13**, 1958.
Prades, J., 1999, Nucl. Phys. B (Proc. Suppl.) **76**, 341.
Prades, J., and A. Pich, 1999, Nucl. Phys. B (Proc. Suppl.) **74**, 309.
Procario, M., *et al.* (CLEO Collaboration), 1993, Phys. Rev. Lett. **70**, 1207.
Quenzer, A., *et al.* (DM1 Collaboration), 1978, Phys. Lett. **76B**, 512.
Raczka, P. A., 1998, Phys. Rev. D **57**, 6862.
Riazzuddin, K., and M. Fayazuddin, 1966, Phys. Rev. **147**, 1071.
Richichi, S., *et al.* (CLEO Collaboration), 1999, Phys. Rev. D **60**, 112002.
Roberts, B. L., 1999, in *High Intensity Muon Sources*, edited by Y. Kuno and T. Yokoi (World Scientific, Singapore), p. 69.
Rodrigo, G., A. Pich, and A. Santamaria, 1998, Phys. Lett. B **424**, 367.
Rojo, J., and J. I. Latorre, 2004, J. High Energy Phys. 01055.
Santiago, J., and F. J. Yndurain, 2001, Nucl. Phys. B **611**, 447.
Schael, S., *et al.* (ALEPH Collaboration), 2005, Phys. Rep. **421**, 191.
Schwinger, J., 1948, Phys. Rev. **73**, 416.
Shifman, M. A., A. L. Vainshtein, and V. I. Zakharov, 1979a, Nucl. Phys. B **147**, 385.
Shifman, M. A., A. L. Vainshtein, and V. I. Zakharov, 1979b, Nucl. Phys. B **147**, 448.
Shifman, M. A., A. L. Vainshtein, and V. I. Zakharov, 1979c, Nucl. Phys. B **147**, 519.
Snow, S., 1993, in *Proceedings of the 2nd International Workshop on τ Lepton Physics*, Columbus 1992, edited by K. K. Gan (World Scientific, Singapore).
Steinhauser, M., 1998, Phys. Lett. B **429**, 158.
Stevenson, P. M., 1981, Phys. Rev. D **23**, 2916.
Surguladze, L. R., and M. A. Samuel, 1991, Phys. Rev. Lett. **66**, 560.
Terent'ev, M. V., 1973, Sov. J. Nucl. Phys. **16**, 87.
't Hooft, G., and M. Veltman, 1972, Nucl. Phys. B **44**, 189.
Vainshtein, A., 2003, Phys. Lett. B **569**, 187.
Van Dyck, R. S., P. B. Schwinberg, and H. G. Dehmelt, 1987, Phys. Rev. Lett. **59**, 26.
van Ritbergen, T., J. A. M. Vermaseren, and S. A. Larin, 1997a, Phys. Lett. B **400**, 379.
van Ritbergen, T., J. A. M. Vermaseren, and S. A. Larin, 1997b, Phys. Lett. B **405**, 327.
Vasserman, I. B., *et al.* (OLYA Collaboration), 1979, Sov. J. Nucl. Phys. **30**, 519.
Vasserman, I. B., *et al.* (TOF Collaboration), 1981, Sov. J. Nucl. Phys. **33**, 709.
Weinberg, S., 1967, Phys. Rev. Lett. **18**, 507.
Weinberg, S., 1977, in *A Festschrift for I.I. Rabi*, edited by L. Motz (New York Academy of Sciences, New York).
Weinberg, S., 1979, Physica A **96**, 327.
Weinstein, A., 2001, in *Proceedings of the 6th International Workshop on τ Lepton Physics*, Victoria 2000, edited by R. J. Sobie and J. M. Roney (North-Holland, Amsterdam).
Werlen, M., *et al.* (UA6 Collaboration), 1999, Phys. Lett. B **452**, 201.
Wetzel, W., 1982, Nucl. Phys. B **196**, 259.
Wilson, K. G., 1969, Phys. Rev. **179**, 1499.
Withlow, L. W., *et al.*, 1992, Phys. Lett. B **282**, 475.
Zielinski, M., 1984, Phys. Rev. Lett. **52**, 1195.
Zyablyuk, K. N., 2004, Eur. Phys. J. C **38**, 215.